



HYDROCARBON POLLUTION AND POTENTIAL ECOLOGICAL RISK OF HEAVY METALS IN THE SEDIMENTS OF THE OTURUBA CREEK, NIGER DELTA, NIGERIA

Clinton Ifeanyichukwu Ezekwe^{1*}, Israel Clinton Utong²

¹Department of Geography and Environmental Management, University of Port Harcourt, PMB 5323 Choba, E-W Rd, 500001 Port Harcourt, Nigeria.

²Environmental Monitoring and Compliance Department, The Shell Petroleum Development Company, POB 263, Rumuobiakani, 500001 Port Harcourt, Nigeria

*Corresponding author, e-mail: Clinton.ezekwe@uniport.ng.edu

Research article, received 10 October 2016, accepted 28 February 2017

Abstract

This study aimed at examining the impact of oil pollution from artisanal oil refineries on the Oturuba river ecosystem using active river bottom sediment. Specific objectives included to determine the level of hydrocarbons and trace metals (Pb, Cd, Zn, Cu, Ni, V and Mg) in the sediments and to relate this with general ecosystem health. The study found elevated concentrations of both hydrocarbons and heavy metals in the range above most sediment quality guidelines exceeding the respective Threshold Effects Level and Probable Effects. Level guideline values and occurring at levels where impairment to biological communities is certain and where toxicity levels can lead to negative impacts on benthic animals or infaunal communities. Heavy metal geochemical accumulation index and potential ecological risk analysis also returned anomalously high concentrations in the range of very highly polluted sediment environments with very high ecological risk indices, thereby ranking the Oturuba Creek as one of the most polluted coastal river systems in the world.

Keywords: sediment pollution; trace metals; artisanal refining; estuaries; Andoni River

INTRODUCTION

The survival of coastal rivers and estuaries which are among the most sensitive and biologically productive habitats on earth is currently being threatened by human activities including oil production. Coastal rivers are dynamic ecosystems with spatial and temporal fluctuations in reach and constituents. Concentrations of organic and inorganic constituents in coastal river systems, especially metals and hydrocarbons are mediated by biogeochemical forcings such as sediment composition and texture, sediment-water redox reactions, pH, temperature, salinity, nutrients and oxygen availability, microbial populations, competition, transportation dynamics and anthropogenic perturbations (Förstner and Salomons, 1981; Whitehead, 2013). These anthropogenic disturbances and naturally induced biogeochemical stressors may impose suboptimal conditions leading to physiological adaptations or forced migration by resident species. For instance, oil pollution in coastal river systems through oil-induced oxygen-deficiency, toxicity, asphyxiation, coating or smothering, which affects gas exchange, thermo-reactions and osmoregulation, can threaten the life-support processes in a river ecosystem by imposing hypoxic conditions thereby affecting community resilience and population dynamics (Luoma et al., 1997; Mendelssohn et al., 2012; Whitehead, 2013).

Sediments are sinks for contaminants in river ecosystems and their physico-chemical properties and response to the chemical dynamics of the hydrological system may enhance subsequent contamination to the ecosystem components to which they are linked. Significant contamination of sediments may lead to species and biodiversity losses (Markovic, 2003; Luoma, 1990) and deleterious food chain reactions from benthic communities to upper trophic levels (Burton, 2002) either through direct adverse impacts on bottom fauna or by becoming long-term sources of toxic substances to the environment. They can also impact wildlife and humans through the consumption of food or water or by direct bodily contact. Of critical importance, is that these impacts may be present even though the overlying water meets water quality criteria (USEPA, 1992) thereby underscoring the importance of sediment quality analysis in monitoring ecosystem integrity.

River bottom or deposited channel materials represent the closest approximation of sediment provenance, movement and deposition, however directly linking sediment chemistry data to observed adverse biological effects on organisms is problematic (USEPA, 2005), hence, a few screening guidelines, indices or benchmarks (below which toxic effects are not expected to occur and above which toxic effects are usually expected) relate chemical concentrations in sediments to their “potential for biological effects” (Bay et al., 2012).

Buchman (2008) presented sediment screening levels based on Threshold Effects Level (TEL), Effects Range-Low (ERL), and Probable Effects Level (PEL) for evaluating sediment quality. TELs define chemical sediment concentration benchmarks where toxic effects are scarcely observed in key indicator organisms while PELs on the other hand define concentrations which when exceeded can cause observable detrimental effects on organisms. ERL thresholds are statistical derivations of the 10th percentile concentration of chemicals in samples identified as toxic occurring between the TEL levels and the PEL benchmark. Also heavy metals in sediments have been used successfully in calculating pre-industrial and anthropogenic pollution sources and ecological risks in sediments (Håkanson, 1980, 1988; Forstner, 1989; Singh et al., 2003; Li et al., 2012) and more recently in the analysis of groundwater contamination in industrial areas (Bhuttiani, 2017).

These benchmarks which have been previously tested and accepted have been applied in this study to measure the impact of artisanal oil refining activities on the ecosystem health of the Oturuba Creek where illegal crude oil refining activities has been ongoing since 2010 and where ambient ecosystem destruction and reduction in fish catch has been observed. This study therefore attempts to show the latent and manifest ecological impacts of hydrocarbon and heavy metal concentrations in sediments of the Oturuba Creek, hence similar ecological systems. It also aims to show the relationships and spatio-temporal spread of heavy metals and hydrocarbons in the Oturuba Creek.

STUDY AREA

Oil was first discovered in commercial quantities in 1956 in Nigeria in the freshwater swamps of the Niger Delta, around Oloibiri, currently in the Bayelsa State of Nigeria. Since then the Niger Delta environment and its eco-systems have been adversely impacted and altered by oil and gas exploration and exploitation. This has triggered a conflict of interest and sometimes armed conflicts between production/facilities host communities on the one hand and the federal government and oil companies on the other. This has led to wanton pipeline vandalism, oil theft, illegal bunkering and illegal refining (using makeshift refineries) of probably stolen crude oil, and consequent oil spills into, and damage to the environment. When oil is spilled, it is washed into water bodies (as in the study area) via surface run off and may persist (bio-accumulate and bio-transform) in the media it attaches to for a very long period of time. About 50% of spilled oil evaporates, others migrate and stray away via the action of wind and tidal waves, others emulsify, while a percentage of it, unnoticeably, sinks to the bottom of the river bed and permeates into bottom sediments (USEPA, 1999).

The Oturuba Creek is a tributary of the Andoni River -a major river which drains the eastern part of the Niger Delta of Nigeria. The creek (Fig. 1) has an approximate length of about 3.66km and width of about 100m, and average depth of about 3.7 metres. The river stretch starts from the Egwede area and drains into the Andoni River in the inter-tidal mud flat mangrove ecosystem terrain characteristic of the eastern Niger Delta coastline. It is a low-lying terrain (< 5 m asl) and consists of about 3-5 m of soft mud with high organic matter content. The Oturuba

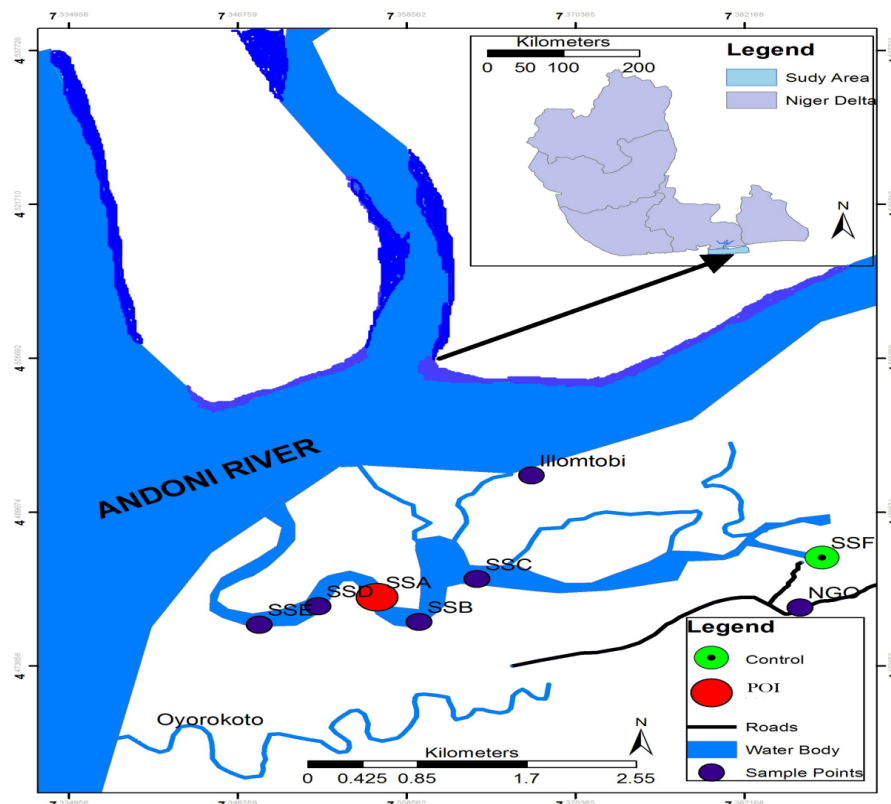


Fig. 1 Location of the study area and the sample sites (SS)

Creek is a permanently saline sheltered river system tied to the tropical deltaic tide influenced Andoni River system with its characteristic silty muds, acidic sediments (pH: 4.09–5.04), high water temperatures (26.2–32.4°C), deep waters (17 fathoms) and wide water salinity ranges (8–21ppt) (Ssentongo, Ukpe and Ajayi, 1986; Ansa et al., 2007; Ansa and Francis, 2007; Ezekwe and Edoghotu, 2015). The study area also falls within the transitional zone of the Aw and Af climate types of the Koppen's climatic classification scheme. It is thus characterized by long hours of day light, high temperatures of about 27°C and high rainfall ($\geq 1,800$ mm).

MATERIALS AND METHODS

Sample sites

Sediment samples were collected from six sample sites after an initial reconnaissance of the study area. The geographical location of each sampling point (Fig. 1) was recorded using handheld GPS equipment (Garmin 76) and described in Table 1.

Table 1 Sampling Sites

Sampling Site	Latitude	Longitude	Site Description
1. SSE	4° 28' 40.675°N	7° 20' 53.685°E	First point upstream near the mouth of the Oturuba Creek (about 1 km from POI) close to the Andoni River.
2. SSD	4° 28' 38.963°N	7° 21' 13.654°E	About 500 m upstream from point of impact (POI).
3. SSA	4° 28' 50.945°N	7° 21' 23.353°E	Point of Impact (POI) where raw waste from the crude oil refining process, refined products and sludge are discharged into the creek
4. SSB	4° 28' 42.957°N	7° 21' 37.046°E	About 500 m downstream
5. SSC	4° 28' 50.374°N	7° 21' 53.592°E	About 1 km downstream
6. SSF	4° 29' 05.78°N	7° 23' 15.43°E	About 3.7 km downstream (Control; un-impacted area).

Visual observation of site1 conditions showed that the site had relatively buoyant biomass; which can be attributed to its location, almost at the point where the Oturuba Creek joined the Andoni River and therefore receives fresh and relatively uncontaminated water from the larger Andoni River system. Oil sheen was only observed

on the surface of the water during ebb tides. Site 2 had oil sheens on the surface of the river with mud flats on both sides of the river showing signs of heavy oil-staining. It was also characterised by scanty and unhealthy looking fauna and flora especially mangroves plants and crabs. Site 3 or the point of impact (POI) was characterized by greasy and muddy surfaces with darkened soils and scorched vegetation. The site was bereft of visible biological activity as no marine organisms were spotted in the vicinity during the fieldwork. Oil sheen and slicks were seen floating freely on the surface of the creek; while site 4 had oil sheen on the surface of the water, especially during low tide. Mangrove plants were sparse with a few marine fauna such as juvenile periwinkle, crabs, mudskipper, etc. in the mangrove mud. The mud had oil stains as in the point of impact but no direct inlet of spilled oil into the water body was observed. This immediate downstream sampling site from the POI was the most impacted section of the creek after site 3. At site 5, mangrove plant species were densely populated and there where sightings of crabs, mudskipper, periwinkles and birds. The mud and surface water showed very little sign of pollution. At site 6, which served as the control site for this study, the mangrove vegetation was dense and green with an abundance of bio-activity (crabs, periwinkles, mudskippers, birds, reptiles and other aquatic invertebrates). The mangrove mud flats and water did not show any visible sign of contamination.

Sample collection and analysis

River bottom sediments were collected from the 6 designated locations in the Oturuba Creek following methods outlined by Marcus et al. (2013). Sediment samples were collected by the grab method in triplicates at low tide in June 2013 (rainy season) and November 2013 (dry season) (APHA, 1998). Samples for hydrocarbon analysis were stored in sterilized bottles, while the samples for the analysis of trace metals were stored in polythene bags previously washed in diluted HCl while those for organic matter analysis were collected in aluminium foils. Samples were stored in polyethylene sealed and stored in ice packed plastic coolers (below 4°C) thereafter, transported to the laboratory and analyzed within 2 days.

The sediment samples were allowed to thaw and were air-dried at ambient temperature ground and sieved through a 0.5 mm mesh. Later, 2 g of each sample was digested using 25 ml 1:3:1 mixture of HClO₄, HNO₃ and H₂SO₄ acids in a water bath. 10 ml deionized water was added to the digest and decanted into 50 ml standard flask and made up to mark with deionized water after rinsing. The Buck Scientific Atomic Absorption Spectrophotometer Model 200A and air-acetylene flame were used for trace metal analyses with quality assurance checked with standard sediment sample PACS-2 using an intra-run Quality Assurance Standard (1 mg/l, Multi-Element Standard Solution, Fisher Scientific) after every 10 samples (Cantillo and Calder, 1990).

The Walkley-Black wet chemistry "reference" procedure for the determination of Total Organic Carbon as described in Schumacher (2002) and applied by Marcus

and Ekpote (2014) was used in analysing total organic carbon (TOC) in this study. 1 g of dried, sieved sediment was put into 250 ml conical flask and digested with 10 ml 0.5 M $K_2Cr_2O_7$ and 20 ml concentrated H_2SO_4 , swirled and allowed to cool. To overcome the concern for incomplete digestion of organic matter, the sample and extraction solutions were gently boiled at 150 °C for 30 minutes and allowed to cool (Walkley and Black, 1934; Tiessen and Moir, 1993). When cool (after 20–30 minutes), 100 ml de-ionized water was added for dilution and 3 or 4 drops of ‘Ferrouin’ indicator was added and titrated with 0.4 N $FeSO_4$ solution (NSW EH, 2015). Results of TOC were reported as percentage and later converted to dry weight (Table 1) by multiplying total organic matter content (%) by sediment bulk density (1.61 g cm^{-3}) and depth (20 cm) of sampling (Pluske et al., 2016).

Samples for hydrocarbon analysis was weighed to obtain wet weight, and then sun-dried and then grounded to powdery form and sieved with a 1.0mm sieve. The sieved samples were stored in well-labelled smaller plastic containers with cover, from where samples were withdrawn for analysis. 5g each of dry powdery samples were weighed out and placed in 250ml beakers. To this was added 30ml of xylene; the beaker was then swirled/shaken for about 5 minutes and allowed to settle, the mixture was later filtered into a clean 100ml standard flask through a Whatmann filter paper that contains about 2g of Anhydrous Sodium Sulphate on a cotton wool. This was done three times and was later made up to the 100ml mark with xylene. The absorbance of the filtrate was measured at 340nm using Hach DR 2800 Spectrophotometer. The corresponding concentrations of Total Hydrocarbon (THC) content were then obtained from the calibration curve and calculated on dry weight basis. Same procedure was applied to the analysis for Total Petroleum Hydrocarbon (TPH), although, after the extraction, the filtrate was treated with silica gel to remove non-petroleum hydrocarbons and re-filtered. The readings were obtained in the same manner with that of THC and the final value calculated as usual (Howard et al., 2009). Calibration of the spectrophotometer (HACH DR 2800) was carried out before each analysis using diluents of a stock solution of 1ml of crude oil in 100ml of xylene at 340nm in line with ASTM (2003) and Howard et al. (2009).

Environmental Impact and Ecological Risk Assessment Methods

Environmental impacts of oil contamination and potential ecological risks were calculated by analysing the relationships, differences and similarities between contaminant concentrations in sample sites. Contaminant concentrations in sediments were further compared with sediment quality guidelines including; the National Ocean and Atmospheric Administration of the USA (NOAA) and the Dutch government intervention values (Verbruggen, 2004) for the protection of ecosystems using the apparent effects threshold (AET), the effects range low (ERL), effects range medium (ERM), the threshold effects and probable effects level (TEL/PEL) (IMO, 2000) and maximum permissible concentrations (MPCs).

Potential Ecological Risk Index (PERI), a diagnostic tool suggested by Håkanson (1980, 1988) for the analysis of contamination in lakes and coastal systems was used to calculate an ecological risk index for the Oturuba river ecosystem. PERI is formed by three basic modules: Degree of contamination (C_D); toxic-response factor (Tr^i); and potential ecological risk factor (Er^i).

The first module of PERI corresponds to the estimate of the degree of contamination (C_D). The C_D is expressed by the sum of the contamination factor of each metal (C_f^i) as:

$$C_D = \sum C_f^i$$

where, C_f^i , is the mean metal concentration (C^i), divided by the pre-industrial concentration of the substance (C_0^i):

$$C_f^i = C^i / C_0^i$$

According to Håkanson (1980, 1988), the potential ecological risk index (PERI) is defined by:

$$RI = \sum Er^i$$

$$Er^i = Tr^i * C_f^i$$

where; RI is calculated as the sum of all risk factors for heavy metals in sediments; Er^i is the monomial potential ecological risk factor; Tr^i is the dimensionless derived toxic-response factor for a given substance (e.g., Cu = 5, Pb = 5, Ni = 5, Zn = 1, Cd = 30), which mainly reflects the heavy metal toxicity level and the degree of environment sensitivity to pollution from a particular heavy metal (Jiao et al., 2015).

C_f^i , C_0^i , and C_n^i are the contamination factor, the concentration of metals in the sediment and the background reference level, respectively. International background values for metals in sediments (shale) include 0.22 mg/kg for Cd, 39 mg/kg for Cu, 68 mg/kg for Ni, 120 mg/kg for Zn, 0.85 mg/kg for Mn (Rodrigues et al., 2006) and 60 mg/kg for Pb (Li et al., 2012).

Håkanson (1980) also proposed the following values to be used in the interpretation of ecological risks in sediments:

- $RI < 150$, low ecological risk for the sediment;
- $150 \leq RI < 300$, moderate ecological risk for the sediment;
- $300 \leq RI < 600$, considerable ecological risk for the sediment;
- $RI \geq 600$, very high ecological risk for the sediment.

In order to assess the intensity of metal contamination in the sediments of the Oturuba Creek, the geochemical accumulation index was calculated using the equation proposed by Singh et al. (2003) to quantify metal accumulation in the sediments, and represent their contamination degree. This index is expressed as follows:

$$I_{geo} = \log_2 C_n / 1.5 B_n$$

where I_{geo} is the geochemical accumulation index; C_n is the total concentration of metal n in the silt/clay fraction;

B_n is the geochemical background value of element n and 1.5 is a correction factor due to lithogenic effects. The I_{geo} classification entails seven grades (0 to 6) of pollution, ranging from no pollution (0) to very high pollution (Forstner, 1989).

RESULTS AND DISCUSSION

Heavy metals, organic matter and hydrocarbons in the sediments

The results of the analysis of sampled sediments are presented in Figure 2. Organic matter concentration ranged between 201 (mg/kg) and 2782.1(mg/kg) with both lowest and highest concentrations occurring in the wet season. Highest concentrations occurred 500m downstream (Site 4) from the point of impact in both seasons.

Concentrations of copper in the sediment ranged between 4.78 – 83.5 mg/kg with highest and lowest concentrations occurring in site 4 and 6 in the dry season respectively. Concentrations also followed the same pattern in the wet season (6.24 mg/kg – 50.02 mg/kg) although with slightly lower concentrations in site 4. Concentrations of copper (4.78 – 83.5 mg/kg) in sediments were above the Dutch maximum permissible concentrations (73 mg/kg) in site 4 in the dry season. Copper concentrations were also above the TEL (18.7 mg/kg) in 7 out of 12 cases and above the ERL (34 mg/kg) in three cases while nickel exceeded TEL limits (15.9 mg/kg) in 7 cases out of 12 in all seasons. Concentrations of zinc ranged between 199.53 and 1007.8 mg/kg, lowest and highest concentrations occurred at site 1 and 6 respectively. The concentrations of zinc were higher in the dry season for all sites apart from site 6 and also above TEL, ERL and PEL guidelines in all seasons.

While lead concentrations (123.3 – 327.5 mg/kg) were above TEL, PEL and ERL in all cases except for PEL in the dry season in site 6 cadmium concentrations (38.1 – 259 mg/kg) were above all the standards in all seasons. For vanadium (1.21 – 5.24 mg/kg) and manganese

(42.71 – 959.4 mg/kg) the only available guideline is the AET (57 and 260 mg/kg respectively). While all the sampling sites were below maximum specified limits for vanadium, manganese exceeded standards in sites 3, 4 and 5 in the dry season and all sampling sites apart from site 6 in the wet season.

Total petroleum hydrocarbons (TPH) in sediments ranged from 3997.9 (mg/kg) dry weight at the POI to 1546 (mg/kg) at site 6 in the dry season. Concentrations in the wet season followed a similar trend with ranges between 5118.5 mg/kg at site 3 and 1727.5 mg/kg in site 6. Total hydrocarbon (THC) concentrations ranged between 5133.6 mg/kg in site 3 and 2151.2 mg/kg in site 6 in the dry season. There was however a slight difference in trend as the POI had a total concentration of 6118.5 (mg/kg) with lowest concentrations (2272.5 mg/kg) downstream in site 5.

Potential ecological impacts of heavy metals and hydrocarbons in the sediments

Species that are intolerant to metal contamination can be adversely affected in a number of ways from heavy metal pollution of marine sediments. Impacts on reproduction and growth can impair the survival of individuals, and affect populations and communities. For instance, copper can be acutely toxic to microalgae at levels between 190mg/kg and 300 mg/kg (Markovic, 2003). In this study, copper occurred between maximum contaminant limits and the low level effects range where biological activities can be impaired. Also, recruitment can also be affected by metal contamination in clams (*Macoma bathilica*) (Langston, 1990; Markovic, 2003). Concentrations of zinc in this study occurred far above these toxic levels. Negative impacts related to metal contamination do not necessarily result from direct toxicity but contaminant-related changes to phytoplankton communities may have serious consequences for higher trophic levels. A change in the phytoplankton community structure can lead to a reduction in preferred prey species,

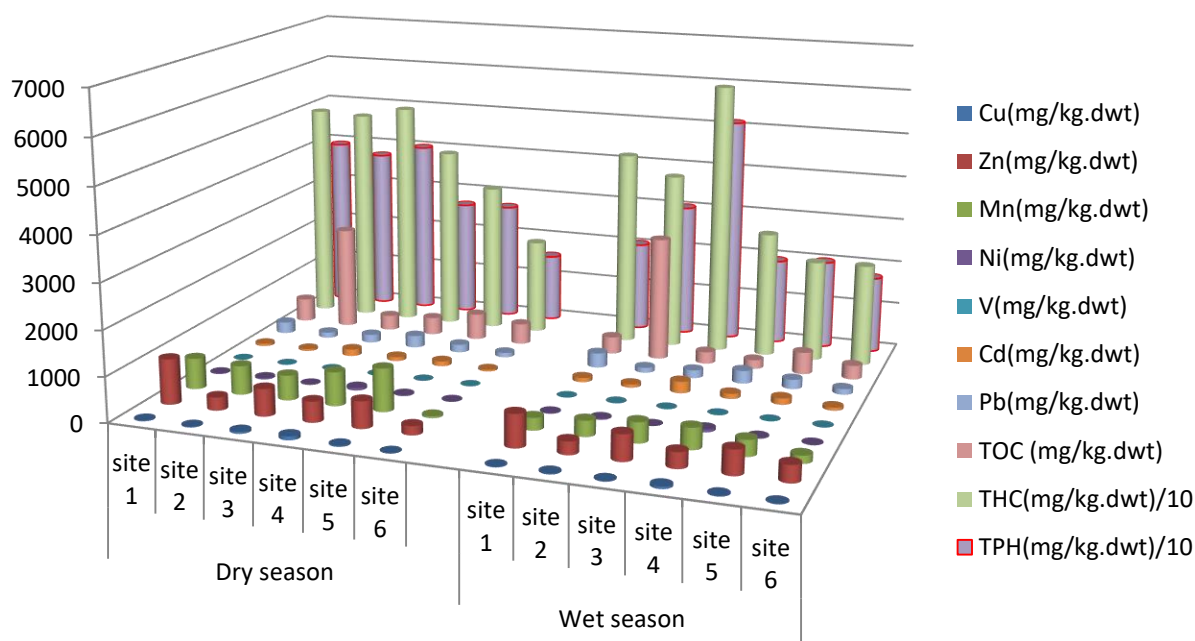


Fig. 2 Hydrocarbons, Heavy metals and TOC in the Oturuba Creek

Table 2 Marine Sediment Quality Guidelines (Modified from NOAA, 2008 and Bay et al., 2012)

Mg/kg	Intervention Dutch Guidelines			Consensus Sediment Guidelines			
	Intervention values	MPC	TEL	ERL	PEL	ERM	AET
P _A H _S	40		1.684	4.022	16.77	44.8	
Mineral oil	1100	5000					
Cu	190	73	18.7	34	108	270	390 Microtop larvae
Zn	720	620	124	150	271	410	410 Infaunal community impacts
Mn							260 Neanthes
Ni	210	44	15.9	20.9	42.8	51.6	110 Echinoderm larva; Bioassay Larvae
V							57 Neanthes
Cd	12	0.68	0.68	1.2	4.21	9.6	3.0 Neanthes
Pb	530	530	30.2	46.7	112	218	400 Bivalve

and ultimately the loss of higher trophic species in those communities. It is possible that the indirect effects triggered by the loss of sensitive species have a much more significant impact on marine communities than indicated by toxicity tests with an individual species (Langston, 1990; Markovic, 2003). All the trace elements in the bottom-sediment samples from this study also exceeded the respective TEL and PEL. According to USEPA (1998), these values are in the range where toxic effects can occur to benthic organisms.

These results suggest that heavy metal and hydrocarbon levels in the study area are at concentrations high enough to impair biological communities and are likely to cause toxicity levels that will lead to negative impacts on infaunal communities (Table 2) including *Leptocheirus* amphipods bivalves, neanthes worms, echinoderm and Oyster larvae (ADEC, 2011). According to Capuzzo (1985), retention of hydrocarbons in lipophilic cellular compartments may result in disruptions in membrane functions or alterations in energetic processes and impairment of an organism's adaptive capacity within its natural habitat. Capacity for metabolism of lipophilic compounds may influence the disposition or removal of aromatic hydrocarbons by marine organisms.

Relationships, spatial and temporal variations of contaminants in the sediments

Organic matter in the study area tended to have a negative relationship with both total hydrocarbon and heavy metal concentrations without showing much variation in both seasons. This is at variance with the findings of Jamil et al. (2014) and the reason for this difference may be a result of pH, salinity and grain size differences (Du Laing, 2009) which were not measured in this study. Heavy metal concentrations increased progressively in both upstream and downstream directions in the dry seasons but tilted downstream in the wet season. THC concentration characteristics in the sampled sites also revealed profound between site variations. This could be indicative of the irregular pattern in waste discharges and spills and the power of tidal influence in redistributing contaminants in the creek's ecosystem.

A correlation matrix can indicate associations and relationships among metals and their sedimentary environments (Table 2-4). High correlation coefficients between different metals in a matrix could mean that they

have common sources, mutual dependence and identical behaviour during transportation and probably deposition. The absence of strong correlations among metals on the other hand may be indicative that the concentrations of these metals are not controlled by a single factor, but may be a pointer to a combination of geochemical support phases and the effects of the mixed association and interactions among the metals (Veerasingam et al., 2012).

Table 2 Proximity Matrix of sampling sites for heavy metals

Correlation between vectors of values in the dry season						
	SSA	SSB	SSC	SSD	SSE	SSF
SSA	1					
SSB	.916	1				
SSC	.934	.985	1			
SSD	.863	.981	.985	1		
SSE	.973	.847	.864	.774	1	
SSF	.739	.493	.475	.343	.828	1
Correlation between vectors of values in wet season						
	SSA	SSB	SSC	SSD	SSE	SSF
SSA	1					
SSB	.923	1				
SSC	.938	.984	1			
SSD	.857	.967	.979	1		
SSE	.974	.858	.873	.776	1	
SSF	.754	.526	.504	.362	.837	1

Distances and similarities between sites were calculated using the Pearson correlation statistics. Results (Table 2) for heavy metals revealed a high level of similarity among sites, although site SSF (background) was least similar to SSB, SSC and SSD in both seasons. The reason for dissimilarities is obvious; however, the similarity between sites SSF (background) and site SSA (POI) is not readily explainable. It may be posited that the tidal nature of the environment may be redistributing contaminants within the marine environment. Results for TOC, THC and TPH (Fig. 3 and Table 3) also show a high level of similarity among sites.

Table 3 Proximity Matrix of sampling sites for TPH, THC and TOC

Correlation between vectors of values in the dry season						
	SSA	SSB	SSC	SSD	SSE	SSF
SSA	1					
SSB	.988	1				
SSC	1.000	.986	1			
SSD	1.000	.992	.999	1		
SSE	1.000	.986	1.000	.999	1	
SSF	.998	.996	.997	.999	.997	1
Correlation between vectors of values in wet season						
	SSA	SSB	SSC	SSD	SSE	SSF
SSA	1					
SSB	.987	1				
SSC	.999	.979	1			
SSD	.996	.997	.992	1		
SSE	.915	.968	.897	.946	1	
SSF	.996	.997	.990	1.000	.946	1

Since the above analysis did not show very distinct relationships, the data was subjected to further multivariate statistical analysis using the Pearson's correlation to test for relationship between contaminants. Results (Table 4) of this analysis (strong – medium correlations verged in red) however revealed very weak relationships among the contaminants; however, only copper and manganese; vanadium and THC; TPH and TOC had any form of significant strong relationship. Subjecting the data to further query by principal component analysis (PCA) using the varimax analysis with Kaiser Normalization rotation method (Table 5); three components were realized accounting for 80.56% of observed variation in the dataset. Principal component one (29.528%) has a strong relationship between TPH and TOC with a moderate association with zinc, cadmium and manganese. This factor is most likely an indication of pollution from uncooked crude oil spilled during transportation and pre-

cooking (refining) operations in the study area. The indicated petroliferous heavy metals have been identified (Marcus and Ekpete, 2014) as key components of crude oil from the part of the Niger Delta.

Factor two which accounts for 26.71% of variance indicates a strong affinity between vanadium and THC. Vanadium is a major constituent of nearly all coal and petroleum crude oils. The most prominent anthropogenic source of vanadium in the environment is the combustion of fossil fuels, particularly residual fuel oils, which also constitute the single largest overall release of vanadium to the atmosphere. While the levels of vanadium in residual fuel oil usually vary by source, concentrations of 1–1,400 ppm have been reported (ATSDR, 2012). The third factor loaded 24.322% and has affinity for copper, lead and nickel. While urban sewage contains substantial amounts of copper, nickel is ubiquitous in the environment while lead is the most abundant heavy metals occurring in nature. This may therefore indicate mobilisation from natural sources and long distance pollution drifted from upstream sources in the Port Harcourt-Elleme-Onne industrial axis located northwest of the study area.

Table 5 Rotated component matrix of variables

	Component		
	1	2	3
Cu	.042	-.082	.887
Zn	.645	-.461	.095
Mn	.506	.137	.656
Ni	-.311	.060	.908
V	.240	.938	.100
Cd	.613	-.391	-.127
Pb	.185	.612	.587
THC (x 0.001)	-.013	.957	-.040
TPH (x 0.001)	.921	.197	.085
TOC (%)	.931	.262	-.042
Extraction Method: Principal Component Analysis. Rotation Method: Varimax with Kaiser Normalization			

Table 4 Pearson's correlation matrix of contaminants

	Cu	Zn	Mn	Ni	V	Cd	Pb	THC (x 0.001)	TPH (x 0.001)	TOC (%)
Cu	1									
Zn	-.014	1								
Mn	.763**	.219	1							
Ni	.509*	.407	.398	1						
V	-.014	-.184	.070	.268	1					
Cd	.074	.229	-.233	.117	-.279	1				
Pb	.458	.592*	.450	.262	-.390	.168	1			
THC (x 0.001)	-.174	.395	.029	.063	.923**	-.372	.498*	1		
TPH (x 0.001)	.130	.459	-.191	.424	.415	.443	.167	.172	1	
TOC (%)	.038	.386	-.278	.448	.436	.531*	-.086	.190	.913**	1

** Correlation is significant at the 0.01 level (1-tailed)

* Correlation is significant at the 0.05 level (1-tailed)

Potential ecological risk of heavy metals in the sediments

Calculated contamination factors for the various metals are Cu: 0.652, Zn: 205.73, Mn: 560.34, Ni: 0.321, Cd: 472.5 and Pb: 3.28, while international toxicity factors for Cd: 30, Ni, Cu, Pb and Zn include 30, 5, 5, 5 and 1 respectively (Li et al., 2012) while toxicity values for Mn and V are not available. Therefore, the degree of contamination (C_D) for the Oturuba Creek system for the analyzed metals is 1,242.82.

Calculated Er^i for metals include 3.26, 205.73, 1.605, 14,175 and 16.4 for Cu, Zn, Ni, Cd and Pb respectively; giving a total value of 14,401.995, with Cd contributing more than 98% of ecological risks followed by Zn with 14.43%. Going by the recommendations of Håkanson (1980), the calculated Er^i for the study area is over 700% beyond the baseline for very high ecological risk metal concentrations. Li et al. (2012) in a study of heavy metal contamination in sediments from a coastal industrial basin in Northeast China concluded that the area "is one of the most polluted of the world's impacted coastal systems". However, evidence from this study shows worse but similar sediment quality situation. Therefore, the Oturuba Creek can be declared to be one of the most polluted coastal rivers in the world.

Index of geoaccumulation (I_{geo})

In order to assess the intensity of metal contamination in the sediments of the Oturuba Creek, the geochemical accumulation index was calculated as proposed by Singh et al. (2003) to quantify metal accumulation in the sediments, and represent their contamination degree. The I_{geo} classification entails seven grades (0 to 6) of pollution, ranging from no pollution (0) to very high pollution (Forstner, 1989).

Table 6 I_{geo} classes, range and sediment quality (Singh et al., 2003)

I_{geo} class	I_{geo} range	Sediment Quality
0	<0	Background concentrations
1	0-1	Unpolluted
2	1-2	Polluted to unpolluted
3	2-3	Moderately polluted
4	3-4	Moderately to Highly polluted
5	4-5	Highly polluted
6	>5	Very highly polluted

Calculation of the geochemical metal accumulation index for the Oturuba river system returned 269.4 for Cu, 2628 for Zn, 11.35 for Mn, 453.9 for Ni, 2.211 for Cd and 685.8 for Pb. This result therefore places metal concentrations in the study area in the range of very highly polluted sediment environment with only cadmium occurring in moderately polluted status (Table 6).

CONCLUSIONS

The Oturuba river system is a sink for wastes and spills from the artisanal refining, transportation and handling of probably stolen petroleum. These activities have led to el-

evated levels of heavy metals and hydrocarbon contaminants in sediments of the river. All the sampled sites in the creek had hydrocarbon concentrations that were above limits for total PAHs in terms of ERL, ERM, TEL, PEL, AET and the Dutch intervention values for the protection of ecosystems. However, only the POI (SSA) exceeded the Dutch maximum permissible concentrations (MPCs) for mineral oils in both season. The results of this study suggest that levels of hydrocarbons are at concentrations high enough to impair biological communities and are likely to cause toxicity levels that will lead to negative impacts on infaunal communities.

Also, all the trace elements in the bottom-sediment samples from this study (except vanadium) exceeded the respective TEL and/or PEL guideline values, which are range where toxic effects occur to benthic organisms (USEPA, 1998). Heavy metal geochemical accumulation index analysis also returned anomalously high metal concentrations in the range of very highly polluted sediment environment with only cadmium occurring in the moderately polluted status.

Heavy metal pollution in the Oturuba Creek has some variability from other river systems in the Niger Delta region. While concentrations of copper and nickel in the study area is similar to those found in the sediments of the Benin River, zinc, vanadium and lead concentrations were far above those found in the same river (Akporido and Ipeaiyeda, 2014) and in the Orogodo River in Agbor Delta State (Issa et al., 2011) all in the far northwestern flank of the Niger Delta. Metal concentrations from this study were also very much higher than those found in the Bonny River system around Okrika (Marcus et al., 2013) located not more than twenty kilometres northwest of the study area, while manganese concentrations in the Oturuba system were very much above those found in the sediments of the Taylor Creek system in Bayelsa Nigeria (Okafor and Opuene, 2007). These not only shows that the Oturuba Creek is heavily polluted but that heavy metal pollution of river sediments may be more related to local anthropogenic inputs than terrigenous sources.

Hydrocarbon concentrations found in the sediments of the Oturuba Creek were below figures found by Akporido and Ipeaiyeda (2014) in the sediments of the Benin River. Also, TPH concentrations found in this study were far above that found in the Qua Iboe River mangrove ecosystem (Benson and Essien, 2009). This may simply be related to the intensity of oil spill-causing activity in the study area.

The potential ecological risk factor (Er^i) for metals calculated for this study showed that Cd contributed more than 98% of ecological risks followed by Zn with 14.43%. Going by the recommendations of Håkanson (1980), the calculated Er^i for the study area is beyond the baseline for very high ecological risk metal concentrations, thereby ranking the Oturuba Creek as one of the most polluted coastal river ecosystems in the world; thereby not only endangering the ecosystem and threatening the livelihoods of the nearly one million people who live along the coastline and depend on the marine environment for sustenance but also the life of those who consume fish from these contaminated rivers. Urgent steps must therefore be taken to stop all illegal and artisanal refining activities in the Andoni River areas of Nigeria.

References

- ATSDR, 2012. Toxicological profile for Vanadium. Agency for Toxic Substances and Disease Registry. Atlanta, GA: U.S. Department of Health and Human Services, Public Health Service. <http://www.atsdr.cdc.gov/toxprofiles/tp58-c6.pdf>
- Akporido, S.O, Ipeaiyeda, A.R. 2014. An assessment of the oil and toxic heavy metal profiles of sediments of the Benin River adjacent to a lubricating oil producing factory, Delta State, Nigeria. *International Research Journal of Public and Environmental Health* 1 (2), 40–53.
- ADEC, 2011. Total Maximum Daily Loads (TMDLs) for petroleum hydrocarbons in the waters of Skagway harbor in skagway, Alaska. Alaska Department of Environmental Conservation, Anchorage, Alaska.
- ADEC, 2004. Sediment Quality Guidelines(SQG). (Technical Memorandum). Alaska Department of Environmental Conservation, Division of Spill Prevention and Response Contaminated Sites Remediation Program, Juneau, Alaska.
- Ansa, E.J, Sikoki, F.D, Francis, A., Allison M. E. 2007. Seasonal Variation in Interstitial Fluid Quality of the Andoni Flats, Niger Delta, Nigeria. *Journal of Appl. Sci. Environ. Manage* 11 (2), 123–127. DOI: 10.4314/jasem.v11i2.55008
- Ansa, E.J., Francis, A. 2007. Sediment Characteristics of the Andoni Flats, Niger Delta, Nigeria. *Journal of Appl. Sci. Environ. Manage* 11(3), 21 – 25. DOI: 10.4314/jasem.v11i3.55071
- APHA, 1998. Standard Methods for the Examination of Water and Wastewater 20th ed. American Public Health Association APHA-AWNA-WPCF. New York 1134 p.
- ASTM, 2003. Test method for oil in water analysis D 3921 – Annual Book of ASTM (American Standard of Testing Materials) Standards Vol. ASTM International U.S.A.
- Bay, S.M., Ritter, K.J, Vidal-Dorsch, D.E., Field, L.J. 2012. Comparison of national and regional sediment quality guidelines for classifying sediment toxicity in California. *Integr Environ Assess Manag* 8 (4), 597 – 609. DOI: 10.1002/ieam.1330.
- Benson N.U., Essien J.P. 2009. Petroleum Hydrocarbons Contamination of Sediments And Accumulation in Tympanotonus Fuscatus Var. Radula from the Qua Iboe Mangrove Ecosystem, Nigeria. *Current Science* 96 (2), 238–244.
- Bhutiani R., Kulkarni D.B., Khanna, D. R., Gautam, A. 2017. Geochemical distribution and environmental risk assessment of heavy metals in groundwater of an industrial area and its surroundings, Haridwar, India. *Energy, Ecology, Environment* 2(2), 155–167. DOI: 10.1007/s40974-016-0019-6
- Buchman, M.F. 2008. NOAA Screening Quick Reference Tables. NOAA OR&R Report 08-1. Seattle, WA Office of Response and Restoration Division, National Oceanic and Atmospheric Administration. 34 pp.
- Burton Jr., G.A. 2002. Sediment quality criteria in use around the world. *Limnology* 3, 65–75. DOI: 10.1007/s102010200008
- Cantillo, A., Calder, J. 1990. Reference materials for marine science. *Fresenius J. Anal. Chem.* 338, 380–382. DOI: 10.1007/bf00322498
- Capuzzo, J.M. 1985. Biological Effects of Petroleum Hydrocarbons on Marine Organisms: Integration of Experimental Results and Predictions of Impacts. *Marine Environmental Research* 17, 272–276. DOI: 10.1016/0141-1136(85)90104-7
- Du Laing G, Rinklebe J, Vandecasteele B, Meers E, and Tack F.M. 2009. Trace metal behaviour in estuarine and riverine floodplain soils and sediments: A review. *Science of the Total Environment* 407 (13), 3972–3985. DOI: 10.1016/j.scitotenv.2008.07.025
- Forstner, U. 1989. Contaminated sediments. In: Bhattacharji, S., Fridman, G. M., Neugebauer H. J. Seilacher A. (Eds.) Lecture notes in Earth Sciences, Springer-Verlag, Berlin 21, 1–157.
- Förstner, U., Salomons W. 1981. Trace metal analysis on polluted sediments. Part I: Assessment of Sources and Intensities. *Environmental Technology Letters* 1, 1–27. <http://edepot.wur.nl/214350>
- Håkanson L. 1980. An ecological risk index for aquatic pollution control: A sedimentological approach. *Water Research* 14, 975–1001. DOI: 10.1016/0043-1354(80)90143-8
- Håkanson L. 1988. Metal Monitoring in Coastal Environments. In: Seeliger, U., Lacerda, L.D, Patchineelam, S.R (Eds) Metals in Coastal Environments of Latin America. Springer-Verlag, 240–257. DOI: 10.1007/978-3-642-71483-2_21
- Howard C.I, Ugwumobong U.G, Horsfall M. 2009. Evaluation of Total hydrocarbon levels in some aquatic media in an oil polluted mangrove, wetland in the Niger Delta. *Applied Ecology and Environmental Research* 7 (2), 111–120. DOI: 10.15666/aeer/0702_111120
- IMO, 2000. Guidance on assessment of sediment quality. Global investigation of pollution in the marine environment (GIPME). International Maritime Organisation IOC-UNEP-IMO. London. Pub no. 439/00
- Issa, B.R, Arimoro, F.O, Ibrahim, M, Birma, G.H, Fadairo E.A. 2011. Assessment of Sediment Contamination by Heavy Metals in River Orogo, Agbor, Delta State, Nigeria. *Current World Environment* 6 (1), 29–38.
- Jamil, T., Lias, K., Hanif, H.F., Norsila, D., Aeisyah, A., Kamaruzzaman, B.Y. 2014. The spatial variability of heavy metals concentrations and sedimentary organic matter in estuary sediment of Sungai Perlis, Perlis, Malaysia. *Science Postprint* 1(1), e00016. DOI: 10.14340/spp.2014.02A0003
- Jiao, X., Teng, Y., Zhan, Y., Wu, J., Lin, X. 2015. Soil Heavy Metal Pollution and Risk Assessment in Shenyang Industrial District, Northeast China. *PLoS One* 10 (5), 1–9. <https://www.ncbi.nlm.nih.gov/pmc/articles/PMC4440741/>. DOI: 10.1371/journal.pone.0127736
- Langston, W. J. 1990. Toxic effects of metals and the incidence of metal pollution in marine ecosystems. In: Furness, R.W., Rainbow, P.S. (Eds.) Heavy metals in the marine environment. CRC Press. Boca Raton, FL. 256 pp.
- Li, X., Liu, L., He, X. 2012. Integrated Assessment of Heavy Metal Contamination in Sediments from a Coastal Industrial Basin, NE China. *PLoS One* 7(6), E39690. DOI: 10.1371/journal.pone.0039690
- Luoma, S.N. 1990. Processes affecting metal concentrations in estuarine and coastal marine sediments. In: Furness, R.W., Rainbow, P.S. (Eds.) Heavy metals in the marine environment. CRC Press. Boca Raton, FL. 256 pp.
- Luoma, S.N, Hornberger, M., Cain, D.J., Brown, C., Lee, B. 1997. Fate, Bioavailability And Effects Of Metals In Rivers And Estuaries: Role Of Sediments. Proceedings of the U.S. Geological Survey (Usgs) Sediment Workshop, February 4-7, 1997.
- Marcus, A.C, Okoye, C.O.B, Ibetu, C.N. 2013. Organic matter and trace metals levels in sediment of bonny river and creeks around Okrika in Rivers State, Nigeria. *International Journal of Physical Sciences* 8 (15), 652–656. DOI: 10.5897/ijps13001
- Marcus, A.C., Ekpete, O.A. 2014. Impact of Discharged Process Wastewater from an Oil Refinery on the Physicochemical Quality of a Receiving Waterbody in Rivers State, Nigeria. *IOSR Journal of Applied Chemistry* 7 (12), 1–8. DOI: 0.9790/5736-071210108
- Markovic, D.L. 2003. Untreated Municipal Sewage Discharge in Victoria Bight, British Columbia, Canada: An Investigation of Sediment Metal Contamination and Implications for Sustainable Development. M.Sc Thesis, Science, Technology & Environment Division. Royal Roads University, Canada.
- Mendelssohn, I.A, Andersen, G.A, Baltz, D.M, Caffey, R.H, Carman, A.R, Fleeger, J,W, Joye, S.B, Lin, Q, Maltby, E, Overturn, E.B., Rozas L.P. 2012. Oil Impacts on Coastal Wetlands: Implications for the Mississippi River Delta Ecosystem after the Deepwater Horizon Oil Spill. *BioScience* (62) 6, 562–576. DOI: 10.1525/bio.2012.62.6.7
- NOAA, 2008. Screening Quick References Tables. Office of Response & Restoration. National Oceanic & Atmospheric Administration.
- NSW EH, 2015. Soil survey standard test method. The New South Wales Office of Environment and Heritage, Online available at: <http://www.environment.nsw.gov.au/resources/soils/testmethods/oc.pdf>
- Okafor, E.C., Opuene, K. 2007. Preliminary assessment of trace metals and polycyclic aromatic hydrocarbons in the sediments. *International Journal of Environmental Science and Technology* 4(2), 233–240. DOI: 10.1007/BF03326279
- Pluske, W., Murphy, D., Sheppard, J. 2016. Total Organic Carbon. Soil Quality Factsheets. <http://www.soilquality.org.au/factsheets/organic-carbon>. Accessed 19th May, 2016.
- Rodrigues M.L.K., Formoso M.L.L. 2006. Geochemical Distribution of Selected Heavy Metals in Stream Sediments Affected by Tannery Activities. *Water, Air, and Soil Pollution* 169, 167–184. DOI: 10.1007/s11270-006-1925-6

- Schumacher, B.A. 2002. Methods for the Determination of Total Organic Carbon (TOC) in soils and sediments. United States Environmental Protection Agency, Environmental Sciences Division National, Exposure Research Laboratory, NCEA-C-1282, EMASC-001 April 2002
- Singh, M., Muller, G., Singh I.B. 2003. Geogenic distribution and baseline concentration of heavy metals in sediments of the Ganges River, India. *Journal of Geochemical Exploration* 80, 1–17. DOI: 10.1016/S0375-6742(03)00016-5
- Tiessen, H., Moir, J.O. 1993. Total and organic carbon. In: Carter M.E. (Ed.) *Soil Sampling and Methods of Analysis*. Lewis Publishers, Ann Arbor, MI. pp. 187–211.
- Ssentongo GW, Ukpe ET, Ajayi TO (1986). Marine fisheries resources of Nigeria: A review of exploited fish stocks. CECAF/ECAF/Se-ries, FAO, Rome, 86/40, pp: 56.
- USEPA, 1992. Sediment Classification Methods Compendium. U.S. Environmental Protection Agency, Sediment Oversight Technical Committee. Office of Water (WH-556). EPA 823-R-92-006. Washington, DC
- USEPA, 1998. The Incidence and Severity of Sediment Contamination in Surface Waters of the United States, Volume 1--National Sediment Survey: U.S. Environmental Protection Agency Report 823-R-97-006, Various Pagination
- USEPA, 1999. Understanding Oil Spills And Oil Spill Response. Office of Emergency and Remedial Response. www7.nau.edu/.../Oil-Spill/EPAUnderstandingOilSpillsAndOilSpillResponse1999.pdf
- USEPA, 2005. Predicting Toxicity to Amphipods from Sediment Chemistry. EPA/600/R-04/030. United States Environmental Protection Agency/ORD National Center for Environmental Assessment Washington, DC
- Veerasingam, S., Venkatachalapathy, R., Ramkumar, T. 2012. Heavy Metals and Ecological Risk Assessment in Marine Sediments of Chennai, India. *Carpethian Journal of Earth and Environmental Sciences* 7(2), 111–124.
- Verbruggen E.M.J. 2004. Environmental Risk Limits for Mineral Oil (Total Petroleum Hydrocarbons). RIVM report 601501021/2004. National Institute for Public Health and the Environment, Bilthoven, the Netherlands.
- Walkley, A., Black, I.A. 1934. An examination of the Degtjareff method for determining organic carbon in soils: Effect of variations in digestion conditions and of inorganic soil constituents. *Soil Sci.* 63, 251–263.
- Whitehead, A. 2013. Interactions between Oil-Spill Pollutants and Natural Stressors Can Compound Ecotoxicological Effects. *Integrative and Comparative Biology* 53(4): 635–647. DOI: 10.1093/icb/ict080.



IMPACTS OF STONE MINING AND CRUSHING ON STREAM CHARACTERS AND VEGETATION HEALTH OF DWARKA RIVER BASIN OF JHARKHAND AND WEST BENGAL, EASTERN INDIA

Swades Pal¹, Indrajit Mandal^{1*}

¹Department of Geography, University of Gour Banga, Malda 732103, West Bengal, India

*Corresponding author, e-mail: indrajitgeofarakka@gmail.com

Research article, received 13 January 2017, accepted 25 May 2017

Abstract

Dwarka River basin (3882.71 km²) of Eastern India in the Chotonagpur Plateau and Gangetic Plain is highly affected by stone mining and crushing generated dust. In the middle catchment of this basin, there are 239 stone mines and 982 stone crushing units. These produce approximately 258120 tons of dust every year and this dust enters into the river and coats the leaves of plants. On the one hand, this is aggrading in the stream bed, increasing sediment load, decreasing water quality, specifically increasing total dissolved solid, pH, water colour, and it also degrades the vegetation quality. Vegetation quality is also degraded as indicated by decreasing of NDVI values (maximum NDVI in 1990 was 0.70 and in 2016 it was 0.48). Considering all these issues, the present paper intends to identify dust vulnerable zones based on six major driving parameters and the impact of the dust on river morphology, water quality and vegetation quality in different vulnerable zones. Weighted linear combination method (in Arc Gis environment) is used for compositing the selected parameters and deriving vulnerable zones. Weight to the each parameter is assigned based on analytic hierarchy process, a semi quantitative method. According to the results, 579.64 km² (14.93%) of the catchment area is very highly vulnerable: Here 581 rivers have a length of 713 km and these rivers are prone to high dust deposition, increased sediment load and water quality deterioration.

Keywords: Dwarka river basin, stone mining, stone crushing, river bed aggradations, sediment load, water quality, vegetation health

INTRODUCTION

Stone crushing industry is an important industrial sector engaged in producing crushed stone of various sizes depending upon the requirement which acts as raw material for various construction activities such as construction of roads, highways, bridges, buildings, and canals etc. It is counted that there are over 12,000 stone crusher units in India (Patil, 2001). In India, the stone crushing industry sector is estimated to have an annual turnover of >US\$ 1 billion and 500,000 principally unskilled or semi skilled rural people engaged in this sector (CPCB, 2009). These stone crushers though socio-economically an important sector, give rise to substantial quantity of fine fugitive dust emissions which create health hazards to the workers as well as surrounding population by causing respiratory diseases.

The dust is generated primarily due to size reduction and handling of the stones at various stages. The major sources of dust generation are the size reductions in the primary, secondary and tertiary crushers. In different stages the amount of dust production varies. The Central Pollution Control Board (CPCB, 2009) reported the proportion of dust contribution at different stages of crushing (see Table 1). The fine-grained dust production depends on the type of the crusher and the parent rock. Primary crushers produce 1- 10% of fines, secondary crushers produce 5 – 25% fines, and tertiary crusher produce 5 – 30% fines. Similarly limestone contains 20–25% of fines; sandstone contains 35–40% fines, whilst igneous and

metamorphic rocks contain 10–30% fines (Mitchell 2009). Blatt and Tracy (1997) analyzed the composition of stone dust emitting from a stone crusher unit. They documented that the chemical composition was SiO₂-72.04%; Al₂O₃-14.42%; K₂O-4.12%; Na₂O- 3.69%; CaO-1.82%; FeO₃-1.22%; MgO-0.71%; TiO₂-0.30%; P₂O₅-0.12% and MnO₂-0.05%. This proportion varies according to composition of the rock from which crushing is done. Average dust contamination level in the atmosphere is 0.10 mg/m³ in USA (Moran et al., 1994; Tucker et al., 1995, IARC,1997; US EPA, 1996). The actual area of the source of the dust generation is quite small (about 0.5- 1 m²) at each source, but as the dust rises it spreads and typically the area in which it spreads is more than 10 to 15 times larger (CPCB, 2009) than the area of actual emission at about 3 to 8 m height. Mining must be planned so that after the mining process the dumped land can be reclaimed by vegetation and agriculture.

The problems of waste rock dumps become devastating to the landscape around mining areas (Goretti, 1998; Sarma, 2005). The dust adversely affects visibility, reduces growth of vegetation, agricultural crops and hampers aesthetics of the area as well as river system (CPCB, 2009). Sharma and Kumar (2016) pointed out that dust deposition on agricultural field reduces productivity of rice and carbohydrate content within the rice grain. Such dust is one of the most visible, invasive, and potentially irritating impacts associated with quarrying, and its visibility often raises concerns that are not directly proportional to its impact on human health and

the environment (Howard and Cameron, 1998). It has noteworthy impact on landscape and biological communities of the Earth (Down, 1997; Bell et al., 2001) and leads to ecosystem disturbance. Natural plant communities get disturbed and the habitats become impoverished due to mining, presenting a very rigorous condition for plant growth (Shivacoumar et al., 2006; Mishra and Kumari, 2008). The unscientific mining of minerals poses a serious threat to the environment, resulting in the reduction of forest cover, erosion of soil in a great scale, pollution of air, water and land and reduction in biodiversity (Pandey and Pandey, 2010; Prasad et al., 2010; Saha and Padhy, 2011; UNESCO, 1998). Most of the plants experience physiological alterations before morphological injury symptoms become visible on their leaves (Liu and Ding, 2008). Rai et al. (2010) reveals that the foliar surface was an excellent receptor of atmospheric pollutants leading to a number of structural and functional changes. Increasing dust concentration in atmosphere will raise the temperature state of the environment and hamper the ambient ecological condition (Ziaul and Pal, 2016). Site conditions that affect the impact of dust generated during extraction of aggregate and dimension stone include rock properties, moisture, ambient air quality, air currents and prevailing winds, the size of the operation, proximity to population centres, and other nearby sources of dust (Bell et al., 1977). Drainage direction and volume both channelized or unchannelized form is also an important vector for spreading these effects in its surrounding. Degree of drainage slope controls the dispersal rate of sediment and dust from the place of origin and pools and riffle condition, variability of discharge regulate persistence of materials within the channel or swiping off the same (Sipos et al., 2014; Nagy and Kiss, 2016). Dust concentrations, deposition rates, and potential impacts tend to decrease rapidly away from the source (Howard and Cameron, 1998).

Table 1 Particulate emission factors for stone-processing operations. Source: Pollution Data Division of Environment Canada (2008)

Sources	Emission factors kg/10000kg production		
	Total Particulate Matter(TPM)	PM ₁₀	PM _{2.5}
Drilling	0.000 800	0.000 040	0.000 002
Primary crushing	0.005 800	0.000 290	0.000 017
Secondary crushing	0.001 208	0.000 290	0.000 017
Tertiary crushing	0.001 208	0.000 290	0.000 017
Screening	0.004 286	0.000 420	0.000 124
Conveying and handling	0.007 327	0.000 720	0.000 213

Most of the previous studies mainly concentrated on impact of mining and crushing dust on vegetation and human health (Pyatt and Haywood, 1989; John and Iqbal, 1992; Grewal et al., 2001; Prajapati and Tripathi, 2008; Rai et al., 2010; Saha and Padhy, 2011; Sharma and Kumar, 2016). But the present study intends to find out

the impact of stone mines and stone crushing units on surrounding rivers specifically in terms of stone dust deposition within stream bed and water quality of the river. This study also aimed to find out the vulnerable zones to stone dust considering the fact that the region nearer to the stone mines and crushing units are more vulnerable to dust. Although the dimension of contamination is multi furious like effect on human health, agricultural production, water quality, stream morphology etc. but concentration mainly is given on to the stream morphology, water quality and vegetation health in the dust affected areas. Figure 1(A-D) shows the logic behind setting such objective.



Fig. 1 Field evidences highlights the problems of stone dust (A) crushing of stone and admixing dust in the atmosphere (B) draining of heaped up dust to the river (C) deposition of dust in the channel bed and banks (D) thick dust layer to the tree leaves

STUDY AREA

The Dwarka River is a tributary of Mayurakshi River. Originating at Kushpahari of Santhal Parganas in Jharkhand it has been flowing through eastern Chotonagpur plateau fringe area of Jharkhand and West Bengal, ultimately it joins the Dwarka Babla river near Hizole wetland (88°4'12.93"E; 24°4'42.27"N) in Murshidabad flood plain of West Bengal (Fig. 2). This basin area is covering an area of 3882.71 km² with along its 156.54 km. long main channel and some major tributaries like Brhamni, Bamni, Gambhira, Borkunda, Ghagar etc. It comprises a small portion of Chotonagpur plateau fringe (Santhal Pargana Upland) at its upper course (40% of the total basin area) and Rarh plain (Birbhum Rarh); Moribund deltaic West Bengal (Murshidabad Plain) in the lower course. It lies to the north of river Mayurakshi and to the south of river Bansloi. Two major faults lines namely Rajmahal fault line (RFL) and Gaibandha fault line (GFL) and one normal faults line are existing within the south west to north-west part of the basin. There are two seismic points situated one at upper (Sismicity Hypocentral Depth 25-70 km) and another is at the lower catchment (Sismicity Hypocentral depth more or less 25 km) of the Dwarka river basin (Fig. 3).

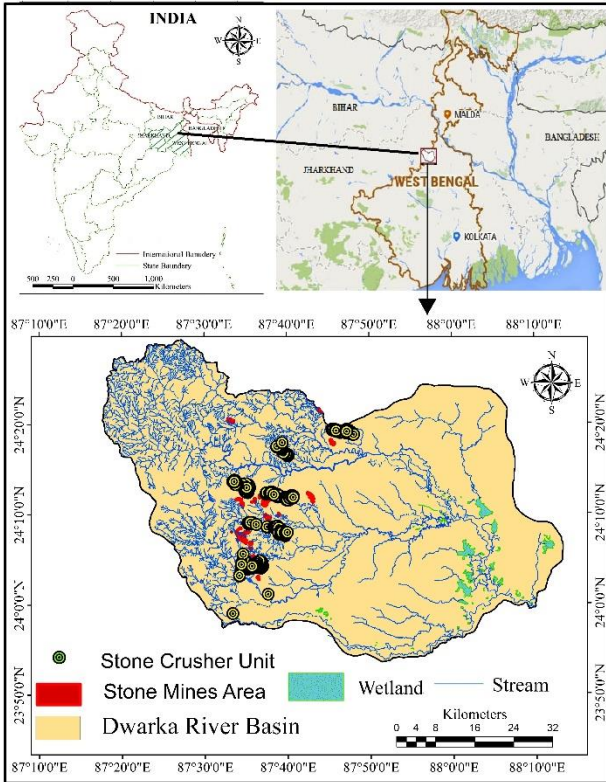


Fig. 2 Location of the studied Dwarka River basin showing the drainage, stone mines and crushing sites

Geologically the upper part of the basin dates back to the deposition of Dharwanian sedimentary followed by Hercinian orogeny from Cambrian to Silurian period. The extreme eastern part of the upper basin is characterized by unclassified granitic gneiss with enclaves of metamorphic geomaterials. The middle catchment is mostly characterized by the deposition of Lateritic soil and hard clays impregnated with Caliche nodules. The platform of this region was set through the tectonic activities associated with tertiary epoch. The lower catchment is mostly characterized by recent alluvial deposition of alternative layers of sand, silt and clay attributed by alleviation river diversion, flooding and consequent shaping by twin action of Bramhani (main tributary of Dwarka) and Dwarka River. The upper basin area of undulating well drained tract of Chotonagpur fringe have fragile coarse lateritic soil containing siliceous matter, karoline, magnesium and iron oxide and sandy gravelly soil or gravelly soil with proxi-

mate rich pegmatite rock (Let, 2012). Elevation of the basin ranges from 14m to 497m, out of total basin area, 58.88% area lies below 76m asl Maximum slope of this river basin is 5.76° in the isolated hillocks of upper and upper middle catchments of the basin. Almost flat surface is found in the Murshidabad plan region where drainage deranging is observed. Total 2552 river units were identified with 3297.49 km length with seven orders hierarchy (Strahler, 1964). Distribution of stream frequency in different orders and their respective lengths is shown in Table 2. Average stream frequency and density are respectively 0.710 nos./km² and 7.15 km./km²

Administratively, the study region includes Pakur and Dumka Districts of Jharkhand and Birbhum and Murshidabad Districts of West Bengal. There are 16 CD Blocks (Kandi, Khargram, Berhampore, Nabagram of Murshidabad and Nalhati, Rampurhat, Mahammadbazar, Muyureshwar of Birbhum), 3 urban centres (Rampurhat, Nalhati, Kandi) within the study area. Among these Pakur, Mhammadbazar region is rich with stone mining and crushing of stone. At present 239 numbers of stone mining units covering an area of 7.62 km² are found at the middle catchment of the basin with 982 number of stone crusher units (Fig. 2). Most of the stone mining and stone crushing units are found at 40-110 m (asl) elevation in the plateau fringe area.

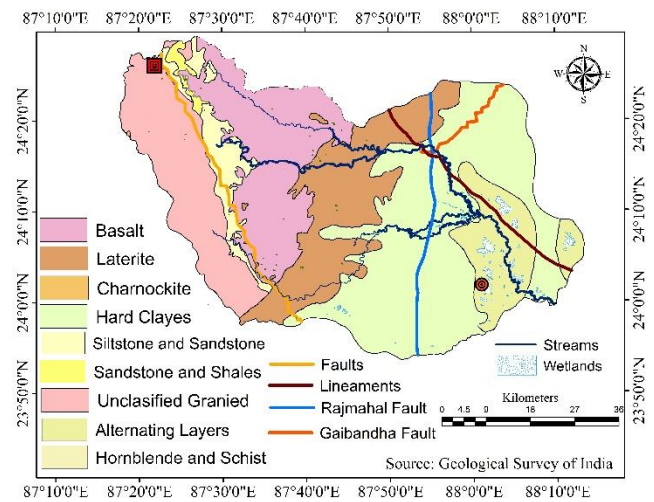


Fig.3 Geological map of the studied catchment

These soils are quite acidic, deficient in organic matter, poorly aggregated and possess low water holding capa-

Table 2 Order-wise number & length of the streams and some other morphometric aspect. Method followed for calculating morphometric properties: stream order after Strahler (1964), bifurcation ratio after Schumm (1956), mean bifurcation ratio after Strahler (1957), stream frequency after Horton (1932) and drainage texture after Horton (1945)

Stream Order	Number of Stream	Total Length (km)	Bifurcation Ratio	Mean Bifurcation Ratio	Stream Frequency (Df/km ²)	Drainage Texture
First	2058	1521.65		3.998	0.710	7.15
Second	349	638.18	5.896			
Third	115	468.55	3.034			
Fourth	22	207.56	5.227			
Fifth	4	111.59	5.500			
Sixth	3	272.83	1.333			
Seventh	1	77.12	3			
Total	2552	3297.49				

city. Transported secondary laterites and lateritic alluvium soils are found at the middle part of the basin (Chakraborty, 1970). These lateritic regolith is carried out by the main river and tributary system (Jha, 1997; Jha and Kapat, 2003; Jha and Kapat, 2009). These lateritic material Fine silty alluvium soil is found at the lower catchment of the basin. The average rainfall is 1500-1600mm Out of which 80% occurs during monsoon season (June to October). Volume of runoff is also maximum in this time. Bank full rivers found in this time. But upstream parts and streams of the upper catchment do not continue as bank full state even during peak monsoon time. Rest periods of a year shows almost dry rivers in the upper catchment of a basin. Wind direction highly varies seasonally. Out of 365 days in a year 123 to 162 days wind comes from southern and south western directions, 53 to 71 days wind comes from north eastern direction, 31-52 days wind comes from eastern and south eastern direction.

MATERIALS AND METHODS

Method for Evaluating Vulnerability

At first, six parameters have been taken into account as stated below for finding out stone dust vulnerability zones namely (1) stone crusher site (Scd); (2) stone mines site (Smd); (3) land use/land cover (Luc) (4) vegetation health (Ndvi); (5) surface slope (Sa); (6) surface runoff (Sro) Stone mining and crusher units have been identified from Google Earth satellite imageries and GPS survey where necessary. These are also identified from topographic sheets of Survey of India (SOI, 1972). These two layers are prime because the adjacent areas will be highly affected with stone dust (Down and Stocks, 1997; Howard and Cameron, 1998; Bell et al., 2001; CPCB, 2009) and its effects will decrease away from these sites (Bell et al., 1977). Vegetation health was identified from Landsat 8 (OLI) satellite imageries (path/row 139/43; spatial resolution 30m.; date of acquisition 12th january 2016) using NDVI technique of Rouse et al. (1973) (see Equation 1). NDVI of all three phases is calculated for the month of januray. NDVI value indicating vegetation usually varies from 0-1. 1 indicates good quality canopy density. Vegetation presence with greater density resists free spreading of dust from source points (Howard and Cameron, 1998; CPCB, 2009). Land use types surrounding the stone mine and crushing centres is a prime factor of stone dust vulnerability. Presence of human habitat, agricultural land and quality water bodies will up heave the degree of vulnerability (UNESCO, 1998; CPCB, 2009). Size of the stone mine area and size of crusher unit can exert multiplier effects on environment. It is true that if size of these units increase, volume of dust production soars up. Average surface slope is another important factor for draining subsided dusts through overland or channel flow. It is calculated from data received from Shuttle Radar Topographic Mission (SRTM) Digital Elevation Model (DEM) of United States Geological Survey (USGS) following the method of Wentworth (1930). United States Department of Agriculture (USDA, 1986) developed Natural Resources Conservation Service (NRCS) method

for estimating runoff and developed equation for it (Eq. 2), where, Q is actual surface runoff in mm, P is rainfall in mm., I_a is $0.4S/0.3S/0.2S/0.1S$ (season and climatic region specific) initial abstraction (mm) or losses of water before runoff begins by soil and vegetation (such as infiltration, orrainfallinterception by vegetation), $0.3S$ is usually used for wet, $0.1S$ is used for dry seasons based on the pattern of ppt. and evaporation ratio. S is the potential maximum retention. S can be calculated using Equation 3. For further details of this methods one can consult USDA (1986).

$$NDVI = \frac{(IR\ band - R\ band)}{(IR\ band + R\ band)} \quad (Eq.1)$$

$$Q = \frac{(P - I_a)^2}{P - I_a + S} \quad (Eq. 2)$$

$$S = \frac{25400}{CN} - 254 \quad (Eq. 3)$$

Scaling of the data layers

Scaling of data layers within their sub layers according to the magnitude of the sub classes and their influences toward the objective have been done using spatial analyst extension of Arc GIS environment, according to a 10 point scale. Natural break method is assigned for reclass of the individual layers. One example can be illustrated regarding distribution of scale to the parameter. Suppose stone crusher site is one of the parameters for measuring vulnerability of stone dust. This particular parameter is subdivided into 10 sub classes (distance classed) based on the proximity of crusher site. Ten rank is given to the sub class very adjacent to the crusher units and descends toward outside distance considering the fact that area nearer to crushing site will be affected intensively. If any parameter controls such stone dust vulnerability in reverse direction (higher magnitude of sub class value indicates less influence to the vulnerability), 10 rank should be provided to the low sub class value (Khatun and Pal, 2016). Such ranking helps all the data layers to be unidirectional. The influencing direction and scale consideration of the parameters has been shown in the table below (Table 5).

Assignment of Weight to the Parameters

The selected parameters applied in this study have not equal control on stone dust vulnerability. Here, a specific weight is distributed to all parameters following the Analytic Hierarchy Process (AHP) (Saaty, 1980), a semi quantitative method for weight assignment (Palaka and Jai Sankar, 2015). The AHP is a method to derive ratio scales from paired comparisons. The input can be obtained from subjective opinion such as satisfaction, feelings and preference. AHP allows some small inconsistency in judgment because humans are not always consistent (Saaty, 1980). The ratio scales are derived from the principal

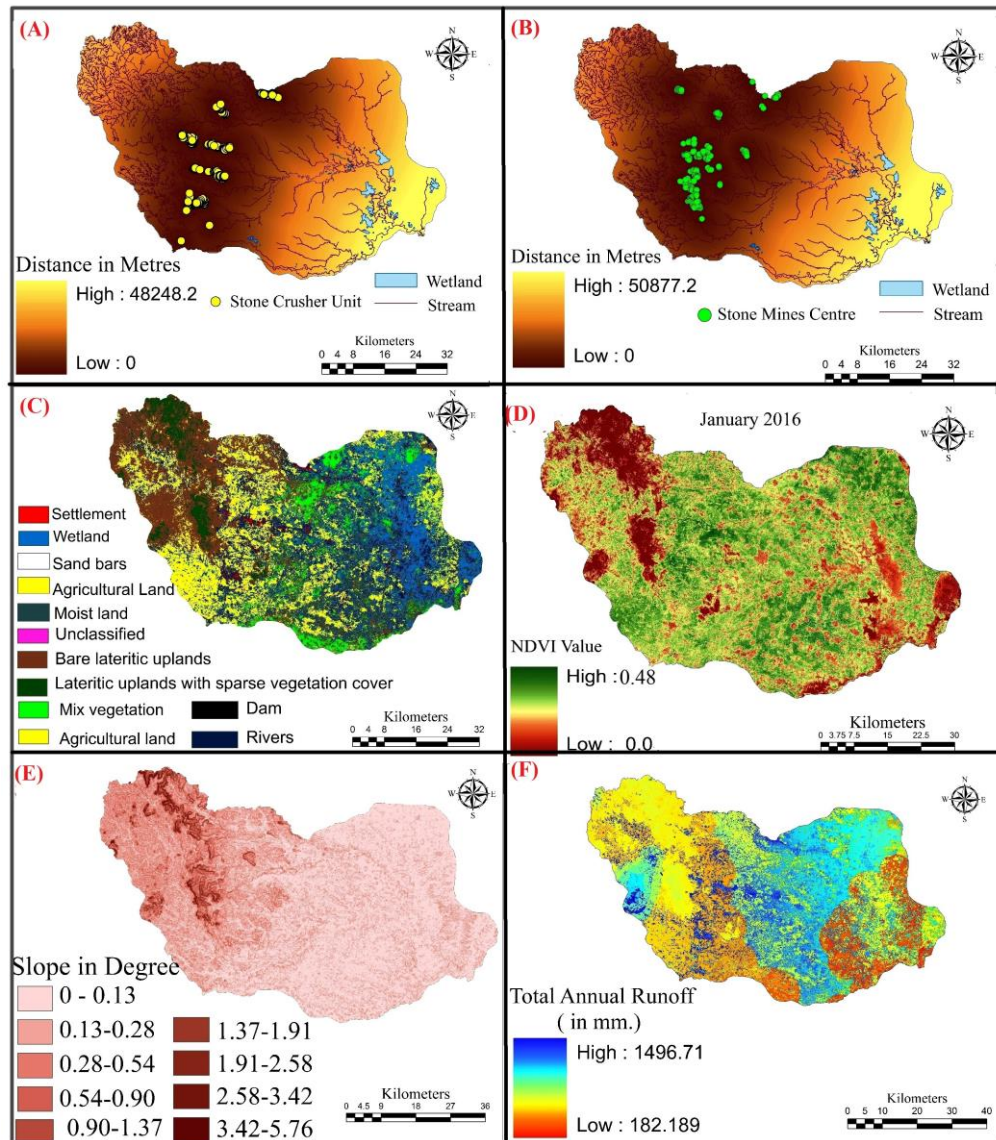


Fig.4 Selected parameters as spatial data layers used for evaluating vulnerability to stone dust (A) Distance map from stone crusher (B) Distance map from stone mines (C) Land use/land cover (LULC) (D) NDVI map (E) Surface slope (F) Surface runoff

Eigen vectors and the consistency index is derived from the principal Eigen value. The relative importance values are determined with Saaty's 1–9 scale (Table 3), where a score of 1 represents equal importance between the two themes, and a score of 9 indicates the extreme importance of one theme compared to the other one (Saaty, 1980). A matrix has been done for comparing the classes in order to achieve the priority. A pair wise comparison matrix is derived using Saaty's nine-point importance scale based on thematic layers used for zoning up the soil erosion susceptibility. Because six parameters were applied in the study, the matrix has 6 X 6 cells (Table 4). The diagonal elements of the matrix are always 1 and therefore it only needed to fill up the upper triangular matrix. Based on the judgment value by comparing one thematic layer with other upper triangle matrix is filled. To fill the lower triangular matrix, only reciprocal values of the upper diagonal are calculated. If a_{ij} is the element of row i column j of the matrix, then the lower diagonal is filled using this formula: a_{ij}

$= 1/a_{ji}$. After the completion of the comparison matrix as weights for the selected parameters have received with 4 % check consistency level.. Here maximum weight is found at stone crushing site (0.408) data layer followed by stone mine site (0.234) (Table 5).

Compositing of Parameters

After assigning weight to the parameters, scaling of the parameters, Weighted Linear Combination (WLC) method of Eastman (2006) was used for compositing all the selected parameters and deriving vulnerability map using spatial analyst tool in ArcGIS environment. This function can be presented using the following formula.

$$WLC = \sum_{j=1}^n a_{ij} w_j \tag{Eq. 4}$$

Where, a_{ij} = i^{th} rank of j^{th} attribute; w_j = weightage of j^{th} attribute.

Table 3 Saaty's 1-9 scale of relative importance (Saaty, 1980)

Scale	1	2	3	4	5	6	7	8	9
Importance	Equal	Weak	Moderate	Moderate	Strong	Strong Plus	Very Strong	Very, Very Strong	Extreme

Table 4 Pair wise comparison matrix for the applied parameters

	Stone Crusher Site	Stone Mines Site	Land Use Land Cover (LULC)	Vegetation Health	Surface Slope	Surface Runoff
Stone Crusher Site	1	2	3	4	5	6
Stone Mines Site	1/2	1	2	3	4	5
Land Use Land Cover (LULC)	1/3	1/2	1	2	3	4
Vegetation Health	1/4	1/3	1/2	1	2	3
Surface Slope	1/5	1/4	1/3	1/2	1	2
Surface Runoff	1/6	1/5	1/4	1/3	1/2	1

Table 5 Modes of ranking of the intra sub class of parameters and distribution of priority based weightage

Parameters	Sub-class	Rank (Highest rank: 10)	Weight of parameters
Stone Crusher Site (Distance from crusher sites)	natural breaks	1-10	0.408
Stone Mines Site (Distance from stone mines centre)	natural breaks	1-10	0.234
Land Use/Land Cover (LULC)	Healthy Vegetation	1	0.144
	Unhealthy Vegetation	2	
	Mix Vegetation	3	
	Lateritic upland	4	
	Moist land	5	
	Water body	6	
	Settlement area	7	
	Bare Land	8	
	Agricultural Field	9	
Open Field	10		
Vegetation Health	natural breaks	1-10	0.095
Surface Slope	natural breaks	1-10	0.067
Surface Runoff	natural breaks	1-10	0.051

This weighted linear combination has been done using raster calculator tool in Arc GIS environment. Asproth et al. (1999), Jiang and Eastman (2000); Mendes and Motizuki (2001); Araujo and Macedo (2002); Rinner and Malczewski (2002); Malczewski et al. (2003); Makropoulos and Butler (2005) are some of the successful users of WLC mainly for land use suitability.

Based on compositing of the raster layers vulnerability model is generated. Equation 3 represents the WLC equation of the selected six parameters. $Sdv_{wlc} =$ Stone dust vulnerability on the basis of weighted linear combination:

$$Sdv_{wlc} = (Scd * 0.408) + (Smd * 0.234) + (Luc * 0.144) + (Ndvi * 0.095) + (Sa * 0.067) + (Sro * 0.051) - (Eq. 4).$$

Methods for Measuring Stream Bed Aggradations

From four different vulnerable zones, 81 sample tributaries have been taken into account and the sample distribution in different areal extent of vulnerable zones have been done following the rule of stratified random sampling. In all cases, the entire length of stream is not lying within a single zone. From each stream segment in respective zone, at least 5 cross sections have been carried out using dumpy level for understanding the channel bed aggradations. Most of the rivers in this region is composed with bed rock and stone duct loosely deposited over the bed. Therefore, while doing cross section, cross section over the bed rock and over the deposited dust surface have taken. Gap between two cross section is majorly stone dust in most of the stream segments. Along downstream course from the stone mining and crushing centres, mixing of stone dust and other sediments from other sources has become so complex and difficult to segregate only the volume of stone dust. Zone wise average aggradations have been calculated for understanding the spatial variation.

Methods for Measuring Water Quality

Stratified random sampling is carried out as done earlier from different vulnerable zones. Altogether 81 samples we have collected within 1st to 15th July, 2016. Total dissolved soild (TDS), pH, water colour have measured from laboratory testing of the sample. A Tested results have been compared with BIS (10500) Standards of Inland Surface Water (1991) both for measuring drinkability and irrigability.

Methods for Detecting Vegetation Quality Change

According to Nayar (1985), leaf area is the main component of tree canopies and the leaf area index gives quantitative data of the depth of canopies. Forest canopies constitute the bulk of photo synthetically active foliage and biomass in forest ecosystems (Lowman and Wittman, 1996). Therefore, any fluctuation in chlorophyll, carbohydrate or protein content of foliar tissues of dominant tree species of a forest can be treated as disturbances in

overall growth of forest biomass. For detecting vegetation quality change, normalized difference vegetation index (NDVI) of Rouse et al. (1973) is used for 1990, 2011 and 2016 from the Landsat satellite imageries of the respective periods. Three images representing different seasons (pre monsoon, post monsoon and winter) are taken into account for showing the average range of NDVI value. Separately, season specific NDVI images are calculated for each season of the respective years and then average is carried out for showing yearly state. For 1990, Landsat TM (resolution: 30m.; Date of acquisition-05th january 1990) and for 2011 and 2016 Landsat OLI (spatial resolution: 30m.; Date of acquisition respectively 11th january 2011 and 12th January 2016 images have been taken. Usually NDVI value 0-1 indicates vegetation; value nearer to 1 depicts high quality vegetation or good canopy density.

RESULTS AND DISCUSSION

Based on weighted linear combination of the concerned parameters, vulnerability model has been prepared. WLC value ranges from 1.39-9.01 for entire basin. But it is assumed that effects of stone dust do not extend after a certain distance from the emitting units. Therefore, instead of considering entire range of WLC value, only higher range of WLC value is considered (>5) and classified this range into four categories. It is found that out of total basin area altogether 579.64 km². (14.93%) belongs to very high vulnerable categories and the high vulnerable category covers 09.06 of the catchment area. The first zone is highly affected by stone dust. Streams of this region receive huge volume of dust both in form of aerosols and dust with drainage. Number and length of the rivers under different vulnerable zones have been counted and measured thereafter. From this approach it is found that 581 river channels are situated in the very highly stone dust vulnerable zones carrying 713km length, 331 river channel segments are found in the highly vulnerable zone with the length of 496km; 198 river channels (323km) are situated on the moderately vulnerable zone and 113 stream channels covering a length 228 km is found in the low vulnerable zone.

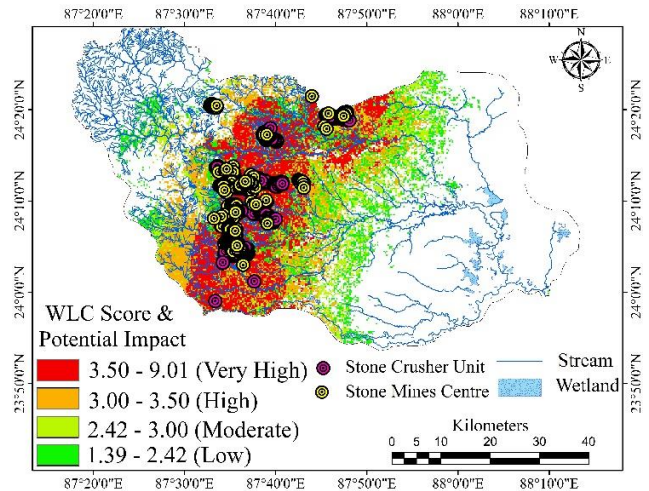


Fig. 5 Vulnerable zones and affected streams

Table 6 Potential impact classes of stone dust and their respective area, stream association

Potential Impact	Pixel Count	Area (km ²)	Area (%)	No. of Streams	Stream Length (km)
3.50-9.01	8240	579.64	14.93	581	713
3.00-3.50	4998	351.77	09.06	331	496
2.42-3.00	4732	332.74	08.57	198	323
1.39-2.42	5854	411.95	10.61	113	228

Impacts of Stone Dusts on Channel Bed Aggradations and Sediment Load

This field measurement in the one hand helps a lot to understand the impacts of stone dust and on the other hand it also introspects that how far the vulnerability model is valid. It is assumed that if rate of channel bed aggradations is very high and water quality is transformed substantially validity of the model inferred. For successful completion of this work during field study 81 tributaries have been selected on the basis of stratified random sampling

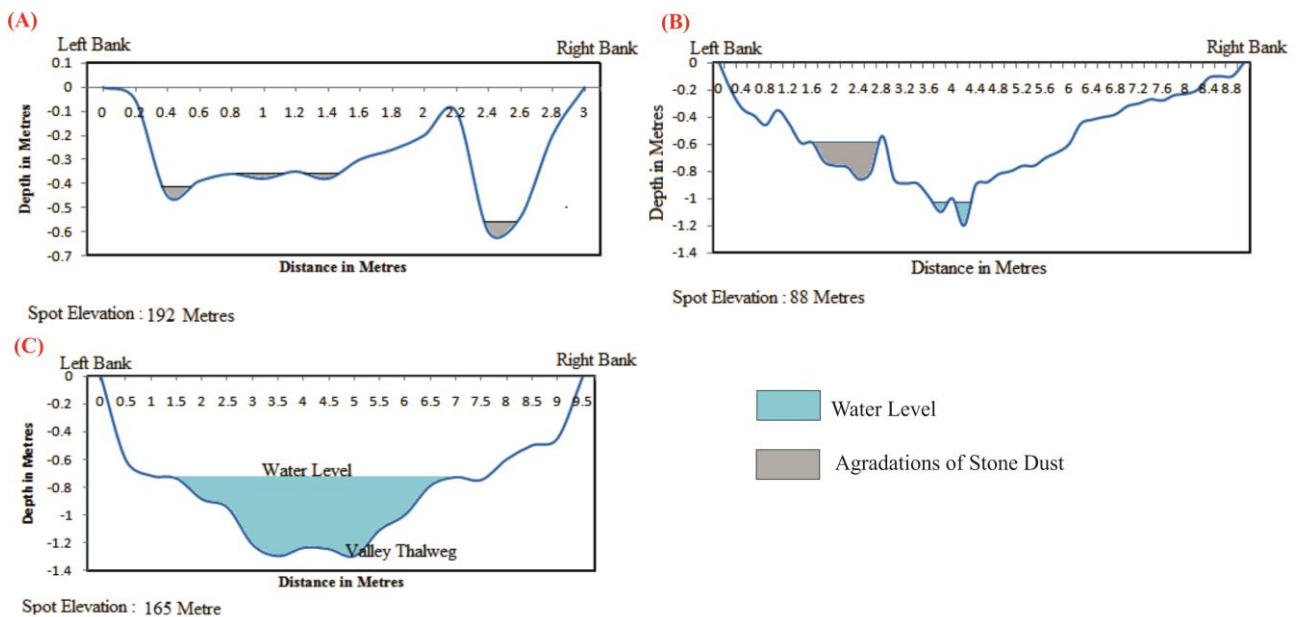


Fig.6 River cross profile and stone dust deposition in (A) very high (B) high and (C) low vulnerable zones

from different vulnerability classes. Twenty tributaries have been selected from very high vulnerable zone, 25 from highly, 20 from moderately and 16 from lowly vulnerable stone dust affected zones. From each stream at least 5 cross sections have been drawn to know the average situation of stream bed aggradations due to dust. In the very high vulnerable zone, depth of dust deposition ranges from 0.09 to 0.20 metre and average depth of dust deposition 0.125m. Range of depth of dust deposition on river bed in the highly vulnerable zone is 0.09 to 0.19 metre with an average of 0.096m. Average depth of dust deposition on rivers within moderately and low vulnerable zones is 0.083 and 0.061 metres respectively (Table 8). It is to be mentioned that channel segments away from crushing unit truly show only dust. But it is clear that dust decreased away from the emitting units.

Impacts on Stream Load Characters

Most of the streams are over loaded with huge amount of dust especially those are located at very proximate region of mining and stone crushing centres. Due to such conditions, thick dust is deposited over the channel bed. During monsoon time carrying capacity of the streams increases, thus they carry the loose materials. Suspended load increases due to stone dust during early monsoon (June and July) because deposited dusts over surface drains to the river during initial period of over land flow and admixture with tributaries. Suspended and bed load varies directly downstream from stone mine and crushing units. Average suspended load is 15762g/m³ during monsoon time in the very high vulnerable zone, followed by 12456 g/m³ in the highly vulnerable zone. In the low vulnerable zone, it is recorded that average load volume is 6782g/m³. which is low enough and in this area maximum proportion of it is contributed by eroded soil not by the dust. This information also supports the vulnerability models. Studies also recorded that this volume of load decreases downstream with varying rate depending on the dust product ability of the mining and crushing centres, discharge volume of the rivers where these are in fluxed, slope of the region, nature of wind. Here it should be mentioned that effect of this dusts exerts down slope. So the vulnerability zones indicated by the model do not exhibits uniform results even within a single vulnerability zone. In the upslope part around a mining or crushing centre is less affected because stream flow does not carry such dust in this situation. Airborne dust mainly affects the upslope regions. Most of the cases load is almost 3-7 times lesser than down slope regions.

Table 7 Sample tributaries and their characteristics in different vulnerable zones

Vulnerable class	Selected tributaries	Range of depth of dust deposition on river bed(m)	Average depth (m)	pH	Avg. TDS (mg/l)
Very high	10	0.08-0.22	0.128	9	2487
High	6	0.09-0.16	0.092	8-8.5	2321
Moderately	5	0.03-0.08	0.074	8.2	(1543
Less Vulnerable	7	0.001-0.08	0.058	8.2	1256

Impact on Water Quality

PH value as an indicator of water quality specifically neutrality of water reveals that in the very high vulnerable zone pH value of river water is above 9. Huge influx of stone dust is principally responsible for such transformed water quality, in the highly vulnerable zone, pH value is 8-8.5 (Table7). But in low vulnerable zones, pH value of the river water is 8.2 and it is near to normal. From this analysis it can be stated that both channel bed aggradations and water quality status is beyond normal situation in the very high and high vulnerable zones and therefore, this model can be treated as valid.

Total dissolved solid (TDS) is another water quality parameter altered after contamination by dusts. In the highly vulnerable zones, TDS value with an average of 2487mg/l. This value is high very adjacent stream segment to stone mine and crusher centres. This high value is beyond the permissible limit of both drinking (500mg/l) and irrigation (2250mg/l) as per BIS (10500) Standards of Inland Surface Water (1991). In the less vulnerable zone, this TDS value (1256mg/l) crossed permissible limit for drinkability but it is irrigable.

Water colour appeared as grey of black drain water according to degree of vulnerability. Even the animals do not drink this water because of huge suspended particulate matters in water. Repetitive supply of water to the agricultural field can heap up huge volume of dust to the field and can alter the basis texture and composition of the soil. Aquatic environment specifically fishing is strongly affected in these segments. Although these stream segments were not highly worth for fish availability and fishing, but during monsoon season, fishing was practiced. But due to alteration of such physico-chemical parameters, such ambient environment has become altered.

Impacts on Vegetation Quality

The middle catchment of the Dwarka river basin is highly affected due to the stone crushing and mining dust. Vegetation coverage has been decreased rapidly due to the construction of a new mine and crushing sites.

The effect of dust pollution on plants is observed in this study as it has reduced the quality of vegetation in study area. The average NDVI value of 1990 was 0.470, whilst in 2011 it dropped to 0.54 and finally it is reduced to 0.48 in 2016 (Fig. 7A, 7B and 7C). This decline of NDVI since 1990 to 2016 focuses on degradation of forest quality. Most of the forest in this area is dominated by *Shorea robusta* and *Madhuca indica*, two broad leaf vegetation species and these are highly sensitive to stone dust.

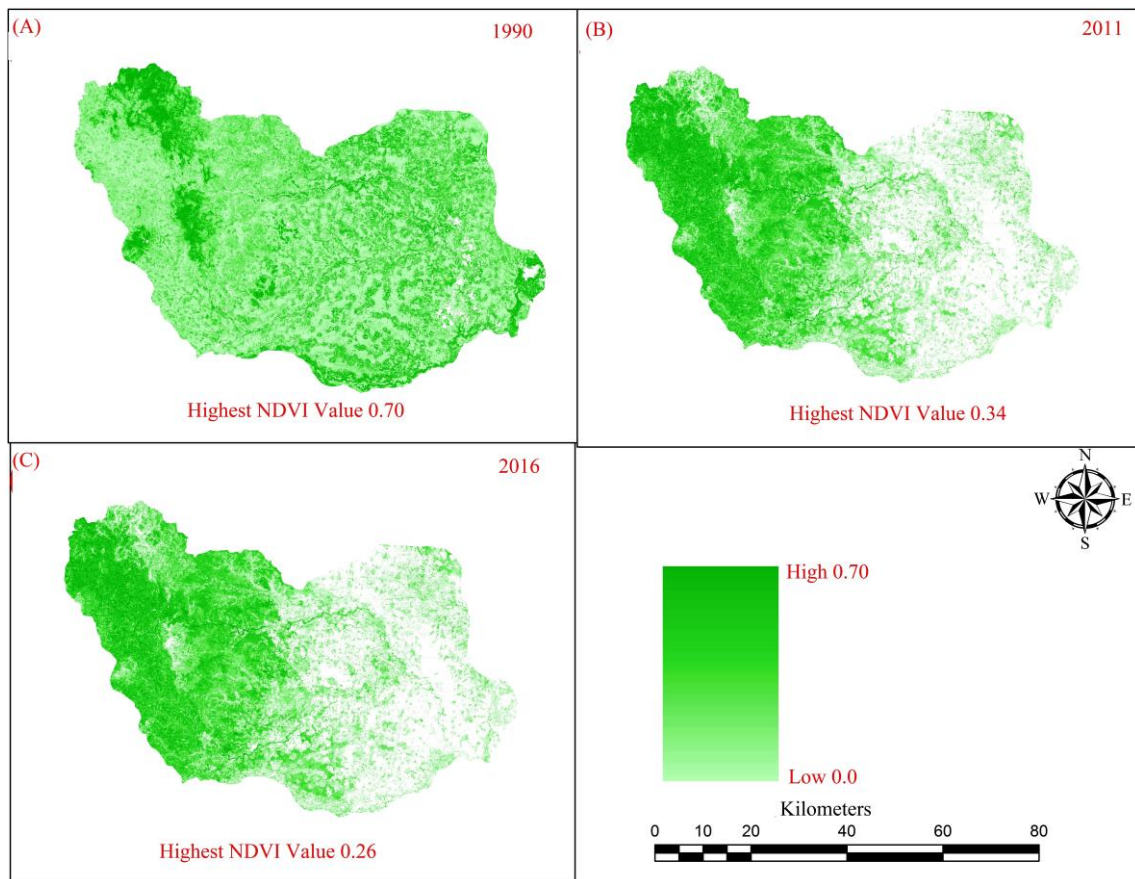


Fig.7 Vegetation Health (using NDVI) (A)1990 (B) 2011 (C) 2016

Saha and Padhy (2011) documented that high rate of dust deposition in the leaves decelerates rate of photosynthesis and food availability within the plant body and it causes weakening of vegetation health. During non monsoon time effects of dust becomes more prominent because of thick dust coating over leaves. In this time due to lack of rainfall, this thick dust coat becomes thicker. Apart from dust effects, continuous emission of hot smoke from crushing unit in the vegetation contiguous area causes partial plant cell damage. Apart from qualitative damage of vegetation, due to installation of stone mines and crushing unit within forest area it is also rapidly expunged.

CONCLUSIONS

From the above analysis, it is found that out of the total above mentioned basin area, a 14.93% area is very highly potential for dust vulnerability. Within this zone, 581 numbers of streams having a length of 713 km are found to be highly affected. Channel bed aggradations, increasing sediment load within water, degradation of water quality beyond permissible limits are some evident effects of dust emissions and spreading. Continuous deposition of such stone dust over vegetation causes qualitative degradation of vegetation as indicated by declining of NDVI values between 1990, 2011 and 2016. Due to mining activities, removal of prestigious forest has been rapidly degrading. Certainly, this fact is not solely responsible for deteriorating forest quality. Coarse grain laterite soil (Chokraborty, 1970), and mass scale soil erosion (6-

8t/ha/y) are another controlling factors for tree felling and degradation of vegetation (Jha and Kapat, 2009; Pal, 2016). The formation of dust layer on plant body damage plant tissue which reduces rate of photosynthesis. Dust particles emitted from stone crushing activity reduces the pigmentation in plant leaves (Saha and Padhy, 2011). Dust fall on open land reduces its fertility of soil (CPCB, 2009). Deposition of dust particles exerts stresses on plant which reduces productivity of plants.

Along with deterioration of forest environment, degradation of aquatic habitat is also vital issue. Fishes and other species will be in stress state if high level dust contamination happens and turbidity level raises. Fish prefers to avoid hypoxic waters and favours more highly oxygenated waters (Breitburg, 2000). But such hypo-oxygenated condition happened in the extra admixing of dusts. Rombough (1988) explained different species of fishes have different ability to tolerate low oxygen concentrations, depending on the natural change of dissolve oxygen concentration that fishes encounter in their preferred habitat. Catfishes tolerate wide range of oxygen variation but can't survive if oxygen comes 59% below ambient limit (Randolph and Clemenens, 1976). Opinion taken from local fishermen who were once engaged with fishing activities emphatically opined that river character has been changed and fish is become almost rare in this altered condition. Influx of dusts automatically enhances turbidity level in water. Turbidity impinges on both the density and metabolism of the plant populations present in stream channels (Wallen, 1951; Aldridge et al., 1987). A

study by Clavel and Bouchard (1980) showed that the absorption of light energy by water is proportional to the concentration of suspended sediment. High level of turbidity in river segments adjacent to the stone mine and crushing centres influences first trophic level in same manner. Cordone and Kelley (1961) and Decker et al. (1999) etc. found out the impact of channel morphology, sand mining, dredging on water quality specifically, turbidity, TDS, temperature etc. and all these again exert negative impact on aquatic habitat. Pal et al. (2016) also reported the huge reduction of fish availability in Chandrabhaga river basin after inflowing huge particulate matter from plant. For energizing growing urban sector through supplying building materials, this sector is getting plenty of attentions to the concerned authorities and loss of forest issues is quite sacrificed. Such situation is also explored in different parts of the country with variable intensities. Pal et al. (2016) identified the effect of fly ash on Chandrabhaga river of Chotonagpur plateau fringe area. They identified that this river is highly affected by thick (>0.5m) dust deposition and as result simplification of unique topographic features and ecological deterioration. Dinda (2014) worked on Rupnarayan river and reported that due to aggradations of channel bed through fly ash fish influx is deduced significantly. Saha and Padhy (2011) highlighted how fly ash affected the growth of vegetation and vegetation quality of the Rarh tract of Eastern India. They clearly stated that due to such effect green pigment contents in forest leaves have reduced significantly. This similar condition is found in the present study area also. In long term environmental agenda, such trend is not good at all. In this paper, attention is paid for a few issues only as mentioned above but apart from all these, human health hazards is also another major emerging problem in this area. The labourers working in this sector are highly exposed to respiratory diseases. During field investigation, opinion of the labourers has been taken into account regarding their health hazard. Dust generated from mining and crushing unit should be used for filling of abandoned mines, fertilizer preparation, road and rail way constructions. But for a successful project, it should be kept in mind that sectoral coordination in this regard is highly necessary.

References

- Aldridge, D.W., Payne, B.S., Miller, A.C. 1987. The effects of intermittent exposure to suspended solids and turbulence on three species of freshwater mussels. *Environ Pollut* 45: 17–28. DOI:10.1016/0269-7491(87)90013-3
- Araujo, C.C., Macedo, A.B. 2002. Multicriteria geologic data analysis for mineral favorability mapping: application to a metal sulphide mineralized area, Ribeira Valley Metallogenic Province Brazil. *Nat. Resour. Res.* 11: 29–43.
- Asproth, V., Holmberg, S.C., Hakansson, A. 1999. Decision Support for spatial planning and management of human settlements. In: International Institute for Advanced Studies in Systems Research and Cybernetics. In: Lasker, G.E. (Ed.), *Advances in Support Systems Research*, Windsor, Ont, Canada 5: 30–39.
- Bell, F.G., Bullock, Lindsey, P. 2001. Environmental Impacts Associated with an abandoned mine in the Witbank Coalfield, South Africa., *International Journal of Coal Ecology* 45: 195–216. DOI: 10.1016/S0166-5162(00)00033-1
- BIS. 1991. Bureau of Indian Standard, Mainak Bhavan, 9 Bahadur Shah Zafar Maro, New Delhi 110002.
- Blatt, H., Tracy, R.J. 1997. *Petrology igneous, sedimentary, and metamorphic* (2nd ed.). New York Freeman P: 66–67.
- Breitbart, D.L., Keister, J.E., Houde, E.D. 2000. Effects of bottom-layer hypoxia on abundances and depth distributions of organisms in Patuxent River, Chesapeake Bay. *Marine Ecology Progress Series*, 205, 43–59. DOI:10.3354/meps205043
- Chakrabarty, S.C. 1970. Some consideration on the evolution of phylogeny of Bengal. Geography Institute. Presidency College, Calcutta, pp. 20–21.
- Clavel, P., Bouchard, B. 1980. Incidences des extractions de granulats d'alluvions et de certains travaux hydrauliques, sur le periphyton, la production primaire et la production secondaire dans trois cours d'eau du massif central. *Ann Stat Biol Besse en Chaudesse* 14: 350.
- Cordone, A.J., Kelley, D.W. 1961. The influences of inorganic sediment on the aquatic life of streams. *Calif Fish Game* 47(2): 189–228.
- CPCB, 2009. Comprehensive Industry Document Stone Crushers, Central Pollution Control Board, Govt. Of India, Series: COINDS/78/2007-08, 1.1 – 8.21, www.cpcb.nic.in
- Decker, C., Keyes, J., Jackson, C.R., Shelton, J., Jackson, B. 1999. Effects of sand dredging on channel morphology, invertebrate communities and fish communities in Urban Dekalb County streams. In: Hatcher KJ (ed) *Proceedings of the 1999 Georgia Water Resources Conference*, held March 30–31, 1999, at the University of Georgia. Institute of Ecology, University of Georgia, Athens, pp 324–326.
- Dinda, S. 2014. Developmental project and its impact on adjacent river ecology: A case study of Kologhat thermal power plant, West Bengal, India, *International Journal of Geomatics and Geosciences* 5(2): 225–230.
- Down, C. 1974. The Relationship Between Colliery-waste Particle Sizes and Plant Growth. *Environmental Conservation*, 1(4), 281–284. DOI: 10.1017/S0376892900004902
- Eastman, J.R. 2006. Idrisi Andes – Tutorial, Clark Labs, Clark University, Worcester, MA. Gajanan N. Supe., et., al. Effects of Dustfall on Vegetation., *International Journal of Science and Research (IJSR)* 4 (7).
- Goretti, K.K.M. 1998. The environmental impacts of underground coal mining and land cover changes analysis using multi-temporal remotely sensed data and GIS. Unpublished M.Sc. thesis (cited in Sarma K), International Institute Aerospace Surveys and Earth Sciences (ITC), The Netherlands.
- Grewal, K.S., Yadava, P.S., Mehta, S.C., Oswal, M.C. 2001. Direct and residual effect of fly ash application to soil on crop yield and soil properties. *Crop. Res.* 21: 60–65.
- Horton, R.E. 1932. Drainage Basin Characteristics. *Trans. Am. Geophys. Union* 13, 350–361. DOI: 10.1029/TR013i001p00350
- Horton, R.E. 1945. Erosional Development of Stream and their Drainage Basins: Hydrological approach to quantitative morphology. *Geol. Soc. Am. Bull.* 56: 275–370. DOI: 10.1177/030913339501900406
- Howard, B., Cameron, I. 1998. Dust control: Best Practice Environmental Management in Mining, *Environment Australia*, 72–73
- IARC, 1997. Silica, some silicates, coal dust and para-aramid fibrils. Lyon, International Agency for Research on Cancer, *IARC Monographs on the Evaluation of Carcinogenic Risks to Humans* 68: 1–242.
- Jha, V.C. 1997. Laterite and landscape development in tropical lands, a case study. In: Nag P, Kumara V, Singh J (ed) *Geography and Environment, Concept* 1: 12–144.
- Jha, V.C., Kapat, S. 2009. Rill and gully erosion risk of lateritic terrain in South-Western Birbhum District, West Bengal, India. *Soc Nat (Online)* 21(2): 141–158.
- Jha, V.C., Kapat, S. 2003. Gully erosion and its implications on land use, a case study. *Land degradation and desertification*. Publ., Jaipur and New Delhi 156–178.
- Jiang, H., Eastman, J.R.. 2000. Application of fuzzy measures in multicriteria evaluation in GIS. *Int. J. Geogr. Inform. Syst* 14: 173–184. DOI: 10.1080/136588100240903
- John, S., Iqbal, M.Z. 1992. Morphological and anatomical studies on leaves of different plants affected by motor vehicle exhaust. *Journal of Islamic Academy of Sciences* 5: 21–23.
- Khatun, S., Pal, S. 2016. Identification of Prospective Surface Water Available Zones with Multi Criteria Decision Approach in Kushkarani River Basin of Eastern India, *Archives of Current Research International* 4(4): 1–20. DOI:10.9734/ACRI/2016/27651

- Let, S. 2012. Hydro-geomorphic Appraisal of Dwarka River Basin, Ph.D thesis submitted in Visva- Bharati University, Santiniketan, West Bengal, India 167–169.
- Lowman, M.D., Wittman, P.K. 1996. Forest canopies: methods, hypotheses, and future directions. *Ann. Rev. Ecol. and Syst.* 27: 55–81. DOI:10.1146/annurev.ecolsys.27.1.55
- Mendes, J.F.G., Motizuki, W.S. 2001. Urban quality of life evaluation scenarios: the case of Sao Carlos in Brazil. *CTBUH Rev* 1(2): 1–10.
- Moran, J.B. Linch, K.D., Cocalis, J.C. 1994. An emerging issue: Silicosis prevention in construction. *Applied Occupational and environmental hygiene* 9(8): 539–542. DOI: 10.1080/1047322X.1994.10388367
- Liu, Y.J, Ding, H. 2008. Variation in air pollution tolerance index of plants near a steel factory; implication for landscape- plant species selection for industrial areas. *WSEAS Transactions on Environment and Development* 4: 24– 32.
- Makropoulos, C., Butler, D. 2005. Spatial ordered weighted averaging: incorporating spatially variable attitude towards risk in spatial multi-criteria decision-making. *Environ. Modell. Software* 21 (1): 69–84. DOI:10.1016/j.envsoft.2004.10.010
- Malczewski, J. 2004. GIS-based land-use suitability analysis: a critical overview. *Prog Plan* 62(1): 3–65. DOI:10.1016/S0305-9006(03)00079-5
- Mishra, R.D., Kumari, P. 2008. Effect of dust pollution on chlorophyll and characteristics of maize. *Adv. Biol. Res* 26 (1-2): 62–67. DOI:10.20546/ijcmas.2016.505.080
- Mitchell, C. 2009. Quarry Fines and Waste, British Geological Survey, Natural Environment Research Council, Keyworth, Nottingham, NG12 5GG.
- Nagy, J., Kiss, T. 2016. Hydrological and Morphological Changes of the Lower Danube Near Mohács, Hungary, *Journal of Environmental Geography* 9 (1–2), 1–6. DOI: 10.1515/jengeo-2016-0001
- Nayar, M.P. 1985. Tree Canopies. Air Pollution and Plants: A State of the Art Report. Ministry of Environment and Forests, New Delhi, India.
- Pal, S. 2016. Identification of Soil Erosion Vulnerable Areas in Chandrabhaga River Basin: a Multi-criteria Decision Approach, *Model. Earth Syst. Environ.* 2(5), 1–11. DOI: 10.1007/s40808-015-0052-z
- Pal, S., Mahato, S., Sarkar, S. 2016. Impact of fly ash on channel morphology and ambient water quality of Chandrabhaga River of Eastern India. *Environ Earth Sci* 75:1268. DOI: 10.1007/s12665-016-6060-0
- Palaka, R., Jaysankar, G. 2015. Identification of Potential Zones for Groundwater Recharge in Kosigi Mandal, Kurnool District, using Remote Sensing and GIS, *International Journal of Current Engineering and Technology* 5: 12–19.
- Pandey, D.D., Pandey, K. 2010. Effect of particulate pollutant on chlorophyll of rice leaf. *Adv. Biol. Res.* 28(1): 167–168.
- Patil, M.A. 2001. Environmental management scenario in stone crusher industry sector and cleaner production possibilities, *TERI Information Monitor on Environment Science* 6 : 83–92.
- Pollution Data Division of Environment Canada. 2008. Criteria Air Contaminants Emissions Inventory 2006 Guidebook. Emissions and Projections Working Group of the Canadian Council of Ministers of the Environment. 57–61.
- Prajapati, S.K., Tripathi, B.D. 2008. Seasonal variation of leaf dust accumulation and pigment content in plant species exposed to urban particulates pollution, *Journal of Environmental Quality* 37: 865–870. DOI:10.2134/jeq2006.0511
- Prasad, S.N., Mishra, C.P., Sinha A.P. 2010. Effect of cement dust pollution on nutritional quality of *Dichanthium annulatum*. In Proc. Of National Seminar on Environmental pollution. A threat to living world. Organized by P.G. Dept. of Botony, Nalanda College, Biharsharif held on 27-28 March: 19.
- Pyatt, F.B., Haywood, W.J. 1989. Air borne particulate distributions and their accumulation in tree canopies, Nottingham, UK. *The Environmentalist* 30: 18–23.
- Rai, A., Kulshreshtha, K., Srivastava, P.K., Mohanty, C.S. 2010. Leaf surface structure alterations due to particulate pollution in some common plants. *The Environmentalist* 30: 18–23. DOI: 10.1007/s10669-009-9238-0
- Randolph, K.N., Clemens, H.P. 1976. Some factors influencing the feeding behaviour of channel catfish in culture ponds. *Trans Am Fish Soc* 105: 718–724. DOI: 10.1577/1548-8659(1976)105<718:sfitfb>2.0.co;2
- Rinner, C., Malczewski, J. 2002. Web-enabled spatial decision analysis using ordered weighted averaging. *J. Geogr. Syst* 4 (4): 385–403. DOI:10.1007/s101090300095
- Rombough, P.J. 1988. Growth, aerobic metabolism, and dissolved oxygen requirements of embryos and alevins of steelhead *Salmo gairdneri*. *Can J Zool* 66(3): 651–660. DOI: 10.1139/z88-097
- Rouse, J.W., Haas, R.H., Scheel, J.A., Deering, D.W. 1973. Monitoring Vegetation Systems in the Great Plains with ERTS. Third ERTS Symposium, NASA SP-351 I, 309-317.
- Saaty, T.L. 1980. The Analytic Hierarchy Process. McGraw-Hill, New York
- Saha, D.C., Padhy, P.K. 2011. Effects of stone crushing industry on *Shorea robusta* and *Madhuca indica* foliage in Lalpahari forest. *Atmospheric Pollution Research* 2: 463-476. DOI: 10.5094/apr.2011.053
- Sarma, K. 2005. Impact of Coal Mining on Vegetation: A Case Study in Jaintia Hills District of Meghalaya, India., International Institute for Geo-information Science and Earth Observation., Enschede, The Netherlands & IIRS, NRSA, Department of Space., Dehradun, India.
- Schumm, S.C. 1956. Evolution of Drainage Systems and Slopes in Badland of Perth Amboy, New Jersey, *Geol. Soc. Am. Bull.* 67: 597–646. DOI: 10.1130/0016-7606(1956)67[597:eod-sas]2.0.co;2
- Sharma, S.B., Kumar, B. 2016. Effects of stone crusher dust pollution on growth performance and yield status of rice (*Oryza sativa*, L.), *Int. J. Curr. Microbiol. App. Sci* 5(5): 796–806. DOI: 10.20546/ijcmas.2016.505.080
- Shivacoumar, R., Jayabalou, R., Swarnalatha, S., Balakrishnan, K. 2006. Particulate matter from stone crushing industry: Size distribution and health effects. *Journal of Environmental Engineering- ASCE* 132: 405–414. DOI: 10.1061/(asce)0733-9372(2006)132:3(405)
- Sipos, G. Blanka., V. Mezösi., G. Kiss., T. van Leeuwen, B. 2014. Effect of Climate Change on the Hydrological Character of River Maros, Hungary-Romania. *Journal of Environmental Geography* 7 (1–2), 49–56. DOI: 10.2478/jengeo-2014-0006
- Strahler, A. N. 1964. Quantitative geomorphology of drainage basins and channel networks. In Chow, V.T. (ed.) Handbook of Applied Hydrology, McGraw-Hill, New York. 439–476.
- Strahler, A.N. 1957. Quantitative Analysis of Watershed Geomorphology. *Trans. Am. Geophys. Union*, 38, 913–920. DOI: 10.1029/TR038i006p00913
- Strahler, A.N. 1964. Quantitative Geomorphology of Drainage Basins and Channel Networks. In Chow, V.T. (ed.) Hand book of Applied Hydrology, MacGraw Hill Book Company, New York, Section 4–11.
- Tucker, D.M., Reger, R.B., Morgan, W.K.C. 1995. Effects of silica exposure among railroad workers. *Applied occupational and environmental hygiene* 10(12): 1080–1085. DOI: 10.1080/1047322X.1995.10389099
- UNESCO, 1985. Living in the Environment. UNESCO/UNEP.
- US Department of Agriculture Soil Conservation Service 1972. National Engineering Handbook, section 4, Hydrology. US Government Printing Office, Washinton DC. 544.
- USDA, 1986. Urban hydrology for small watersheds; technical releases 55. Natural resources conservation services, Conservation engineering divisions.
- US EPA, 1996. Ambient levels and noncancer health effects of inhaled crystalline and amorphous silica: health issue assessment. Washington, DC, US Environmental Protection Agency, Office of Research and Development (Publication No. EPA/600/R-95/115; National Technical Information Service Publication No. PB97-188122).
- Wallen, E. 1951. The direct effect of turbidity on fishes. *Bull Okla Agric. Mech Coll (Biol)* 2:27.
- Wentworth, C.K. 1930. A Simplified method of determining the average slope of land surface. *America Journal of Science*, Series 5 (Newhaven Connecticut), 20: 184–190. DOI: 10.2475/ajs.s5-20.117.184
- Ziaul, S., Pal, S. 2016. Image Based Surface Temperature Extraction and Trend Detection in an Urban Area of West Bengal, India. *Journal of Environmental Geography* 9 (3–4), 13–25. DOI: 10.1515/jengeo-2016-0008



GROUNDWATER: QUALITY LEVELS AND HUMAN EXPOSURE, SW NIGERIA

Adeyemi Olusola^{1*}, Opeyemi Adeyeye¹, Olufemi Durowoju¹

¹Department of Geography, Osun State University, P.M.B 4404, Osogbo, Osun State, Nigeria

*Corresponding author, e-mail: adeyemi.olusola@uniosun.edu.ng

Research article, received 13 February 2017, accepted 6 April 2017

Abstract

Groundwater serves as a source of freshwater for agricultural, industrial and domestic purposes and it accounts for about 42%, 27% and 36% respectively. As it remains the only source of all-year-round supply of freshwater globally, it is of vital importance as regards water security, human survival and sustainable agriculture. The main goal of this study is to identify the main cause-effect relationship between human activities and the state of groundwater quality using a communication tool (the DPSIR Model; Drivers, Pressures, State, Impact and Response). A total of twenty-one samples were collected from ten peri-urban communities scattered across three conterminous Local Government Areas in Southwestern Nigeria. Each of the groundwater samples was tested for twelve parameters - total dissolved solids, pH, bicarbonate, chloride, lead, electrical conductivity, dissolved oxygen, nitrate, sulphate, magnesium and total suspended solids. The study revealed that the concentrations of DO and Pb were above threshold limits, while pH and N were just below the threshold and others elements were within acceptable limits based on Guidelines for Drinking Water Quality and Nigeria Standard for Drinking Water Quality. The study revealed that groundwater quality levels from the sampled wells are under pressure leading to reduction in the amount of freshwater availability. This is a first-order setback in achieving access to freshwater as a sustainable development goal across Less Developed Communities (LDCs) globally. To combat this threat, there is the need for an integrated approach in response towards groundwater conservation and sustainability by all stakeholders.

Keywords: groundwater, DPSIR, cause-effect, peri-urban, communication tool

INTRODUCTION

Clean, safe and adequate availability of freshwater is vital to the survival of all living organisms and the smooth functioning of ecosystems, communities and economies (Ibeh and Mbah, 2007; Akoteyon, 2013). Availability and access to freshwater is also a global concern and a major unit of the sustainable development goals (SDGs). In terms of availability, two major sources of freshwater are surface water and groundwater. Groundwater provides a valued fresh water resource to human population and constitutes about two-third of the fresh water reserves presently occupying various spaces across the world. Groundwater is used for agricultural, industrial and domestic purposes. It accounts for about 50% of livestock and irrigation usage and just under 40% of water supplies, whilst in peri-urban areas, 98% of domestic water use is from groundwater (Todd, 1980; Stigter et al., 2006). Groundwater can be put into different uses such as domestic, agricultural and industrial activities. These activities put a demand on groundwater thereby attenuating the remaining portion of available groundwater reserves (Sangodoyin and Agbawhe, 1992). Activities such as these not only put pressure on global groundwater reserves but also affect the quality of groundwater (Oluwande, 1983; MacDonald et al., 2005; Stigter et al., 2006; Akoteyon, 2013). Groundwater quality comprises the physical, chemical and biological qualities (Phillips et

al., 2013). It becomes polluted when its quality is disturbed, whether the physico-chemical or the biological property.

Groundwater pollution can also be described as water contamination. It occurs when pollutants are released to the ground and make their way down into groundwater. It can also occur naturally due to the presence of minor and unwanted constituents, contaminants or impurity in the groundwater, in which case it is more likely referred to as contamination rather than pollution (Phillips et al., 2013). In most tropical climes such as Nigeria, increase in the rate of population, a corollary effect of increase in the level of urbanization, industrial and agricultural activities are perceived to pose serious pollution threats with all its concomitant health hazards on groundwater quality especially in urban and peri-urban areas (Kehinde et al., 1989; Adelana et al., 2008). Groundwater in some climes contain specific ions (such as fluoride) and toxic elements (such as arsenic, lead and selenium) in quantities that are harmful to health, while others contain elements or compounds that cause other types of problems (such as the staining of sanitary fixtures by iron and manganese).

Most peri-urban towns in tropical countries such as Nigeria are heavily populated due to rapid urbanization because of urban renewal processes; a growing planning process in urban planning, closeness to major urban centres, etc. It is based on this background that this research seeks to assess groundwater quality levels

across three conterminous Local Government Areas (LGAs) in Osun State. These three LGAs (Boluwaduro, Ifelodun and Boriipe) are close to Osogbo, the Osun State Capital and they have been enjoying influx of people from Osogbo who are settling down in these areas. These three LGAs have been experiencing population growth (NPC, 2006) and are fast becoming urbanized with unchecked physical planning process coupled with observed sanitary issues and difficulties in the use of freshwater especially for drinking purpose; the area becomes ideal for this kind of study. These factors (urbanization, unchecked physical development and sanitation issues, offshoot of population growth) are impacting on freshwater availability within the study area and thereby reducing its quality. With the present global challenge on freshwater, there is the need for developing countries such as Nigeria to drive policies that will protect her freshwater reserves and ensure sustainability. One of the channels through which the nations of the world can achieve protection and sustainability is encouraging more research into groundwater reserves using human-environmental models that can be used to understand interactions between nature and man in order to drive policies that are long sustainable and achievable. The aim of this study is to assess the spatial variation in groundwater quality across three conterminous LGAs in Osun State and present a sustainable water management approach. To achieve this aim, this study employed the use of DPSIR (Driving force, Pressure, State, Impact and Response) Model in understanding the importance and functions of groundwater quality in Boluwaduro, Boriipe and Ifelodun LGAs in Osun State. The main goal of this model is to identify the main cause-effect relationship between human activities and the state of water quality and present

a response approach geared towards sustainable freshwater availability. Borja et al. (2005) used the model together with other methodologies to identify the relevant pressures and impacts of water quality changes in estuarine and coastal areas. Danielopol et al. (2003) reviewed the changes in the status of groundwater ecosystems and the important driving forces, resulting from the direct or indirect impacts of human activities. Their discussion divided the environmental pressures which are largely produced by human activities in two major classes, namely; groundwater quantity problems and the critical depletion of aquifers in many parts of the world and groundwater quality problems, where the systems are overloaded with contaminants. An application of the DPSIR model based on the uniqueness of the study area and its peculiarities (being a tropical community, peri-urban zone, its absolute dependence on freshwater through groundwater abstraction and increasing emergence of light industries) becomes very relevant and sets to add more to growing body of knowledge on integrated water quality studies especially in tropical climes and offers a unique solution for similar Less Developed Communities (LDCs) across the world. Also, given globally recognized water scarcity, using the worlds accessible freshwater in a sustainable manner becomes critically important.

STUDY AREA

Three LGAs were investigated in this research – Ifelodun, Boluwaduro and Boriipe (Fig. 1, 7°55'N, 4°40'E; 7°57'N, 4°48'E; 7°57'N, 4°48'E). Ifelodun has an area of 114km² with a population of 96, 444 with its headquarters located at Ikirun, Boluwaduro has an area of 144km² and a population of 70,954, with its headquarters located at Atan-Ayegbaju while Boriipe with an area of 132km² and a population of 138,742 as at 2006 census has its headquarters at Iragbiji.

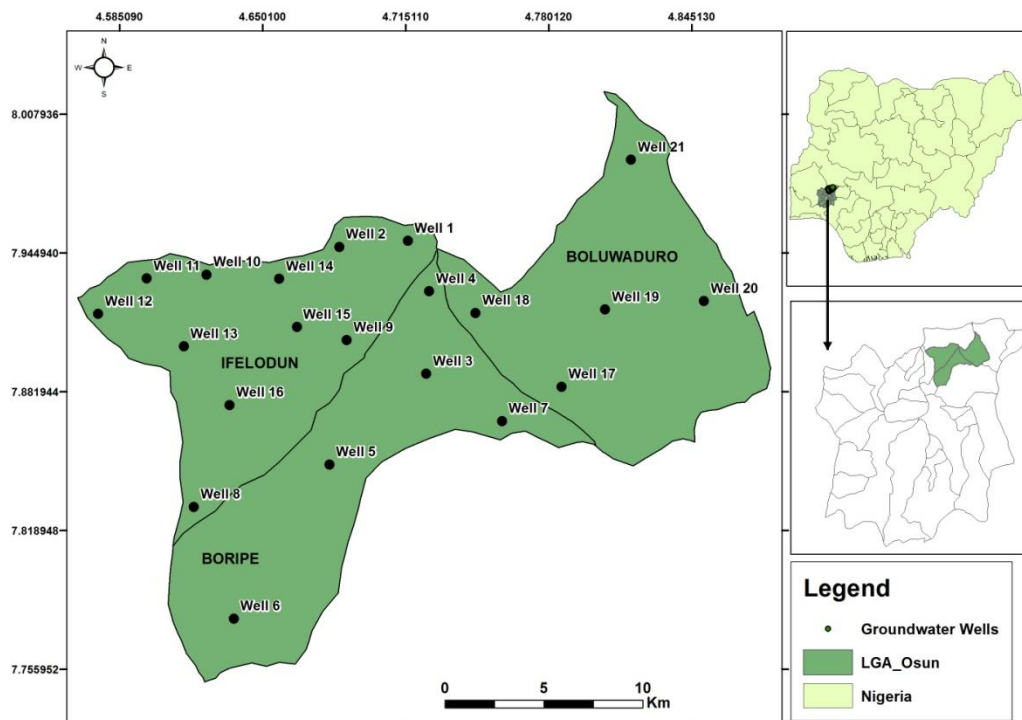


Fig. 1 Map showing study area and groundwater sampling points

The study area (Fig. 1) receives an average rainfall of 1,150 mm a year; it lasts from April to late October or early November (South-westerly winds prevail), though it eases off in July or August (August Break). The dry season lasts from November to March which is the period of intense harmattan when the North-easterly dusty wind prevails, mixed with occasional intense heat. Osun State is an inland state, lying mainly in the tropical rainforest, in the deciduous forest area which spreads towards the grassland belt of the study areas. Climate here is less humid and hot than the greater part of South-Western Nigeria although the effect of the harmattan wind is strongly felt in the dry season. The towns are situated on a raised land which is well over 500 meters above the sea level and is drained by the tributaries of River Osun.

Various economic activities are being carried out within the study areas. Sizeable numbers of the populace within the zone are civil servants who also are into one form of petty trading. Market structures within the zone are mostly periodic with few ones being patronized on a daily basis. The area boasts of various industries from local craft ones to light industries (food crops processing plants, auto-mechanic workshops, etc.) and few heavy industries (Iron smelting, metal fabrication, etc.). Due to large expanse of available arable land, the area is intensively cultivated for various crops while some are already being converted into industrial sites.

METHODOLOGY

Field survey was carried out before sample collection. This was necessary in order to examine the general characteristics of the area, determine the most feasible routes for sample collection and identify wells and their characteristics. Communities where samples were taken are Iree, Obagun, Otan-Ayegbaju, Ada, Oba, Erinpa, Ikirun, Eko-Ajala, Iragbiji located within the Local Government Areas Boripe, Boluwaduro and Ifelodun (Table 1). These areas were identified during the course of the reconnaissance and it was gathered that their source of groundwater which is mostly from wells is not too safe for drinking.

DPSIR model

DPSIR model is a chain of causal links starting with 'driving forces' (economic sectors, human activities) through 'pressures' (emissions, waste) to 'states' (physical, chemical and biological) and 'impacts' on ecosystems, human health and functions, eventually leading to political 'responses' (prioritization, target setting, indicators). Describing the causal chain from driving forces to impacts and responses is a complex task, and tends to be broken down into sub-tasks, e.g. by considering the pressure-state relationship. A 'driving force' is a need. Examples of primary driving forces for an individual are the need for shelter, food and water, while examples of secondary driving forces are the need for mobility, entertainment and culture (Kristensen, 2004). Driving forces lead to human activities such as transportation or food production, i.e. result in meeting a need. These human activities exert 'pressures' on the environment, as a result of production or consumption processes.

Table 1 Location of sampled groundwater wells

ID	Geographic coordinates		Depth (m)	Flow
	Nothing	Easting		
Well 1	07°55' 46.221"	04°40' 30.370"	7	Perennial
Well 2	07°55' 44.207"	04°40' 20.006"	2	Seasonal
Well 3	07°56' 08.450"	04°43' 41.446"	2	Perennial
Well 4	07°56' 11.886"	04°43' 46.192"	8	Seasonal
Well 5	07°56' 13.011"	04°43' 30.199"	12	Seasonal
Well 6	07°53' 27.352"	04°42' 47.338"	12	Seasonal
Well 7	07°53' 32.399"	04°42' 46.743"	12	Seasonal
Well 8	07°54' 22.510"	04°41' 12.610"	2	Seasonal
Well 9	07°54' 20.596"	04°41' 15.500"	2	Perennial
Well 10	07°56' 33.035"	04°37' 34.008"	6	Perennial
Well 11	07°55' 02.547"	04°34' 31.910"	2	Seasonal
Well 12	07°55' 03.512"	04°34' 28.859"	6	Perennial
Well 13	07°54' 31.711"	04°34' 41.251"	14	Seasonal
Well 14	07°55' 37.113"	04°39' 13.297"	7	Perennial
Well 15	07°55' 13.326"	04°40' 08.198"	14	Seasonal
Well 16	07°55' 07.601"	04°40' 09.509"	2	Seasonal
Well 17	07°56' 22.387"	04°44' 39.922"	14	Seasonal
Well 18	07°56' 19.271"	04°44' 40.429"	2	Seasonal
Well 19	07°56' 19.115"	04°44' 38.494"	2	Seasonal
Well 20	07°56' 50.558"	04°47' 24.027"	12	Seasonal
Well 21	07°56' 51.940"	04°47' 24.439"	12	Seasonal

As a result of pressures, the 'state' of the environment is affected; that is, the quality of the various environmental compartments (air, water, soil etc.) in relation to the functions that these compartments fulfil. The 'state of the environment' is thus the combination of the physical, chemical and biological conditions. The changes in the physical, chemical or biological state of the environment determine the quality of ecosystems and the welfare of human beings. In other words, changes in the state may have environmental or economic 'impacts' on the functioning of ecosystems and human lives (Kristensen, 2004). A 'response' by society or policy makers is the result of an undesired impact and can affect any part of the chain between driving forces and impacts. DSPIR was applied as a guiding model for a well-developed water quality study in the light of sustainable freshwater management.

Driving forces and Pressures

The need for shelter, healthy living and improved financial status were identified as the driving forces acting upon the sustainable use of freshwater supply within the zone. A corollary effect of these forces is increased population growth which in turn affects urbanization and industrialization. As a basic pressure, population growth was analysed using existing records between 2006 and 2011 (NPC, 2006) and possible contamination sources that predispose groundwater to pollution were identified on the field.

State and Impact

The state of the groundwater in terms of its quality was determined from the Laboratory using standard protocols and measures (APHA et al., 2008) at the University of Ibadan, Department of Agronomy. A total of twenty-one (21) samples were collected from ten (10) peri-urban communities scattered across the three Local Government Areas (Boripe, Boluwaduro and Ifelodun). The water samples were collected with the aid of Polyethylene bottles (APHA et al. 1998) and each location was determined using a Global Positioning System. Also, the state of each of the wells was determined in terms of depth and volume of water was qualitatively described using seasonality. At the time of sampling, bottles were thoroughly rinsed two to three times with the well water. The samples were taken immediately to the laboratory to determine their physico-chemical properties. Each of the groundwater samples was analyzed for 12 parameters: Total Dissolved Solids (TDS), pH, Bicarbonate, Chloride, Lead, Electrical Conductivity, Dissolved Oxygen, Nitrate, Sulphate, Magnesium and Total Suspended Solids using standard laboratory procedure (APHA et al., 1998).

The spatial variation of the physico-chemical properties was determined using charts across the 21 communities. Based on WHO and Nigeria standards, average values of each of the parameters were compared against the WHO standard to ascertain the level of exposure to risks being posed by the consumption of freshwater within the study area. Risk map for threatening parameters was produced using ArcGIS 10.1 in form of dot map using proportional circles.

Response

The present capacities of major stakeholders were evaluated to understand how to cope with the impact of polluted groundwater and finally presenting a required management intervention that is both long-term and short-term.

RESULTS

Driving Forces and Pressures

The driving forces identified within the study area are population growth and urbanization. These activities arise as a result of human needs for food, water, shelter and health. Due to population increase (NPC, 2011) across the area, there is increase in the rate of urbanization and agricultural practices. On the average, across the three LGAs,

population increased by over 14%. By 2050, it is expected that global water demand will increase by 55 percent (Cap-net, 2016) mainly due to growing demands from manufacturing, thermal electricity generation and domestic use. As population increases across the study area (Fig. 2) so does production of wastewater and other products that predisposes groundwater to being polluted. By 2020 the proportion of urban population in LDCs is predicted to surpass 50% and it is expected that 57% of the world's population will live in cities (UN Report, 1997). Going by the trend, peri-urban communities are likely to have greater influx of urban dwellers of which a large proportion will be poor. This in itself implies increase in pressure on domestic and drinking water supply, sanitation and food supply (Danielopol et al., 1997).

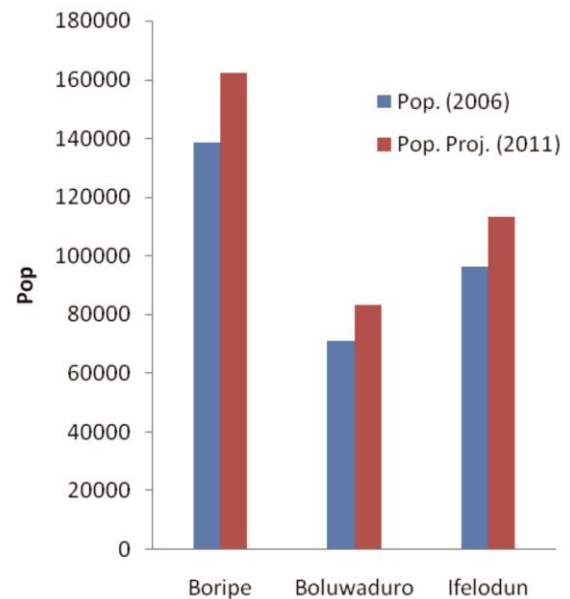


Fig. 2 Graphical representation of population growth across the study area

Agricultural practice exerts pressure on the environment and it is a major source of high concentration of nitrate in groundwater in wells, through the application of chemical manure. Fertilizers and pesticides applied to crops eventually reach underlying aquifers particularly if the aquifer is shallow and not protected by an overlying layer of low permeability materials.

State and Impact

The values in Table 2 shows that well 13 has the highest pH value followed by well 6. pH is a measure of the acidic or basic nature of a solution pH average (6.5) value for groundwater is within the permissible level (Table 3). It has been noted in the Nigeria Standard for Drinking Water Quality (NSDWQ, 2007) that pH usually does not have a direct bearing on consumers of water. DO is a measure of the amount of oxygen level in a body of water. It is affected by pressure, temperature and salinity. Average value for DO across the studied wells is 10.6. The average value for DO here is above the threshold limit (NSDWQ, 2007). Excess dissolved oxygen in water bodies can cause external bubbles (emphysema), a rare occurrence that affects the skin and other tissues (Kumar et al., 2007).

Table 2 Physico-chemical result of groundwater analyses across the twenty-one communities

ID	pH	EC ($\mu\text{S/cm}$)	TDS mg/l	TSS mg/l	Cl mg/l	NO ₃ mg/l	SO ₄ mg/l	HCO ₃ mg/l	Ca mg/l	Mg mg/l	Pb mg/l	DO mg/l
Well 1	6.71	542	20.5	1.4	17.8	0.8	1.2	0.07	20.5	3.1	0.34	11
Well 2	5.66	432	18	0.5	35.5	0.6	1.1	0.19	19.1	3.8	0.35	9
Well 3	6.83	512	21.8	1	22.5	0.9	1	0.1	18.5	2.9	0.43	10
Well 4	6.71	842	22.4	1.5	27	1.3	1	0.12	17.35	2.2	0.32	12
Well 5	6.83	422	20.6	1.19	25.6	1.1	1.5	0.16	19.8	1.7	0.2	13
Well 6	6.24	362	33.2	0.8	24.5	1.2	0.9	0.08	17.3	1.8	0.19	11
Well 7	6.31	392	30.4	0.65	21.5	1	1.6	0.07	21.5	1.9	0.17	12
Well 8	6.55	545	26.8	1.11	20.6	1.4	1.1	0.06	22.8	2.15	0.22	9
Well 9	6.53	792	20	0.92	17.3	1.7	1.2	0.05	26.1	2.35	0.3	8
Well 10	6.71	382	25.5	0.85	35.5	1.8	0.8	0.16	25.3	2	0.26	8
Well 11	6.75	372	24.2	0.7	18	0.4	1	0.2	18.75	4.19	0.4	8
Well 12	6.82	322	23.2	1.1	21	1.1	1.1	0.02	22.8	2.6	0.28	9
Well 13	9.92	682	17.9	0.6	18.5	0.9	0.7	0.16	27.33	2.8	0.49	12
Well 14	6.36	332	16.5	0.9	13.8	1.1	1.7	0.14	35.1	3.3	0.31	13
Well 15	6.23	352	14	0.3	12.9	0.7	0.9	0.1	29.2	4.8	0.33	11
Well 16	6.54	662	13.6	0.45	18	0.9	1.6	0.09	18.7	2.9	0.21	12
Well 17	6.26	352	20.3	0.25	19.2	0.7	1.4	0.11	16.5	3.15	0.26	12
Well 18	6.55	342	18.6	0.4	21	1.1	1.6	0.16	17.1	2.9	0.18	11
Well 19	6.52	342	19.1	0.3	16	1.3	0.8	0.12	19.3	1.6	0.14	11
Well 20	6.85	602	12.7	0.22	13	0.8	1	0.1	18.6	1.45	0.1	10
Well 21	6.8	852	14.8	0.18	20	1.1	1.7	0.08	17.8	2.15	0.11	11
Average	6.70	496.90	20.67	0.73	20.91	1.04	1.19	0.11	21.40	2.65	0.27	10.62

For calcium, well 14 appeared with the highest value and well 6 for TDS. Well 2 and 10 has the highest value for Cl. Calcium concentration, Cl and TDS appears with an average of 21.40mg/l, 20.9 mg/l and 20.6mg/l respectively and they are well within acceptable standard (Table 3). The palatability of drinking water rated by panels of tasters in relation to its TDS level is as follows: excellent, less than 300 mg/l; good, between 300 and 600 mg/l; fair, between 600 and 900 mg/l; poor, between 900 and 1,200 mg/l; and unacceptable, greater than 1,200 mg/l (WHO, 1996a, b). TDS concentrations across sampled wells are quite low and there is the tendency for the water to become flat and insipid in taste (Kumar et al., 2007).

Table 3 Nigeria Standard for Water Quality (NSDWQ, 2007)

Physico-chemical parameters	NSDWQ
pH	6.5 -8.5
EC ($\mu\text{S/cm}$)	1000
TDS (mg/l)	500
TSS (mg/l)	500
Chloride (mg/l)	250
Nitrate (mg/l)	50
Sulphate (mg/l)	100
Bicarbonate (mg/l)	-
Calcium (mg/l)	75
Magnesium (mg/l)	0.20
Lead (mg/l)	0.01
Dissolved oxygen (mg/l)	5.0

Magnesium (Mg) concentration as observed in the study is higher than the sulphate (SO₄) level. Well 15 has the highest concentration level of Mg exceeding the permitted level without any known effect on human health. As for sulphate, well 14 and 21 has the highest concentration level. SO₄ has an average concentration of 1.13mg/l lower than the permitted class given by NSDWQ (2007). It has been noted that low SO₄ concentration has no effect on human health.

Well 10 has the highest level of nitrate concentration. Across the studied wells, NO₃⁻ has an average value of 1.04mg/l which is well within the permitted standard globally. For lead, the highest concentration was observed in well 13 (0.49mg/l). Lead across the study wells presents an average value of 0.266mg/l exceeding the permitted threshold level of 0.01 mg/l. From the study, Lead has been found to be highly concentrated in most wells across Obagun, ObaOke, Oba – Oke and Iree. Most wells across the study area are shallow and particularly these wells are sited close to auto-repair workshops, such as; auto mechanic, auto welding and auto painting. Wastes disposal from these workshops found their way into the soil profile and contaminate the aquifer level resulting in groundwater pollution due to their shallowness. Pb is quite deadly and it results in several diseases which are harmful to the human health especially children. The presence of Pb above the normal threshold (WHO, 1996a; NSDWQ, 2007) results in carcinogenic diseases,

Table 4 Groundwater Quality Matrix (Red: High Risk; Yellow: Medium Risk; Blue: No risk

	pH	EC	TDS	TSS	Cl	NO ₃ ⁻	SO ₄	HCO ₃ ⁻	Ca	Mg	Pb	DO
IFELODUN	Yellow	Blue	Blue	Blue	Blue	Blue	Blue	Yellow	Blue	Blue	Red	Red
BORIBE	Yellow	Blue	Blue	Blue	Blue	Blue	Blue	Yellow	Blue	Blue	Red	Red
BOLUWADURO	Yellow	Blue	Blue	Blue	Blue	Blue	Blue	Yellow	Blue	Blue	Red	Red

interference with Vitamin D metabolism and it affects mental development in infants. Bicarbonate, HCO₃⁻, is always expected to be quite high especially in groundwater levels with low levels of calcium and magnesium. It serves as a control on water pH. Well 2 has the highest Bicarbonate level (0.19mg/l). The average value for HCO₃⁻ across the studied sites is 0.111 mg/l. The highest concentration level of TSS was observed in well 4 (1.5mg/l), and an average of value of 0.696 mg/l across all wells. TSS is well within the permitted level.

It is quite clear that most wells within the study area are quite shallow. Hence, they are susceptible to contamination from activities around. The deepest well is about 12 meters (Table 1). This explains the reason why some of the wells are seasonal. The extraction is from weathered regolith not deep enough to sustain water availability all year round. The shallowness of the well suggests that contaminants get into the freshwater zone rather easily. The pathway through which most of the groundwater within the study area gets polluted is through point sources as observed across the studied wells. From the state of groundwater quality across the studied wells vis-a-vis the WHO (1996a) and NSDWQ (2007), levels Dissolved Oxygen (DO) and Lead (Pb) within the wells poses high risk to human health and survival within the study area (Table 4). Nitrate and pH are just within par while the rest are well within acceptable limit (Table 4). The two high risk parameters are presented in Fig. 3 and 4 to show variation in concentration across the study area.

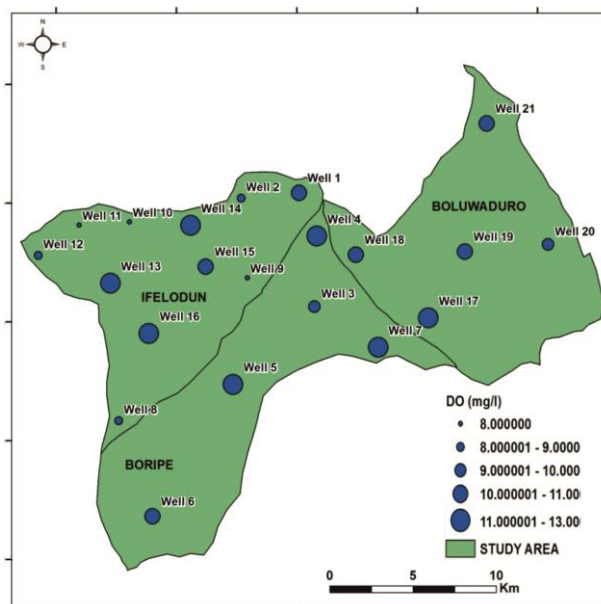


Fig.4 Risk map showing DO concentration in the study area

Response

The cycle of hydrological processes sustains life and serves as a means of providing freshwater on the earth surface (Cap-net, 2016). Freshwater is a natural asset that must be protected to ensure that the essential ecosystem services it provides continue. Expected response based on observed pressures and impact is to recognize that water is a scarce resource used for many different purposes, functions and services; therefore, water management has to be holistic and carefully consider different demands in view of available resources and threats. It is therefore expected that effective management of groundwater should encompass seeking non-conventional water sources, such as reclaiming or desalinating. Also, addressing source-point pollution (i.e. precluding waste streams from entering natural water bodies) is among measures that can effectively curb this problem. Specifically, all water producing wells within the study area should meet minimum standards for well construction mostly in terms of depth. Furthermore, proper well location with minimum standards from potential sources (auto repair workshops, dumpsites, etc.) of contamination must be set. On the part of the government, regulatory bodies should be empowered and made to employ the polluted pay principle and good practice should be adopted. In order to effectively achieve the expected goal and meet global sustainable demands, alongside desirable socio- economic development by prioritizing social equity, environmental sustainability and economic efficiency, health-sanitation officers should be properly equipped to enforce environmental healthi-

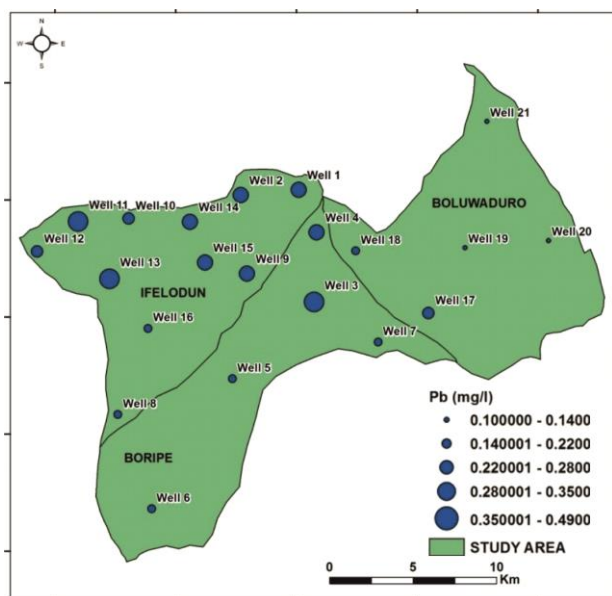


Fig3 Risk map showing Pb concentration in the study area

ness. A more drastic approach to solving polluted groundwater across peri-urban centres in LDCs is the establishment of central borehole system carefully constructed in clusters of communities based on stakeholder participation right from the feasibility study to the construction of the water system.

CONCLUSION

The information obtained from this shows that two the levels of two parameters were found to be at above the threshold, two parameters were found to be at around the threshold limit while the remaining eight parameters were within the acceptable limits. In addition, the research has shown that groundwater quality levels from the sampled wells are under pressure threat due to increase in population and urban activities. These drivers put a lot of pressure on the environment thereby increasing pollution risk from point sources such as dumpsites, metals from auto-repair workshops and chemicals due to intense agricultural practices. The resultant impact is that there is a grave danger on health especially on the urban poor utilizing groundwater for human consumption without any form of treatment.

Globally, there is little or nothing that mankind can do to change water availability in the natural water cycle. However, on a local scale, natural water cycle supports numerous smaller man-made water cycles that critically alter overall water availability. There is therefore the need for better management, i.e. improved economic efficiency of these man-made water cycles to ensure sustainable development. Reducing pollution and collecting, recycling and reusing wastewater are a first order approach to tackle this menace within these communities and other LDCs in order to sustain human lives and create an environment that is sustainable and liveable.

References

- Adelana, S.M.A., T.A. Abiye, D.C.W. Nkhuwa, C. Tindemugaya, M.S. Oga. 2008. Urban groundwater management and protection in Sub-Saharan Africa. In: Adelana S.M.A and MacDonald, A.M (eds) Applied groundwater studies in Africa. CRC, Boca Raton, FL, pp 231–260
- Akoteyon, I. S. 2013. Hydrochemical Studies of Groundwater in Parts of Lagos. *Southwestern Nigeria. Bulletin of Geography, Physical Geography Series* (6), 27–42. DOI: 10.2478/bgeo-2013-0002
- APHA, AWWA, WEF 1998. Standard Methods for the Examination of Water and Wastewater. 20th Edn., APHA, Washington, DC.
- Borja, A, Galparsoro I, Solaun O, Muxika I, Tello M, Uriarte A, et al 2005. The European Water Framework Directive and the DPSIR, A methodological approach to assess the risk of failing to achieve good ecological status. *Estuar Coast Shelf Sci* 66:84–96. DOI: 10.1016/j.ecss.2005.07.021
- Cap-Net, 2016. Ecosystem functions and services: Integrated water resources management. Training Manual. Online available at: www.cap-net.org
- Danielopol, D, Griebler, C, Gunatilaka, A, Notenboom J. 2003. Present state and future prospects for groundwater ecosystems. *Environ Conserv* 30(2): 104–30. DOI: 10.1017/s0376892903000109
- Ibeh, L.M., Mbah, C.N. 2007. Surface characteristics of urban rivers in Enugu South eastern Nigeria. *World Journal of Biotechnology* 8(2), 1412–1417.
- Kehinde, M.O., Loehnert, E.P. 1989. Review of African groundwater resources. *Journal of African Earth Sciences* 9, 179–185. DOI: 10.1016/0899-5362(89)90019-5
- Kumar, M., Kumari, K., Ramanathan, A.L., Saxena, R. 2007. A comparative evaluation of groundwater suitability for irrigation and drinking purposes in two intensively cultivated districts of Punjab, India. *Env. Geol.*, 53: 553–574. DOI: 10.1007/s00254-007-0672-3
- MacDonald, A.M., Kemp, S.J. Davies, J. 2005. Transmissivity variations in mudstones. *Ground Water* 43, 259–269. DOI: 10.1111/j.1745-6584.2005.0020.x
- NPC (National Population Census) 2006. Details of the breakdown of the national and state/provisional population totals. Official Gazette 96 (2), 1–42, Federal Republic of Nigeria, Abuja.
- National Population Commission. 2011. Nigeria's over 167million population: Implications and challenges. Retrieved March, 10, 2012
- NSDWQ, 2007. Nigerian Standard for Drinking Water Quality. Nigerian Industrial Standard NIS 554, Standard Organization of Nigeria, p30.
- Oluwande, P. 1983. Guide to tropical environmental health engineering. Nigerian Institute of Social and Economic Research Ibadan (NISER), Ibadan, pp. 141-147.
- Phillips, A.J., Gerlach, R., Lauchnor, E., Mitchell, A.C., Cunningham, A.B., Spangler, L. 2013. Engineered applications of ureolytic biomineralization: a review. *Biofouling* 29(6), 715–733. DOI: 10.1080/08927014.2013.796550
- Sangodoyin, A.Y., Agbawhe, O.M. 1992. Environmental study on surface and groundwater pollutants from abattoir effluents. *Biore-source Technology* 41(3), 193–200. DOI: 10.1016/0960-8524(92)90001-e
- Stigter, T. Y., Ribeiro, L., Carvalho Dill, A. M. M. 2006. Application of a groundwater quality index as an assessment and communication tool in agro-environmental policies - Two Portuguese case studies. *Journal of Hydrology* 327(3–4), 578–591. DOI: 10.1016/j.jhydrol.2005.12.001
- Todd, D.K., Mays, L.W. 2005. Groundwater Hydrology, 3rd edition. John Wiley and Sons Inc. p, 652.
- UN Report (United Nations Report) 1997. World Urbanization Prospects: The 1996 Revision. New York, USA: UN Secretariat, Population Division.
- WHO (World Health Organisation), 1996a. Guidelines for Drinking Water Quality, vol. 2: Health Criteria and Other Supporting Information, second ed. World Health Organisation Press, Geneva.
- WHO (World Health Organisation), 1996b. Water Quality Monitoring: A Practical Guide to the Design and Implementation of Freshwater Quality Studies and Monitoring Programmes. E and FN Spon, London, UK.



SPATIOTEMPORAL ASSESSMENT OF VEGETATION INDICES AND LAND COVER FOR ERBIL CITY AND ITS SURROUNDING USING MODIS IMAGERIES

Shwan O. Hussein^{1*}, Ferenc Kovács¹, Zalán Tobak¹

¹Department of Physical Geography and Geoinformatics, University of Szeged, Egyetem u. 2-6, H-6722 Szeged, Hungary

*Corresponding author, e-mail: shwan.huseen1@su.edu.krd

Research article, received 28 March 2017, accepted 2 May 2017

Abstract

The rate of global urbanization is exponentially increasing and reducing areas of natural vegetation. Remote sensing can determine spatiotemporal changes in vegetation and urban land cover. The aim of this work is to assess spatiotemporal variations of two vegetation indices (VI), the Normalized Difference Vegetation Index (NDVI) and Enhanced Vegetation Index (EVI), in addition land cover in and around Erbil city area between the years 2000 and 2015. MODIS satellite imagery and GIS techniques were used to determine the impact of urbanization on the surrounding quasi-natural vegetation cover. Annual mean vegetation indices were used to determine the presence of a spatiotemporal trend, including a visual interpretation of time-series MODIS VI imagery. Dynamics of vegetation gain or loss were also evaluated through the study of land cover type changes, to determine the impact of increasing urbanization on the surrounding areas of the city. Monthly rainfall, humidity and temperature changes over the 15-year-period were also considered to enhance the understanding of vegetation change dynamics. There was no evidence of correlation between any climate variable compared to the vegetation indices. Based on NDVI and EVI MODIS imagery the spatial distribution of urban areas in Erbil and the bare around it has expanded. Consequently, the vegetation area has been cleared and replaced over the past 15 years by urban growth.

Keywords: MODIS, remote sensing, vegetation index, NDVI, EVI, land cover, time series

INTRODUCTION

The rate of urbanization is increasing throughout the world. According to recent United Nations estimations, the majority of the world's population is living in urban areas and the overall proportion is expected to reach 65% in the middle of the 21st century (United Nations, 2014). However according to the World Bank (2015) the urban population in Iraq was already 69.5% in 2015.

A gradual increase in the percentage of build-up land results in a reduction of the vegetated areas. Urbanization alters environmental conditions such as climate, biodiversity, quality of water and air that has a substantial impact on human comfort and health. The impacts may become pronounced when they interact on a global scale. Therefore a better understanding of the effect of urbanization is required to support greener sustainable development and climate change strategies (Imhoff et al., 2010). Possible solutions include the creation of green spaces, that are irrigated and fertilized, which are found to considerably reduce the negative consequences associated with transformation into urban environment (Gregg et al., 2003). Remote sensing of urban expansion and vegetation clearing provides information on the spatial and temporal patterns of urban development and its impacts to the environment.

MODIS sensor is able to provide information necessary for monitoring ecosystem dynamics at adequate spatiotemporal resolution using vegetation indices such as

EVI and the NDVI. VIs are spectral transformations of two or more bands designed to enhance the properties of vegetation to allow reliable spatial and temporal inter-comparisons to photosynthetic health and canopy structural changes. NDVI is chlorophyll sensitive, while EVI is more responsive to canopy structural variations including leaf area index (LAI), canopy type and architecture. The VIs complements each other and improves upon the detection of vegetation changes and the extraction of canopy biophysical parameters (Huete et al., 2002). NDVI was found to be highly sensitive to the vegetation presence as well as its density and dynamics (Zhang et al. 2006). For this reason, the MODIS NDVI can be employed in the quantification of green biomass and vegetation cover. A recent study in China by Li et al. (2010) found that MODIS NDVI was highly correlation with the field verification data of vegetation cover and had obvious advantages for predicting natural vegetation coverage than EVI within their study area.

MODIS VIs are sensitive to multi-temporal vegetative biophysical and canopy changes. Both NDVI and EVI have a good dynamic range and sensitivity for monitoring and assessing spatial and temporal variations in vegetation amount and condition. NDVI generally has a higher range of values over semiarid sites, and the opposite for more humid forested sites with a lower range (Huete et al., 2002). With the support of satellite imagery time-series data it became possible for researchers to obtain phenological information at various spatial and temporal intervals. Looking at publications in the

area, it should be stated that the first use of satellite data in the identification of key phenological parameters using NDVI was described in publications by Tucker and Myneni (Tucker et al., 2001; Myneni et al., 2007).

However, there is a range of recent studies in developed and developing countries, focused on the application of Moderate Resolution Imaging Spectroradiometer (MODIS) to model trends in vegetation patterns. Mertes et al. (2015) demonstrated a methodology over East Asia to monitor urban land expansion at continental to global scales using MODIS data, including a multi-temporal composite change detection approach based on MODIS 250 m annual maximum EVI. The study explained that EVI data improved the classification results and is capable of distinguishing between landscape changes in urban environment. A publication by Yuan and Bauer (2007) demonstrated a strong correlation between percent impervious surface and land surface, covering twin cities of Minnesota. Lunetta et al. (2006) preferred MODIS Normalized Difference Variation Index (NDVI) for a time series for southern Virginia with the available MODIS quality indicators. Colditz et al. (2006) demonstrated the effects of different quality levels of MODIS NDVI of evergreen broadleaved forest and savanna in western Africa. It was found that low quality analysis or very lenient settings resulted in a significant decrease in NDVI during the wet season. Therefore, not accurately representing the phenology of evergreen broadleaved forest. A recent study in southern Brazil using MODIS leaf area index has highlighted the merit of the MODIS quality indicators such as NDVI and EVI (Rizzi et al., 2006).

The main driving factors of vegetation growth are precipitation and temperature (Bonan, 2002). Water availability, often directly related to precipitation and its variability, is the driving factor for most semi-arid regions. Several studies have been conducted on the response time between precipitation and phenological activity using satellite-based vegetation indices (Nicholson et al., 1990; Los et al., 2006; Camberlin et al., 2007). Vegetation growth patterns and their connection with climate are studied by vegetation phenology

(Schwartz, 2013). Land surface phenology (LSP) is focused on seasonal features of spatiotemporal variation and LSP is also one of the main ecosystem change indicators (Suepa et al., 2016). With the aid of remote sensing imagery information, it has become possible to establish spatiotemporal phenological changes, which enabled phenological monitoring at global, regional and local scales (Zhang et al., 2005).

The goal of this work is to assess spatiotemporal variations of vegetation indices (EVI and NDVI) in Erbil and its environment between 2000 and 2015, using MODIS satellite data and GIS methods, to determine the impact of urbanization on the spatial distribution and temporal dynamic of urban and surrounding natural and agricultural vegetation cover. This is conducted by evaluating biannual mean vegetation indices captured in March and December to determine spatiotemporal processes. Climate data including rainfall, humidity and temperature is also considered between 2000 and 2015, to enhance the understanding of vegetation change dynamics. Correlation analysis is conducted between each climate variable compared to both vegetation indices. Dynamics of vegetation gain or loss will be evaluated through the study of land cover type changes.

STUDY AREA

The study area for this research is the city of Erbil and its surroundings, which is the capital of Iraqi Kurdistan Region (Fig. 1). Situated in the north-east part of Iraq and lies between longitudes $43^{\circ} 51' 20''$, $44^{\circ} 12' 28''$ and latitudes $36^{\circ} 05' 58''$, $36^{\circ} 15' 54''$ covering an area around 580 km^2 . The total numbers of Iraq Kurdistan residents is approx. 4.8 million people., the area is presented by fertile plains, uphill and mountainous lands (United Nations Development Program, 2016). The Zagros Mountains (3600 m above the sea level) form the main landscape of the north part of the Kurdistan area. Looking at the distribution of vegetation it should be indicated that agricultural areas form approximately 34% of Iraqi Kurdistan while the dominating land cover of this region is

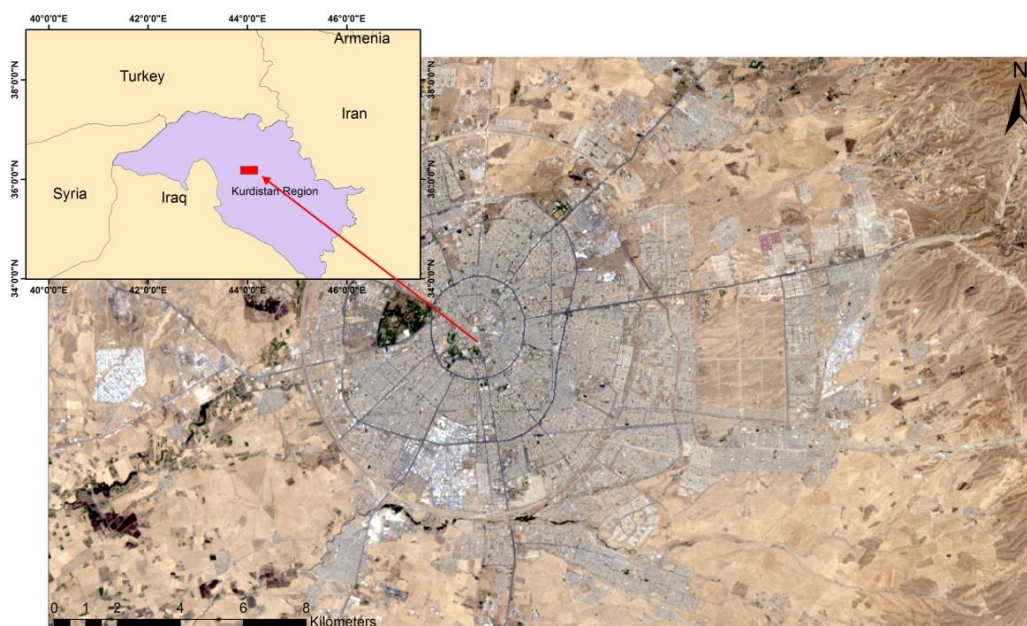


Fig. 1 Overview of Erbil Study area

presented by grasses and forests. The area is mainly characterised as an anticline/syncline system. The Tigris River is located in the southern part of the Erbil Governance. The Iraqi Kurdistan area is heavily employed for agricultural purposes in Iraq (Hameed, 2013) (Fig. 1).

In Erbil Governance approximately 41% and 59% are formed by arable and non-arable lands respectively (SOITM, 2013). The dominating proportion of non-irrigated agricultural crops (93%) is highly dependent on rainfall while the remaining 7% of crops are irrigated. Dominate soil types found in Erbil as well as the adjacent territories are clay and limestone. Their proportions are found to increase with depth. Both the upper and the bottom layers of the Erbil region soil are composed of brown clay. In addition to the indicated types of formations, soils of the city are presented by sand, plaster and gravel (Hameed, 2013).

Erbil City is located in a transition area characterised by Mediterranean and Arid climatic features. The climate is characterized by mild winters and warm/hot summers. An average rainfall range in Erbil area is 300-400 mm per annum with the highest rainfall levels during the period between October and April. The annual relative humidity in the Erbil area is approximately 35% and the monthly average air temperature ranges from 10 °C to 25 °C. The climate of the study area is typically dry in summer with little to no precipitation, while winters are wet (Hameed, 2013). In 2011, the Erbil municipality has a population of 884,299 people and a density of 6000 persons per km² and the population is rapidly expanding.

DATA AND METHODOLOGY

Data

MODIS Vegetation Indices

Vegetation indices such as NDVI and EVI are designed to provide consistent spatial and temporal comparisons of vegetation conditions and cover, allowing biomass productivity monitoring and quantifying changes in vegetation cover (Colditz et al., 2006; Mertes et al., 2015; Rizzi et al., 2006). The study uses a 16 day composite for each NDVI and EVI raster (MOD13Q1), captured by the MODIS-Terra sensor. Blue, red, and NIR reflectance bands, centered at 469 nm, 645 nm and 858 nm respectively, are used to determine the MODIS vegetation indices, with a spatial resolution of 250m (USGS, 2016). MODIS products are computed from atmospherically corrected bi-directional surface reflectance that have been masked for water, clouds, heavy aerosols, and cloud shadows (USGS, 2016). The equations for NDVI and EVI are described below (Huete, et al., 2002).

The NDVI is determined as:

$$NDVI = \frac{NIR - Red}{NIR + Red}$$

The EVI is determined as:

$$EVI = 2.5 \frac{NIR - Red}{NIR + (6 * RED) - (7.5 * BLUE) + 1}$$

The purpose of EVI is to improve on a standard NDVI MODIS product. The benefits of EVI include; enhancement of vegetation signal and sensitivity in biomass abundant regions, reduction of soil and atmospheric effects and the reduction of the smoke impact, generated as the result of biomass combustion in tropical area (Xiao et al., 2009). Improving on NDVI, MODIS includes (EVI) that minimizes canopy background variations and maintains sensitivity over dense vegetation conditions (USGS, 2016). The EVI also uses the blue band to remove residual atmosphere contamination caused by smoke and sub-pixel thin clouds. The MODIS NDVI and EVI products are computed from atmospherically corrected bi-directional surface reflectance that have been masked for water, clouds, heavy aerosols, and cloud shadows (USGS, 2016). MODIS (MOD13Q1) data was employed to create a time series of NDVI and EVI over the study area annually, between 2000 and 2015 to determine variations of vegetation extent.

MODIS Land Cover

The study uses MODIS Land Cover Type Yearly L3 Global 500m resolution (MCD12Q1), Land Cover Type 1 (IGBP) global vegetation classification scheme where selected among five global land cover classification systems. The MODIS land cover product (MCD12Q1) is classified into five land cover classes; Open Shrub land, Grassland, Cropland, Urban/Built-up area and Bare or spare vegetation. MODIS land cover is used to carry out change assessment and distribute NDVI and EVI to in land cover classes.

Climate Data

Average temperature, humidity and total rainfall and for March and December were collected from Erbil station and plotted over the 15 year period (2000-2015). Humidity data was collected at the altitude of 470 m. All climate data was sourced from the Kurdistan region government, Ministry of Agriculture and Water Resources (2016).

Methodology

The year of 2005 was chosen as a moderate year in terms of temperature and rainfall, to avoid the impact of climate extremes on the results. Where average of rainfall and temperatures were extracted for 75 years and the selected year was closer to moderation. Both NDVI and EVI was March the month of highest value, while the lowest levels of vegetation were identified in December (Fig. 2).

The project methodology was summarized in Figure 3. Data compilation and raster statistics were generated in ArcGIS 10.3. Statistical analysis and investigation of possible trends were carried in Microsoft Excel. Pre-processing of satellite data was required and was conducted in the study. Data pre-processing for included checking pixel reliability and vegetation index quality. Bad pixels are omitted from the analysis as they represent clouds, shadows from the clouds and cover the true value of the ground reflectance. Where

the pixel representation must be more than 2/3 of the area, therefore the 2009 data for both March and December contain a very high portion of bad pixels. Several years of data captured in December (2000-2002, 2006-2009 and 2011) also contain very high portions of bad pixels (Table 1).

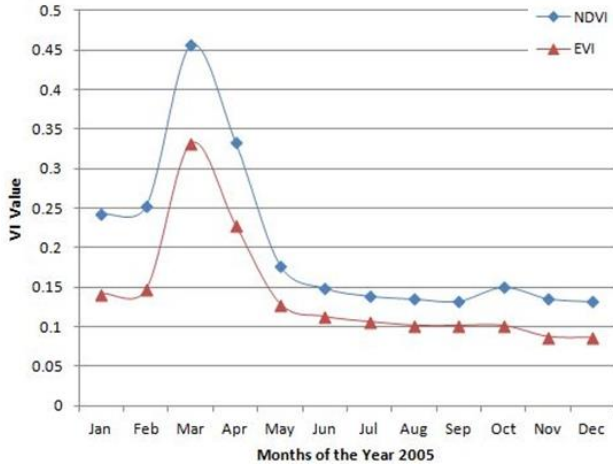


Fig. 2 Mean NDVI, EVI time series from months of the year 2005, showing minimum and maximum values in the study area

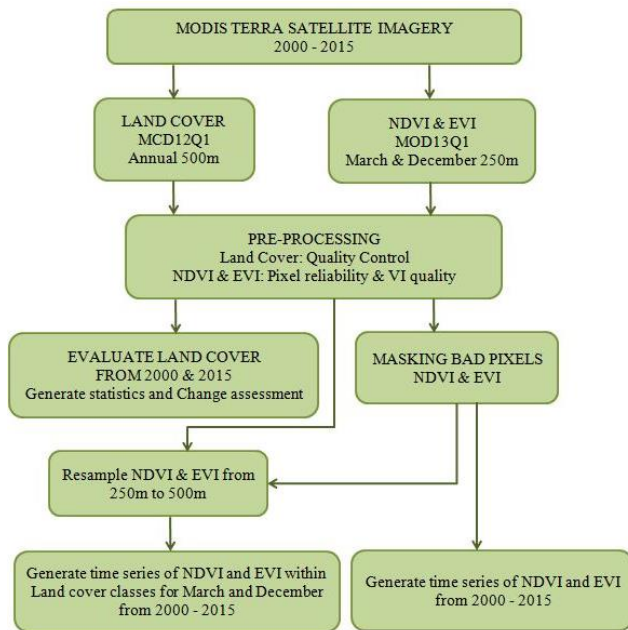


Fig. 3 Methodology summary of the project

Mean NDVI and EVI were generated to provide an average index over the complete study area, allowing the comparison between years to examine a temporal trend. Plots of monthly NDVI and EVI statistics (mean, minimum, maximum and standard deviation) are generated from 2000 to 2015, identifying temporal variations.

MODIS land covers (MCD12Q1) the quality control of the pixels was verified and all were excellent. Conducting detection of change assessment, by comparing the areas of five land covers and generate time series of NDVI and EVI within land cover classes from 2000 to 2015.

Table 1 Summary of QA layers good pixel representation for each year

	March		December
Year	Pixel representation (%)	Year	Pixel representation (%)
2000	100	2000	40.7
2001	100	2001	66.55
2002	100	2002	49.93
2003	100	2003	81.03
2004	100	2004	97.43
2005	100	2005	96.68
2006	100	2006	71.32
2007	100	2007	47.9
2008	100	2008	65.66
2009	56.81	2009	56.83
2010	98	2010	99.47
2011	100	2011	68.02
2012	91.33	2012	87.61
2013	100	2013	90.8
2014	99.88	2014	99.98
2015	100	2015	96.78
Mean	96.63	Mean	76.04

RESULTS

This section presents time series scatter plots of mean NDVI and EVI values and summary statistics including standard deviation, minimum and maximum.

MODIS NDVI and EVI

An obvious difference is apparent between March and December of mean NDVI and EVI over the 15 year period in the same area, presented in Figures 4 and 5. March had significantly higher means and greater variability of VI levels compared to December. December showed some variability at maximum VI levels however the mean was fairly constant with a small peak in 2014. The differences between March and December could be based on seasonal growth variations. After the wet season, March generally has much greater NDVI and EVI values, expect for 2008. In December 2008 NDVI and EVI values were very similar to the averages in March. Both VI in March 2010 showed highest level due heavy rains this month. However both months for NDVI and EVI showed a gradual increasing trend from 2000 to 2015 (Fig. 4 and 5). Important to note is that both NDVI and EVI time series plots appear to have similar patterns.

NDVI and EVI images for March 2002 (baseline) and March 2015 (final year) are compared in Figure 6 to visualize the spatiotemporal variation of vegetation. March had the highest vegetation growth, and will best represent differences in true vegetation coverage extent. It is evident that the spatial distribution of urban areas and/or bare or sparsely vegetated areas surrounding Erbil has expanded over the past 15 years and consequently vegetation surrounding the urban centre has been replaced by urban growth. However it appears that agricultural areas in rural region have expanded possibly to support population growth. The NDVI maps appear to have greater areas of high vegetation health compared to the EVI maps (Fig. 6).

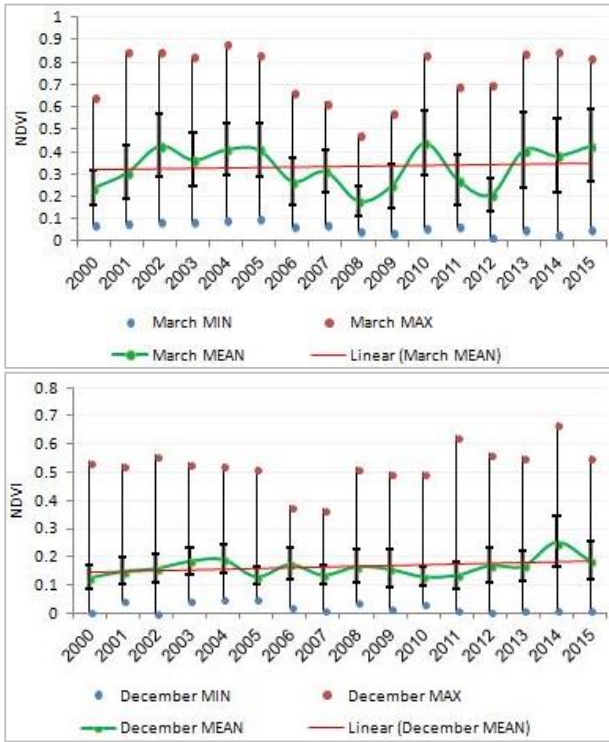


Fig. 4 NDVI Time series from 2000 – 2015 in the whole area, comparing mean, minimum, maximum and standard deviation values for March and December in the study area

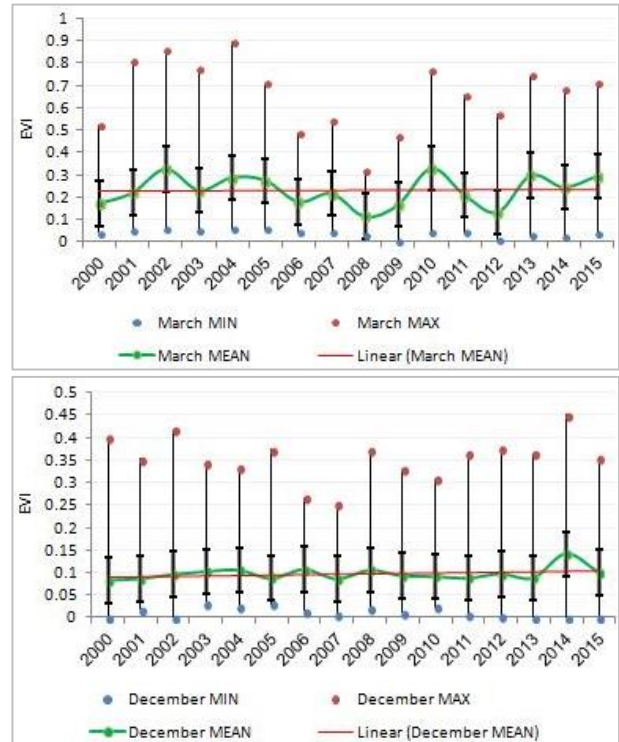


Fig. 5 EVI Time series from 2000 – 2015 in the whole area, comparing mean, minimum and maximum and standard deviation for March and December in the study area

MODIS (MOD13Q1)

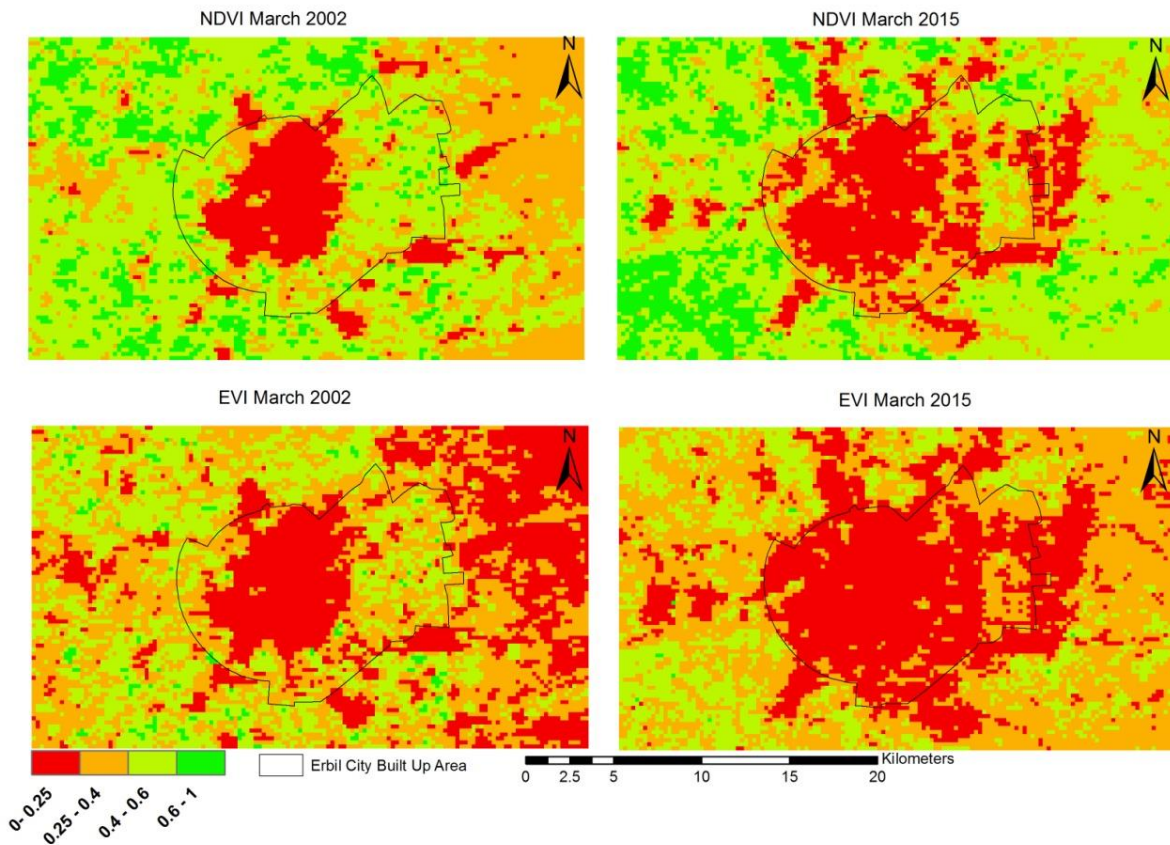


Fig. 6 NDVI and EVI maps for March 2002 and 2015

Interesting to note, there is a decline in urban green spaces such from 2002 to 2015 in both NDVI and EVI images. The green space may still be present, but in poor health or have reduced in size.

The NDVI and EVI values captured in March had a greater variability, compared to data captured in December. Annual MODIS data captured in March was used to calculate land cover statistics for time series for both indices (Fig. 7 and 8). The majority of the years contained VI values with little variation, except for both VI in 2002 2010 and 2014 (Fig. 7 and 8). This may be explained by abrupt climatic changes resulting in vegetation growth or decline. The cropland class had the highest NDVI values over any other class during the 15 year period (Fig. 7), which is expected as healthy green homogeneity crops will exhibit a higher NDVI value compared to open shrub and grassland ecosystems that contain various plant species with varying foliage colours and types. Bare/sparsely vegetated and urban areas displayed the lowest mean NDVI vales over the study area over the 15 year period.

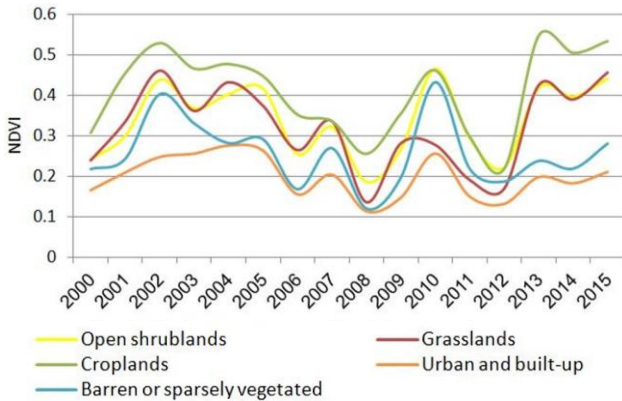


Fig. 7 Mean NDVI values from March 2000–2015, comparing 5 land cover types

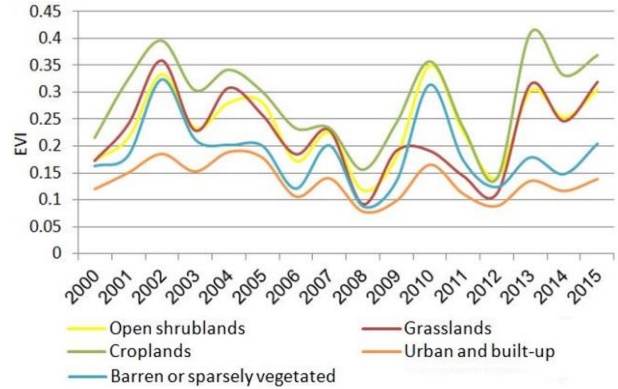


Fig. 8 Mean EVI values from March 2000 – 2015, comparing 5 land cover types

The EVI time series presents as well similar trend, as cropland appear to generally have a greater biomass over grasslands and open shrub land over the 15 year period, (Fig. 7). Cropland EVI exceeds grassland possibly from additional crop irrigation for those years. As expected EVI in urban areas remains relatively low over the study period, however EVI in bare/sparsely vegetated classes seems to spike in 2002 and 2010 (Fig. 8). The spikes may be explained by an increase in sparse vegetation species and opportunistic species such as weeds. Based on Figures 7 and 8 it can be suggested that NDVI is more sensitive than EVI for fluctuations in vegetation health and biomass.

MODIS Land Cover

Figure 9 compares MODIS land cover classification between 2000 and 2015. The foremost visual difference is the reduction of bare or sparsely vegetated land and increase in grasslands. The spatial distribution of the urban area has remained relatively similar at this resolution. Therefore, we verified through Landsat images 30m resolution, where urban and Built-up area 58% increased over

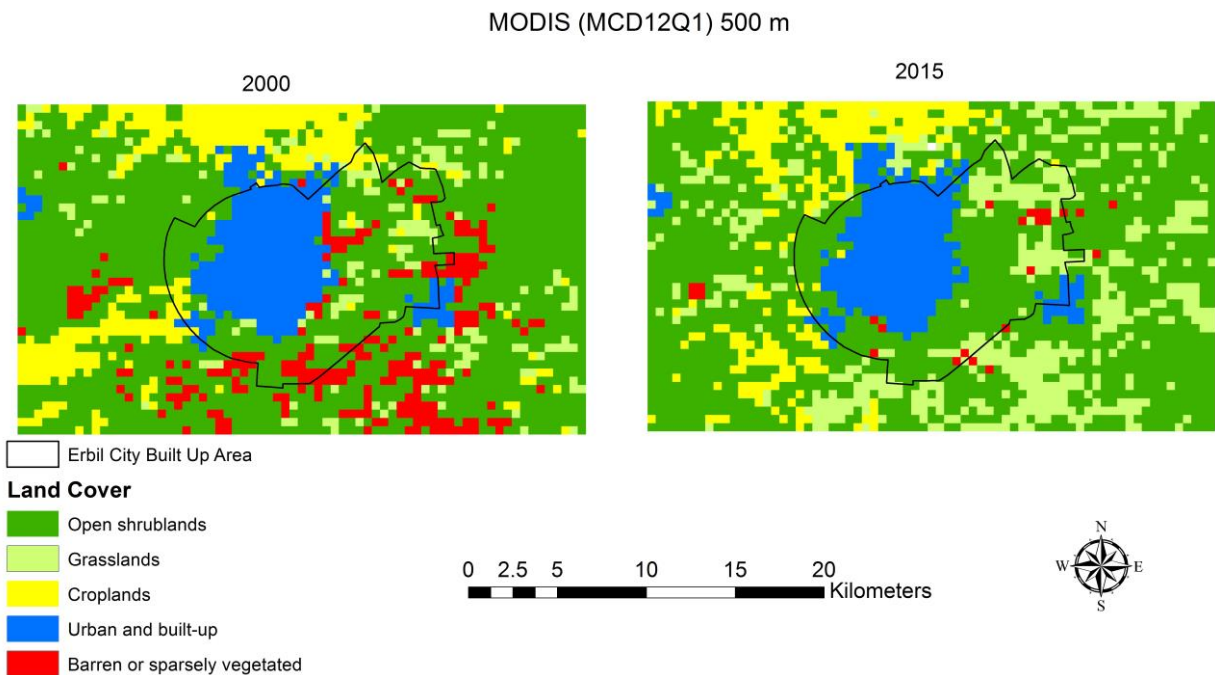


Fig. 9 Comparison of MODIS land cover between 2000 and 2015

the time period (Hussein, 2017). The area of land cover types and percentage differences comparing the baseline year 2000, to the final year 2015, are highlighted in Table 2. Between the 15 years there has been a significant decrease of bare or sparsely vegetated land (90%) and a slight decrease of cropland (18%) and open shrub land (4%). However there has been a 67% increase of grasslands. Based on these observations, we can assume the majority of bare or sparsely vegetated land has transitioned into grassland, outside of the urban center between 2000 and 2015.

Table 2 Land cover area and percentage differences comparing 2000 to 2015

Land Cover	2000	2015	Difference (ha)	Change within Cover type (%)
	Area (ha)	Area (ha)		
Open Shrublands	42825	41050	1775	-4
Grasslands	4375	13150	-8775	+67
Croplands	8275	6775	1500	-18
Urban and Built-up Area	7425	7425	0	No change
Barren or Sparsely Vegetated	6100	600	5500	-90
Total	69000	69000		

Climate

Annual rainfall, average temperature (Fig. 10), and average humidity (Fig. 11) and covering the 16-year period are presented below. Rainfall was considerably high in 2003 and 2006, followed by low rainfall years in 2004, 2010, and 2007 (Fig. 10). After 2007 total rainfall has remained more constant with less variation between years, with a positive increasing trend towards 2015.

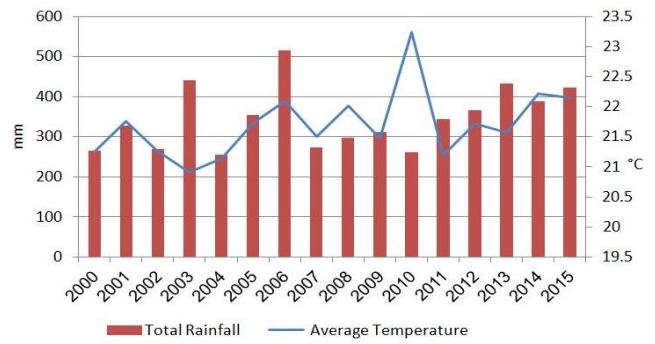


Fig. 10 Total annual rainfall and average temperature time series from 2000 – 2015

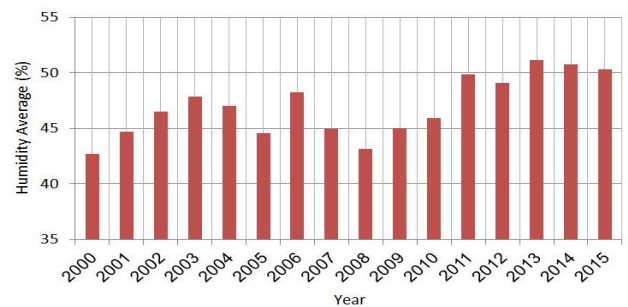


Fig. 11 Annual mean humidity time series from 2000 – 2015

Humidity shares a similar pattern to rainfall, with high averages in 2003 and 2006, followed by lows and then a gradual increasing trend towards 2015 (Fig. 11). Interesting to note, average temperature for 2003 was the lowest over the 16 year period, while in 2006 the temperature was relatively high for that period (Fig. 10). In 2010 average temperature spiked at 23°C, the highest average temperature over the 16 years. By comparison total rainfall was very low in 2010 with average humidity. Average rainfall, humidity and temperature all appear to have generally increased between 2000 and 2015 with various positive and negative fluctuations in-between.

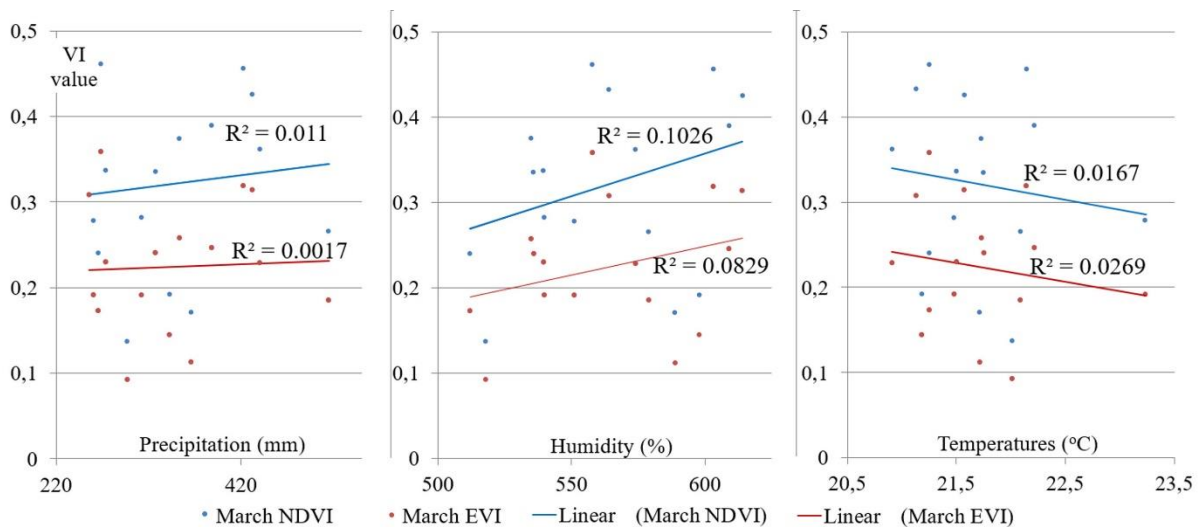


Fig. 12 Time series (2000 – 2015) correlation analysis between rainfall, humidity, temperature and vegetation indices (NDVI and EVI) within grasslands for March

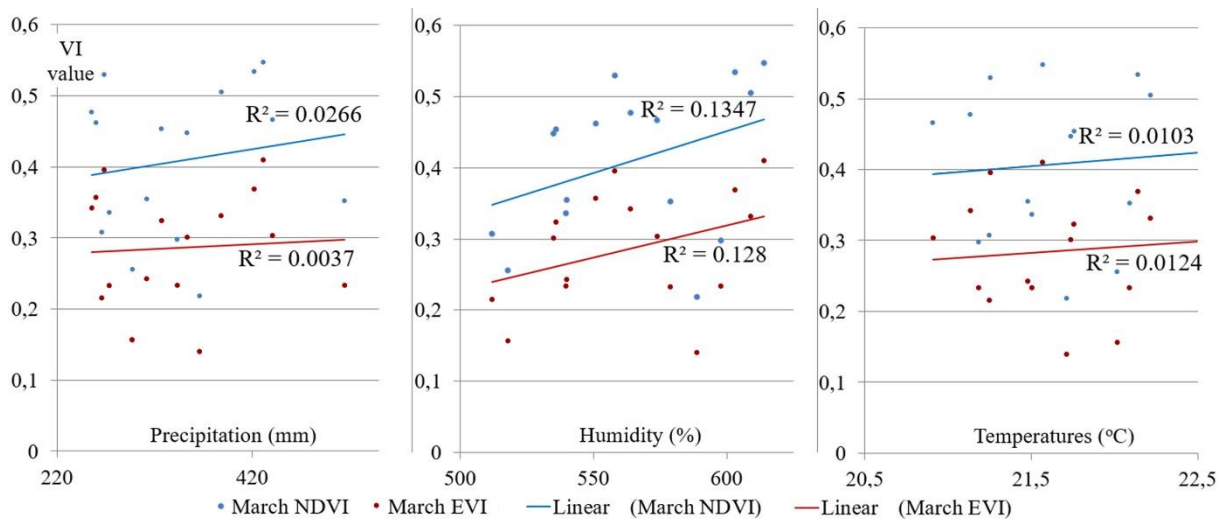


Fig. 13 Time series (2000 – 2015) correlation analysis between rainfall, humidity, temperature and vegetation indices (NDVI and EVI) within croplands for March

Climate variables were compared with NDVI and EVI by correlation analysis (Fig. 12-13). Rainfall, humidity and temperature averages for March were compared to mean NDVI and EVI levels within grasslands and croplands captured in March. There was no strong evidence of correlation between NDVI or EVI and any of the climate variables. All comparisons between climate and NDVI or EVI were not significant.

DISCUSSION

Remote sensing of urban sprawl and green space provides information on the spatial and temporal patterns of human growth that are useful for understanding differences in socioeconomic and political factors as well as environmental and climatic impacts (Mertes et al., 2015). Based on NDVI and EVI MODIS data (Fig. 6) imagery the spatial distribution of urban areas in Erbil and the bare around it has expanded. Consequently the vegetation area has been cleared and replaced over the past 15 years by urban growth.

However it appears that agricultural or grassland areas in rural regions have expanded slightly, to possibly support population growth. Based on our observations, we can assume most of bare or sparsely vegetated land has transitioned into grassland, outside of the urban centre. Urbanization can substantially alter the abundance and distribution of vegetation (Gregg et al., 2003). However this statement is unclear for the city and surrounds of Erbil based on the spatial resolution (250m, 500m) of the MODIS data. A finer imagery resolution of 30m or less is required.

Mapping within an urban landscape is not an easy task, due to the small footprints of features such as parks and trees, mixed between clusters of buildings and roads. Urban areas are typically heterogeneous in both material composition and configuration and with new development they are often highly variable between locations (Mertes et al., 2015). Vegetation indices are useful for extracting green space features from complex urban areas. The NDVI and EVI MODIS imagery with its course

resolution was still able to successfully identify spatial and temporal patterns of human growth in the City of Erbil. Additional research is recommended utilizing imagery of higher resolution such as Landsat with a 30m spectral resolution. To determine the distribution of green space within the urban area of Erbil, Worldview 2 imagery is recommended with 2m spatial resolution.

The urban expansion pattern observed in Erbil is highly dependent on the Tigris River. The city is represented by a matrix of interconnected patches that vary from non vegetated areas such as impervious surfaces to areas of high plant diversity (SOITM, 2013). The combination of vegetated land patches lead to the formation of elevated plant diversity in Erbil (Neil and Wu, 2006). Agricultural activities such as clearing, burning and herbicides uses have impacted plant community distribution outside of the urban centers. However within the urban landscape the observed vegetation patterns or urban green spaces (UGS) are a direct consequence of reconstruction activities, including alteration of urban landscape as well as city gardens and forests. The green areas in Erbil are managed by governments, institutions and individuals. It is expected that the outlined bodies directly control abundance and biodiversity of green spaces within the city. Erbil is one of the oldest cities in the world, therefore it could be expected that the cities preservation activities should be aimed towards green space and plant diversity conversation, however this is not the case (UNESCO, 2016).

Urban Green Spaces are essential constituents of the urban structure that enhance resident's quality of life and behaviour (M'Ikiugu et al., 2012). UGSs contribute to the sustainable development of urban ecosystems and provide a range of ecological and social benefits including; biodiversity and historic landscape feature conservation, regulate local microclimate, protection of air quality, noise absorption and water resources protection. UGS also maintain and improve human well-being by contributing to recreation and aesthetic activities (M'Ikiugu et al., 2012).

CONCLUSION

Spatiotemporal variations of vegetation indices (EVI and NDVI) between 2000 and 2015 was successfully observed using MODIS data. It was evident that the spatial distribution of bare or sparsely vegetated areas surrounding Erbil has expanded over the past 15 years, and consequently vegetation surrounding the urban centre has been replaced by urban growth including grassland or green space. It is suggested the majority of bare or sparsely vegetated land has transitioned into grassland, outside of the urban center between 2000 and 2015.

There was no evidence of correlation between any of the climate variables to NDVI or EVI. March 2010 was a dry, warm period, which spiked VI averages above normal, mainly because of sparsely vegetated or open shrub lands. Opportunistic weed and dry grass species that thrive in these conditions may explain the spike in VI. Overall vegetation indices showed a gradual increasing trend from 2000 to 2015, but vegetation extent decreased based on the land cover information.

Human alteration of the environment has caused a spatiotemporal transition from native plant species to managed monocultures for agricultural purposes or urban development. Considering vegetation distribution in the surroundings of Erbil city it can be stated that according to the collected MODIS data the Iraqi Kurdistan region manifested high levels of vegetation regardless of the period of the year. It is expected that vegetation patterns in this region are highly manipulated and dependent on anthropogenic activity because this region plays an important role in the agricultural infrastructure of the country.

References

- Bonan, G. 2002. Ecological Climatology. Cambridge University Press, p. 690.
- Camberlin, P., Martiny, N., Philippon, N., Richard, Y. 2007. Determinants of the interannual relationships between remote sensed photosynthetic activity and rainfall in tropical Africa. *Remote Sensing of Environment* 106 (2), 199–216. DOI: 10.1016/j.rse.2006.08.009
- Colditz, R., Conrad, C., Wehrmann, T., Schmidt, M., Dech, S. 2006. Generation and assessment of MODIS time series using quality information. *IEEE International Geoscience and Remote Sensing Symposium, IGARSS*, p.6. DOI: 10.1109/igarss.2006.200
- Gregg, J., Jones, C., Dawson, T. 2003. Urbanisation effects on tree growth in the vicinity of New York City. *Nature* 424, 183–187. DOI: 10.1038/nature01728
- Hameed, H. 2013. Water Harvesting In Erbil Governorate, Kurdistan Region, Iraq, Lund University.
- Huete, A., Didan, K., Miura, T., Rodriguez, E.P., Gao, X., Ferreira, L.G. 2002. Overview of the radiometric and biophysical performance of the MODIS vegetation indices. *Remote Sensing of Environment* 83 (1-2), 195–213. DOI: 10.1016/s0034-4257(02)00096-2
- Hussein, S. 2017. The geographical evolution of urban greenness in the city of Erbil based on Landsat imagery. Regional Committee of the Hungarian Academy of Sciences, Pécs, 232–239.
- Imhoff, M., Zhang, P., Wolfe, R., Bounoua, L. 2010. Remote sensing of the urban heat island effect across biomass in the continental USA. *Remote Sensing of Environment*, 114 (3), 504–513. DOI: 10.1016/j.rse.2009.10.008
- Kurdistan Region Government, 2016. Ministry of agriculture and water resources, Iraq.
- Li, Z., Li, X., Wei, D., Xu, X., Wang, H. 2010. An assessment of correlation on MODIS-NDVI and EVI with natural vegetation coverage in Northern Hebei Province, China. *Procedia Environmental Sciences* 2, 964–969. DOI: 10.1016/j.proenv.2010.10.108
- Los, S., Weedon, G.P., North, P.R.J., Kaduk, J.D., Taylor, C.M., Cox, P.M. 2006. An observation-based estimate of the strength of rainfall-vegetation interactions in the Sahel. *Geophysical Research Letters* 33(16), DOI: 10.1029/2006GL027065
- Lunetta, R.S., Knight, J.F., Ediriwickrema, J., Lyon, J.G., Worthy, L.D. 2006. Land-cover change detection using multi-temporal MODIS NDVI data. *Remote Sensing of Environment* 105(2), 142–154. DOI: 10.1016/j.rse.2006.06.018
- M'Ilkiugu, M. M., Kinoshita, I., Tashiro, Y. 2012. Urban Green Space Analysis and Identification of its Potential Expansion Areas. *Procedia - Social and Behavioral Sciences* 35, 449–458. DOI: 10.1016/j.sbspro.2012.02.110
- Mertes, C., Schneider, A., Sulla-Menashe, D., Tatem, A.J., Tan, B. 2015. Detecting change in urban areas at continental scales with MODIS data. *Remote Sensing of Environment* 158(1), 331–347. DOI: 10.1016/j.rse.2014.09.023
- Myneni, R.B., Yang, W., Nemani, R.R., Huete, A.R., Dickinson, R.E. et al. 2007. Large seasonal changes in leaf area of amazon rainforests. *PNAS* 104(12), 4820–4823. DOI: 10.1073/pnas.0611338104
- Neil, K., Wu, J. 2006. Effects of urbanisation on plant flowering phenology. *Urban Ecosystem* 9(3), 243–257. DOI: 10.1007/s11252-006-9354-2
- Nicholson, S., Davenport, M., Malo, A. 1990. A comparison of the vegetation response to rainfall in the Sahel and East Africa, using normalized difference vegetation index from NOAA AVHRR. *Climatic Change* 17(2), 209–241. DOI: 10.1007/bf00138369
- Rizzi, R., Rudorff, B., Shimabukuro Y., Doraiswami, P. 2006. Assessment of MODIS LAI retrievals over soybean crop in southern Brazil. *International Journal of Remote Sensing* 27(19), 4091–4100. DOI: 10.1080/01431160600851850
- Schwartz, M., 2013. Phenology: An Integrative Environmental Science. Springer, London, p.602.
- SOITM, 2013. Erbil City. Turkmen Human Rights: Research Foundation, New York.
- Suepa, T., Jianguo, Q., Lawawirojwong, S., Messina, J. 2016. Understanding spatio-temporal variation of vegetation phenology and rainfall seasonality in the monsoon Southeast Asia. *Environmental Research* 147, 621–629. DOI: 10.1016/j.envres.2016.02.005
- Word Bank, 2015. Data Catalog. <http://data.worldbank.org>
- Tucker, C., Slayback, D.A., Pinzon, J.E., Los, S.O., Myneni, R.B., Taylor, M.G. 2001. Higher northern latitude normalized difference vegetation index and growing season trends from 1982 to 1999. *International Journal of Biometeorology* 11(2), 184–190. DOI: 10.1007/s00484-001-0109-8
- UNESCO, 2016. UNESCO World Heritage Centre. <http://en.unesco.org/>
- United Nations Development Program, 2016. United Nations Development Program. <http://www.undp.org/>
- United Nations, 2014. World urbanization prospects. New York: United Nations, p.32.
- USGS, 2016. Vegetation Indices 16-Day L3 Global 250m. https://lpdaac.usgs.gov/dataset_discovery/modis/modis_products_table/mod13q1
- Xiao, X., Zhang, J., Yan, H., Wu, W., Biradar, C. 2009. Land surface phenology: Convergence of satellite and CO2 eddy flux observation. In: Normeets A. (ed.) Phenology of Ecosystem processes. Springer Sciences+Business Media, New York, 247–270. DOI: 10.1007/978-1-4419-0026-5_11
- Yuan, F., Bauer, M. 2007. Comparison of impervious surface area and normalized difference vegetation index as indicators of surface urban heat island effects in Landsat imagery. *Remote Sensing of Environment* 106(3), 375–386. DOI: 10.1016/j.rse.2006.09.003
- Zhang, X., Friedl, M., Schaaf, C. 2006. Global vegetation phenology from moderate resolution imaging spectroradiometer (MODIS): evaluation of global patterns and composition with in situ measurements. *Journal of Geophysical Research* 111(G04017), 1–14. DOI: 10.1016/j.rse.2006.09.003
- Zhang, X., Friedl, M., Schaaf, C., Strahler, A. 2005. Monitoring the response of the vegetation phenology to precipitation in Africa by coupling MODIS and TRMM instruments. *Journal of Geophysical Research* 110(D12), 1–14. DOI: 10.1029/2004jd005263



CENTURIAL CHANGES IN THE DEPTH CONDITIONS OF A REGULATED RIVER: CASE STUDY OF THE LOWER TISZA RIVER, HUNGARY

Gabriel Jonathan Amissah^{1*}, Timea Kiss¹, Károly Fiala²

¹Department of Physical Geography and Geoinformatics, University of Szeged, Egyetem u. 2-6, H-6722 Szeged, Hungary

²Lower Tisza District Water Directorate, Stefánia 4, H-6720 Szeged, Hungary

*Corresponding author, e-mail: gabbyjonad@yahoo.com

Research article, received 1 March 2017, accepted 26 May 2017

Abstract

The Tisza River is the largest tributary of the Danube in Central Europe, and has been subjected to various human interventions including cutoffs to increase the slope, construction of levees to restrict the floodplain, and construction of groynes and revetments to stabilize the channel. These interventions have altered the natural morphological evolution of the river. The aim of the study is to assess the impacts of these engineering works, employing hydrological surveys of 36 cross sections (VO) of the Lower Tisza River for the years of 1891, 1931, 1961, 1976 and 1999. The changes in mean depth and thalweg depth were studied in detail comparing three reaches of the studied section.

In general, the thalweg incised during the studied period (1891-1931: 3 cm/y; 1931-1961: 1.3 cm/y and 1976-1999: 2.3 cm/y), except from 1961-1976 which was characterized by aggradation (2 cm/y). The mean depth increased, referring to an overall deepening of the river during the whole period (1891-1931: 1.4 cm/y; 1931-1961: 1.2 cm/y; 1961-1976: 0.6 cm/y and 1976-1999: 1.6 cm/y). The thalweg shifted more in the upper reach showing less stable channel, while the middle and lower reaches had more stable thalweg. Although the cross-sections subjected to various human interventions experienced considerable incision in the short-term, the cross-sections free from direct human impact experienced the largest incision from 1891-1999, especially along the meandering sections.

Keywords: thalweg, channel depth, Lower Tisza River, river regulation, morphological changes

INTRODUCTION

Rivers have been altered by human impacts for centuries for economic benefits (flood protection, improvement of shipping routes, energy production, water withdrawal etc.). It is important to understand the consequences of these interventions, since such hydro-morphological and ecological information are crucial to any sustainable future river engineering (Hooke, 1995). The sediment load and its characteristics reflect the overlapped effects of all environmental subsystems of the river's catchment (Fryirs and Brierly, 2001; Fryirs et al., 2007, 2008). If, any of these subsystems change, it should be reflected in the sediment transport, thus in the channel forms of a river (Chruch, 2006; Anderson and Anderson, 2010; Hasanzadeh, 2012). Therefore, alluvial channel morphology is the result of the interactions between channel-bed topography, flow field and sediment movement (van der Berg, 1995; Ferguson, 2010; Latapie et al., 2014; Leigleiter, 2014; Powell, 2014).

Although rivers are natural transporters and exporters of sediments, usually direct human activities on the channel adversely affect this capacity (Yang et al. 2014). The different human impacts have increasingly reduced the amount of transported sediments, as usually

they trap or dredge the sediments i.e. by channel straightening, embanking, widening, removal of riparian vegetation and urbanization (Osei et al. 2015). When these artificial modifications aim to change the channel itself, they are defined as direct human impacts, and include channelization, widening, bank protection, mining and removal of riparian vegetation (Brierly and Fryirs, 2005). On the other hand, when the interventions are not carried out directly on the river but involve the modification of the subsystems within the catchment, and they affect the flow and sediment transfer regime of a river, they are termed as indirect human impacts (e.g. deforestation, land use changes, mining activities and urbanization). These indirect impacts are characterized by spatial and temporal lags of varying intensities. The consequences of these human interventions have been well described on various rivers in the world (Rinaldi and Simon, 1998; Surian, 1999; Liébault and Piegay, 2001; Kondolf et al., 2002; Xu, 2002; Rinaldi, 2003; Yates et al., 2003; Antonelli et al., 2004; Harmar et al., 2005; Pinter and Heine, 2005; Chang, 2008; Kroes and Kraemer, 2013; Kiss and Balogh, 2015; Morais et al., 2016; Nagy and Kiss, 2016).

The riverbeds are quite sensitive to any modification of discharge and sediment supply within the catchment. While the diversion and/or extraction of water from the channel induce aggradation, constructions (e.g. levees and

embankments) increase flow velocity and induce scouring (Landon et al., 1998; Gregory, 2006; Huang et al., 2014). Most European rivers flowed in wide braided channels in the 19th century. However, the 20th century ushered in various forms of human interventions and the concomitant decrease in sediment supply to the channels, therefore most rivers started to narrow and incise (Liébault and Pigay, 2002; Rinaldi, 2003; Surian and Rinaldi, 2003; Liébault et al., 2005; Rinaldi et al., 2005; Wyżga, 2007).

In the Carpathian Basin, diverse direct and indirect human impacts altered the morphology of the Tisza River, which is the second largest river of Hungary. In the 21st century rising flood water levels were recorded on the Tisza River. It could be explained by the catchment-scale runoff increase due to forest clearance, rough grazing, land-use changes, and probably increasing mining and quarrying activities on the catchment (Schweitzer, 2009). Besides these decadal and centurial catchment-scale indirect human impacts, engineering alteration of the channel itself was also responsible for the increasing flood levels. The primary aim of the works was to protect towns and villages, infrastructure and agricultural lands from floods and to support shipping. Therefore, in the late 19th century a system of artificial levees along the Tisza River and tributaries were built, meanders were cut off, new artificial channels were made, and swampy areas were drained by creating drainage canals (Schweitzer, 2009). The superimposed effects of these indirect and direct human impacts had changed the hydrology and morphology of the river.

Although studies have been made to ascertain the impacts of these regulation works, only a short reach of the Tisza River was studied in detail and covered various elements of the channel (Sipos et al., 2007; Kiss et al., 2008). With this study, our goal is to assess the impact of artificial cut-offs and revetment constructions on the depth conditions of the entire Lower Tisza River (ca. 90 km long) channel, highlighting thalweg depth changes between 1891 and 1999.

STUDY AREA

The Tisza River (catchment area: 157200 km², length: 962 km; Lászlóffy, 1982) is the main tributary of the Danube in Hungary. With its source in the North-eastern Carpathian Mountains, it drains the eastern part of the Carpathian Basin flowing through the Great Hungarian Plain. The Hungarian section of the Tisza (L: 596 km, A: 47000km²) is divided into three sections. The studied Lower Tisza River (Fig. 1) stretches from upstream of Csongrád (255 f.km) to the Hungarian–Serbian border

(166 f.km). Based on the degree of human impact and the morphological characteristics, the section was divided into three reaches (Table 1).

Along the Lower Tisza the pre-regulation slope (2.2 cm/km) was increased to 2.9 cm/km by artificial cut-offs. The Maros River, which is the major tributary of the Tisza, has a high-slope (13 cm/km) in its lowland section, thus downstream of their confluence at Szeged the slope of the Tisza increases to 6 cm/km (Kiss et al., 2008; Mezősi, 2009). The Tisza in Hungary has a typical lowland river character, as it transports large amount of fine grained sandy and silty suspended sediment and it has a clayey bed material (Lászlóffy, 1982; Mezősi, 2009; Kasse et al., 2010).

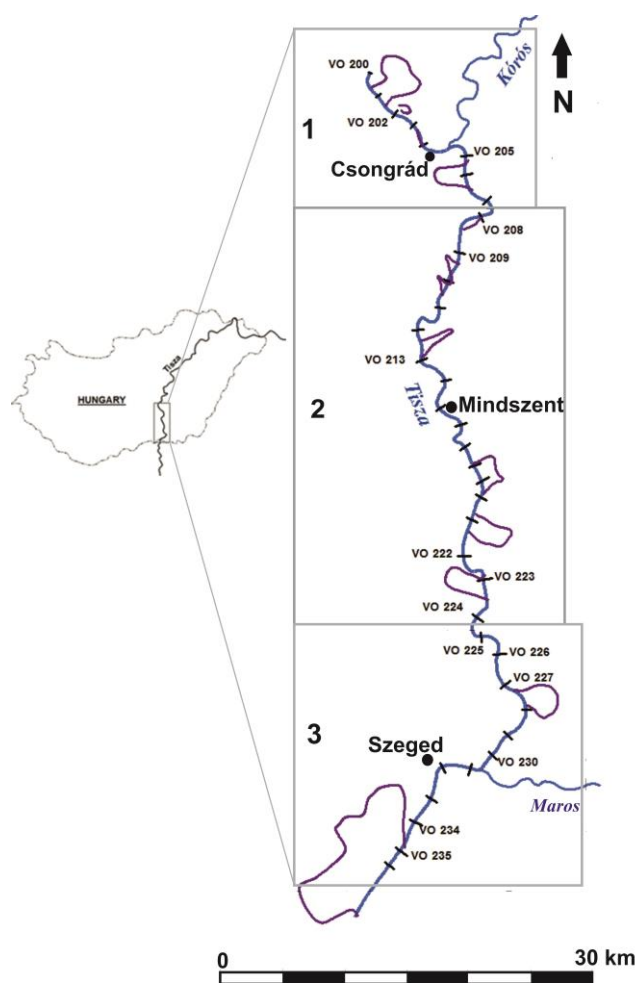


Fig. 1 The studied Tisza section was divided into three reaches based on the morphology of the channel. The studied cross-sections (1-upper reach; 2-middle reach; 3-lower reach) and cut-offs are also indicated.

Table 1 Characteristics of the three river reaches evaluated in this study

Reach	Length (f.km)	Floodplain width			Cut-off (no.)	Revetments	
		Min	Mean	Max		Length (km)	Density (km/km)
Upper	255-238	365	850	1060	3	10.92	0.64
Middle	238-194	560	1000	3200	7	17.53	0.39
Lower	194-166	380	600	975	2	16.03	0.54

Hydrology

The catchment of the Tisza has an annual mean precipitation of 744 mm/y, thus the generated mean run-off is 177 mm/y (mean discharge: 830 m³/s; ICPDR, 2008). On the Tisza, usually two major floods occur. The first flood (March–April) is caused by snow melt, and if the snowmelt is combined with rainfall extremely large floods could develop. The second flood occurs during the summer (June), induced by the early summer rainfall. As the lowland section of the river is long, and its slope is small, this summer flood sometimes superimposes on the preceding spring flood, thus record high floods could develop. The absolute water level change between the highest and lowest water stages is 1355 cm at Mindszent (highest stage measured in 2006: 1062 cm; lowest stage measured in 1968: -293 cm), and 1184 cm at Szeged (highest stage measured in 2006: 960 cm; lowest stage measured in 1968: -224 cm). The discharge also shows considerable hydrological variations. At Szeged, the maximum discharge is 4348 m³/s (in 1932) and minimum value is 58 m³/s (in 2013; Lóczy et al., 2009; Kiss, 2014).

Regulation Works

The late 19th century marked the beginning of catchment-scale engineering interventions on the Tisza River. They involved the disconnection of the Tisza from its wetlands by construction of levees. The flood control levee-system is 2940 km long, and the originally 27000 km² large natural floodplain (which was about a third of the territory of Hungary) was reduced to 21251 km². The aim of artificial levee constructions was to protect the land from inundations and to provide safe areas for agriculture, and to decrease the duration of floods (Szlávik, 2000; Pinke, 2014). Simultaneously, the river was shortened by 38% with 114 meander cut-offs (Dunka et al, 1996; Schweitzer, 2009). As a result of cut-offs, the meandering equilibrium river was transformed into an in-growing meandering one, as its slope almost doubled (Kiss, 2014). The cut-offs accelerated the erosion of the river bed, thus the sediment load increased, which resulted in accelerated deposition on the confined active floodplains (Kiss et al., 2011).

The regulation works in the 20th century continued by the construction of revetments and groynes. Revetments were built to stop the lateral erosion of bends which migrated too close to levees, whilst the groynes facilitated shipping by tightening wide sections and to train sharp bends in order to improve the flood conductivity of the river channel. In total 44% of the banks of the Tisza River were stabilized, mainly between the 1930s and 1960s. However, it started in 1886, whilst the latest was built in 2016.

The second half of the 20th century was the period of dam constructions on Tisza and its tributaries. On the Tisza, three dams (which operate as locks) were built at Tiszalök (1957) and Kisköre (1973) in Hungary, and Törökbecse/Novi Becsej (1976) in Serbia (Bezdán, 2010). The locks were built to impound the water during low stages, thus water withdrawal for irrigation could be secured, but they also produce hydropower and aid navigation. Although they are opened during floods, the

retention of sediments by the dam creates temporal sediment deficit downstream which induces incision (Kiss et al., 2008; Lóczy et al., 2009).

Along the Lower Tisza channel regulations started in 1855, shortening the originally 131 km long studied river section by 30 km, cutting off 12 meanders. The originally 6–8 km wide natural floodplain was reduced to 1 km in average. At Szeged however, the floodplain is just 400 m wide. The levees constricted the floodplain at some sections, thereby reducing its flood conductivity and increasing the flood risk. Therefore, the height of levees was increased too: originally they were just 2.3–3.0 m high, but nowadays their height is 7.0 m, thus they could provide safety despite of the increasing flood levels (Sipos et al., 2007; Kiss et al., 2008; Lóczy et al., 2009; Schweitzer, 2009). In the Lower Tisza 51.4% of the banks are protected by revetments, but their spatial distribution is not even, as it is indicated by the different revetment density of the studied reaches (Table 1).

MATERIALS AND METHODS

To understand the channel depth changes caused by direct human impacts, the maximum and mean depths along cross-sectional profiles were measured and analyzed. The study employed a dataset of hydrological surveys made in 1891, 1931, 1961, 1976 and 1999. The Hydrological Atlas of the Lower Tisza (1974) provided the locations of the surveyed cross-sections and it also showed the bank lines of the river at different dates. The channel surveys were undertaken using fixed geodetic survey points (VO-stones) at approximate spacing of 2.5 km. These VO-stones allowed subsequent surveys at the same cross-sectional profiles at different times. Along a profile the channel depth was measured at 5 m intervals. In the present study relative depths were calculated from the bankfull level, which was determined as lowest point of the bank line (Fig. 2). Based on the cross-sectional profiles the maximum (thalweg) depth and the mean depth for every cross-section were determined. The maximum depth refers to the location of the thalweg. The mean depth was calculated as the arithmetic mean of all depth data of a cross-section.

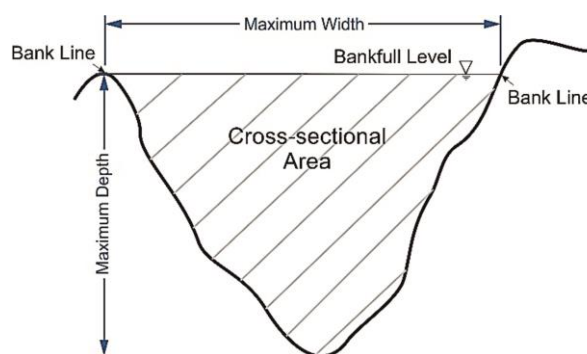


Fig. 2 The depth values were measured from the bankfull level of a cross-section

The spatial data of cut-offs and revetments were provided by Hungarian Lower Tisza Water Directorate. In the study bends and meanders were distinguished, based on Laczay's classification (Laczay, 1982). The sinuosity

of segments was calculated between two inflection points, as the ratio of bend length and chord length (Fig 3). If the sinuosity value was below 1.1, the segment was classified as a bend, if it was above 1.1 the segment was considered to be a meander.

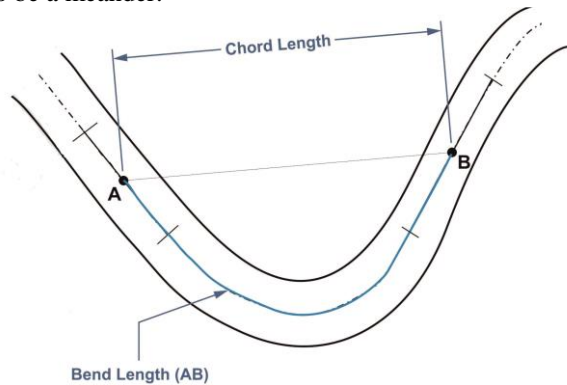


Fig. 3 Determination of inflection points, bend length and chord length along the segments of the river

RESULTS AND DISCUSSION

The presented results include the changes in characteristic depths of the study section, the spatio-temporal variation of the thalweg, and its relative position to the nearest bank. The influence of the various human interventions was also evaluated by comparing the thalweg depth of channel segments influenced by direct and indirect human impact.

A general overview of the studied 36 cross-sections (Fig. 4) indicates that 64% of them are located in slightly sinuous bends, whilst the remaining 36% are situated in meanders. Also, ca. two-third of the cross-sections was under some kind of direct human influence, and only one-third (13) of them is free from direct engineering works, indicating heavy anthropogenic impact on the Lower Tisza River. The cross-sections free from any direct regu

Changes in mean depth of the channel

The mean channel depth gives an indication of the general bed level change of a cross-section, and thus of the studied

segments and reaches. The yearly mean depth changes representative for the entire studied Lower Tisza, indicate incision for all periods (1891-1931: 1.4 cm/y; 1931-1961: 1.2 cm/y; 1961-1976: 0.6 cm/y; and 1976-1999: 1.6 cm/y). The intensive incision of the channel in the first period could be explained by the effect of the cut-offs. The incision continued in the next period (1931-1961) too, though the incision rate reduced by 14%, and this reduction further continued but in a greater extent (50%) between 1961 and 1976. This general reduction in the mean depth of the whole section can be attributed to the gradual evolution of the channel after the first phase of the regulation works towards an equilibrium state. However, in the last period (1976-1999) the channel experienced its highest yearly incision rate. This could be explained by the construction of the revetments which restricted the lateral erosion of the river. This meant the channel could undergo incision readily which resulted in higher incision rate by 1.5 times.

A more detailed analysis of the changes of the mean depth along the studied section (Fig. 5) shows that the location of the greatest incision rates changed by time. While between 1891 and 1931 the greatest incision (12 cm/y) appeared on the upper reach (VO 200), in the next period between 1931 and 1961, it was in the lower reach (10.5 cm/y, VO 225). Between 1961 and 1976, it was measured in the upper reach (14.1 cm/y, VO 207), and finally the incision rate was 9.5 cm/y between 1976 and 1999 which occurred in the middle reach (VO 214). The VO 200 probably incised in response to cut-offs since it is located within an artificial channel, however the remaining sections were all located within meanders. Although most cross-sections referred to incision, some cross-sections had higher incision rates. The period 1976-1999 had its highest aggradation (15.9 cm/y) in the middle reach. The highest rates of aggradation for all the other periods (1891-1931: 8.7 cm/y; 1931-1961: 6.9 cm/y; and 1961-1976: 12.8 cm/y) occurred in the lower reach.

The ratio of the mean depth to the thalweg depth along the studied section of the river (Fig. 6) was also calculated, as it refers to the difference between the mean

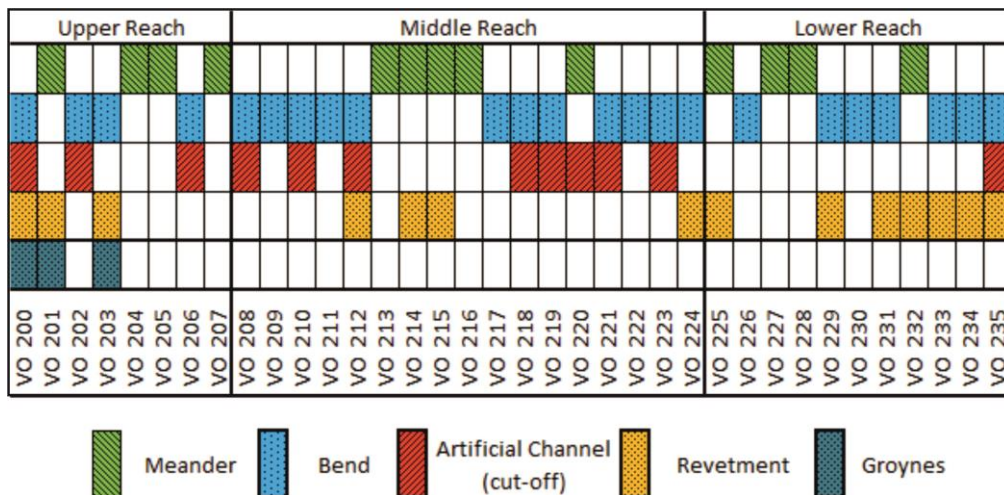


Fig. 4 The studied cross-sections are located in meanders or bends, and various human interventions affected most of their development

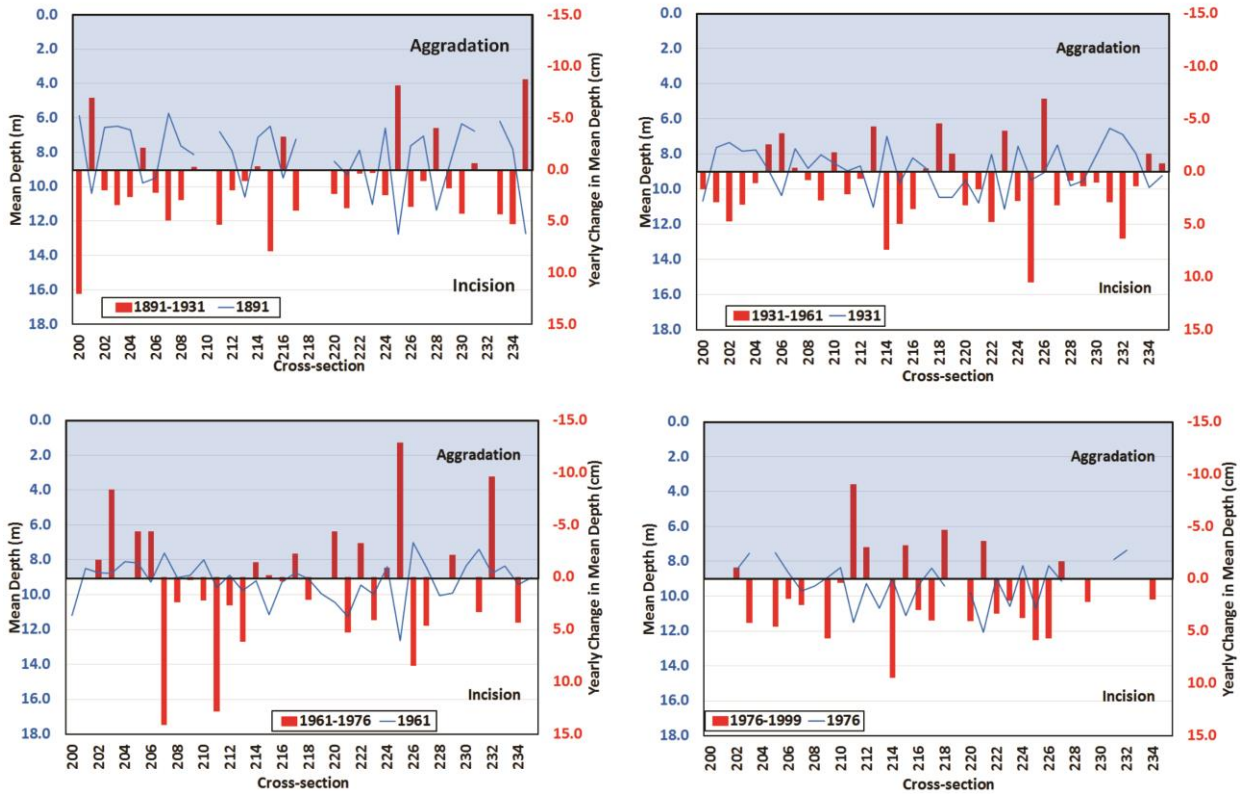


Fig. 5 Changes in mean depth: the mean depth at the beginning of a period between two surveys indicated by blue line; and the yearly change in mean depth in between survey years is indicated by red columns

depth and the thalweg depth: smaller value indicates a greater difference between the thalweg depth and mean depth. The ratio of mean and thalweg depths generally decrease from upstream to downstream (0.70 for upper reach; 0.69 for middle reach; and 0.67 for lower reach), referring to a more even channel bottom towards downstream. However, considering the temporal changes, it is interesting, that the ratio generally increases, referring to more intensive incision of the thalweg itself, than of the bottom of the whole channel.

Changes in the depth of the thalweg

During the studied period the mean thalweg depth of the whole studied section increased from 12.2 m (1891) to 14.1 m (1999), thus by 15.5 %, representing an incision rate of 1.7 cm/y over a century and indicating a general thalweg incision (Fig. 7-9). However, the incision of the

thalweg was not temporally an even process, as at the beginning (1891-1931) the mean thalweg depth increased by 1.2 m which represents an incision rate of 3 cm/y. This incision continued (1931-1961), although its rate became lower (1.3 cm/y). Finally, between 1961 and 1976 the thalweg was subjected to aggradation resulting in the reduction of the mean thalweg depth by 0.3 m (aggradation rate: 2 cm/y). This virtually negated the incision of the previous period. Between 1976 and 1999 the thalweg again experienced incision (2.3 cm/y). These changes could be explained by the human impacts on the studied section: the cut-offs which shortened the channel length caused an increase in bed slope, which resulted in stream power increase. The initial high incision rate could be attributed to the quest of the river to re-establish its equilibrium after the cut-offs.

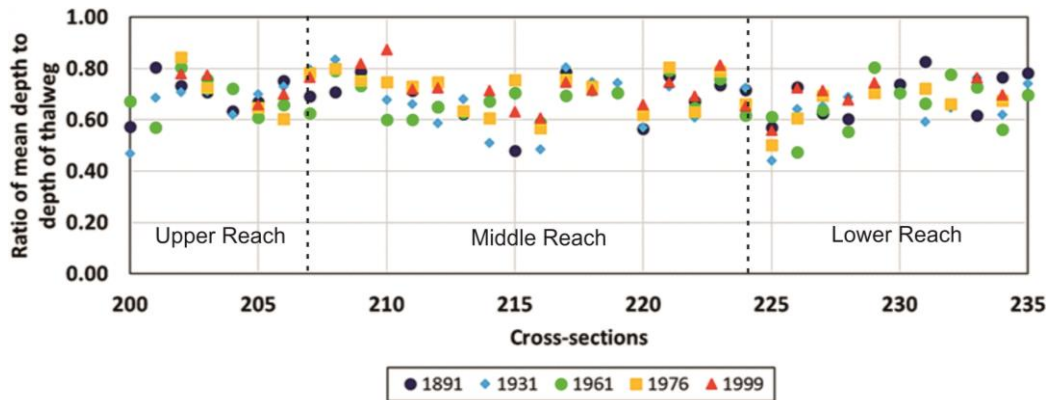


Fig. 6 The variation of the ratio of the mean depth to thalweg along the studied section

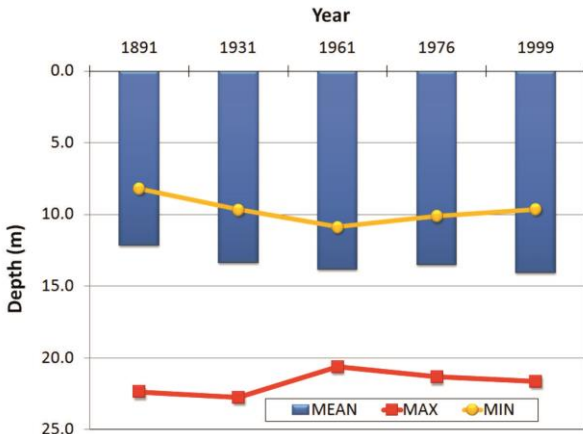


Fig. 7 Variations in mean thalweg depth for the whole studied section

As the channel gradually developed towards quasi-equilibrium, the incision reduced (1931-1961), and the channel evolution process culminated in aggradation (1961-1976), similarly to the stages of the channel evolution model of Simon and Rinaldi (2006). The effect of high floods in the late 20th and early 21st centuries was combined with the effects of revetment and groin constructions, therefore the thalweg started to incise, thus the evolution model distorted. The range (i.e. the difference between the maximum and minimum thalweg depths) was up to 14.2 m in 1891. An increasing minimum thalweg depth and a decreasing maximum thalweg depth caused a reduction in the range until 1961. Afterwards this trend reversed, thus the range increased (1999:

12 m) was still short of the 1891 value. This reduction in ranges points to the development of a uniform channel, implying that although the channel was progressing to equilibrium after the cut-offs, the construction of the revetments and groynes initiated another cycle of dis-equilibrium.

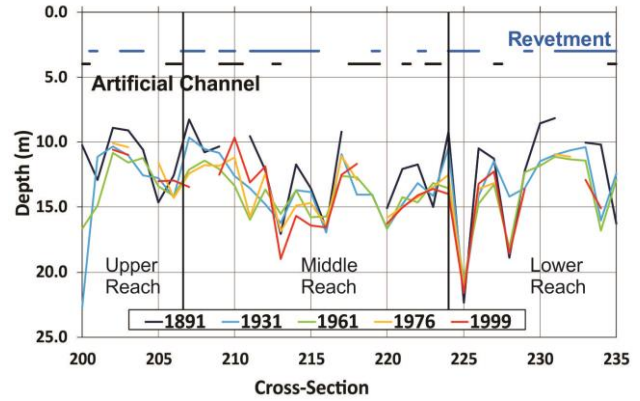


Fig. 8 Variation of thalweg depth along the studied section for various survey years

The spatio-temporal changes of the thalweg were studied comparing the three reaches of the Lower Tisza. The upper and middle reaches show significant changes in thalweg depth, while in the lower reach the thalweg remained relatively stable (Fig. 8). This could be explained by (i) the ponding effect of the Danube and Maros Rivers on the Tisza (Vágás, 1982) and by (ii) the artificially more stabilized and straightened lower reach. The areas of maximum incision along the channel occur mainly downstream of the cut-offs. This means the scouring action of the increased

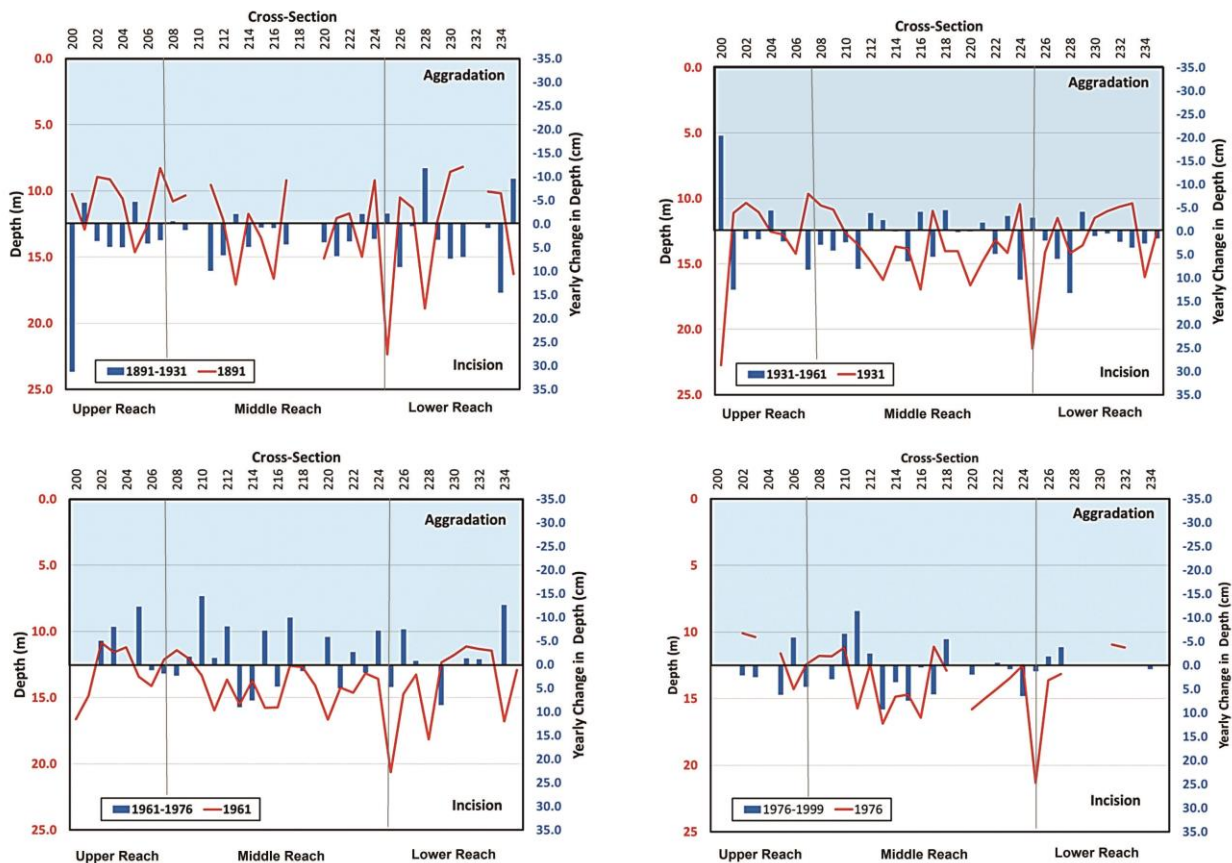


Fig. 9 Changes in thalweg depth: the thalweg depth at the beginning of a period between two surveys is indicated by red line, and the yearly change in thalweg depth in between survey years is indicated by blue columns

stream power was more pronounced at the end of the artificial segments (cut-offs) of the river channel.

The location of the thalweg within the cross-sectional profile was studied in detail too: the greater the ratio between the location of the thalweg to the closest bank and the channel width, the farther is the thalweg to the banks (Fig 10). Considering the whole, ca. 100 year-long period, it seems that the thalweg migrated closer to the banks in the upper reach, whilst the changes within the middle reach are smaller, and in the lower reach the thalweg migrated away from the bank. The trends also show that the location of the thalweg had the greatest range of variations in the upper reach, referring to frequent thalweg changes: in some cross-sectional profiles the thalweg shifted almost across half of the channel width. Although along the middle reach at some cross-sections the thalweg shifts were very small, in general the lower reach had the narrowest range. This implies the lower reach was more stable compared to the middle and upper reaches, although there were some very stable locations within the middle reach.

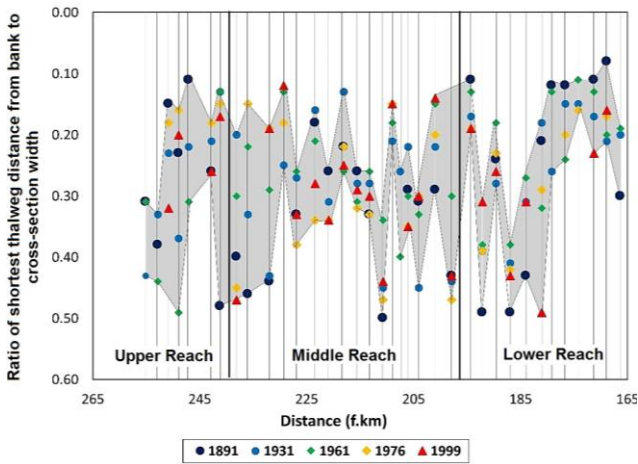


Fig. 10 Variation of the thalweg location relative to the whole cross-section width (the shaded area refers to the range of changes in the position of the thalweg)

The mean thalweg depth values of the upper reach were generally lower than the whole section, and the deepest thalweg depth was characteristic of the lower reach. The incision of the thalweg depth of the three different reaches (Fig. 11) during the whole period reflects an increasing trend towards downstream, as the mean depth of the thalweg increased by 1.3 m (1.2 cm/y) in the upper reach, by 1.7 m (1.6 cm/y) in the middle and 2.5 m (2.3 cm/y) in the lower reach.

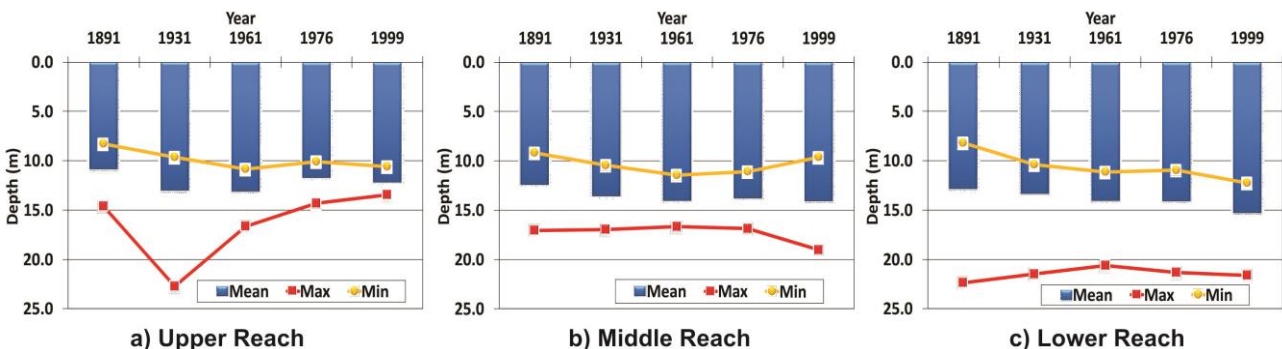


Fig. 11 Variations in thalweg depth values within the various reaches

Effect of human impacts on the evolution of the thalweg depth

To evaluate the role of engineering works on channel evolution, the channel segments not affected directly by cut-offs and revetments were compared to segments created by cut-offs and affected by revetments.

Effect of cut-offs

At the beginning, the mean thalweg depth in non cut-off segments was 11.7 m, while it was 13.7 m in artificial segments (Fig. 12). The higher mean thalweg depth in the artificial segments could be attributed to the initial scouring induced by the artificial channels of the cut-offs. However, by 1999, the mean thalweg depth in the non cut-off segments had increased by 21% to 14.2 m (2.3 cm/y), while in case of artificial segments almost zero net change was recorded. With the exception of 1961-1976 when the channel experienced a general aggradation, there was consistent incision of the mean thalweg depth within the non cut-off segments. In the artificial segments, although there was no net change between 1891 and 1999, there was a depth increase of 0.9 m from 1891 to 1931 (2.2 cm/y), which was followed by a consistent reduction of mean thalweg depth (1931-1961: 1.3 cm/y; 1961-1976: 2 cm/y and 1976-1999: 0.9 cm/y). The incision within the non-cut-off segments are partly due to the construction of revetments (80% of revetments built in segments which were not created by cut-offs) which restricted the lateral erosion within the channel, and therefore increased

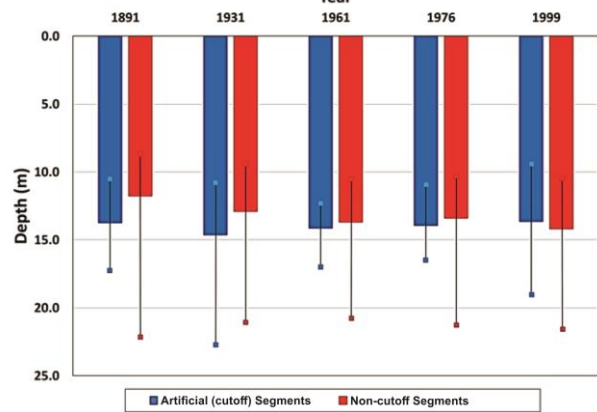


Fig. 12 Comparison of mean thalweg depths for cross-sections within segments affected and not affected by cut-offs, including the range (maximum-minimum) of thalweg depths

scouring of the channel bed to complement the sediment deficiency. Another important factor is the location of a cross-section within a meander or bend. For an alluvial channel, due to the asymmetric nature of cross-sections in meanders, thalweg depths are generally deeper in meanders than in bends or straight segments (Dey, 2014). This statement is also valid for the Lower Tisza (Fig. 13), as the mean thalweg depth of meandering segments is deeper by 3 m than of the non-meandering segments. Within the studied section, more than 90% of the meanders are located in the non-cut-off segments which contributed to its depth increments. However, the relatively narrower widths of the artificial channels also meant that the channel had the tendency to scour with the initially high stream power.

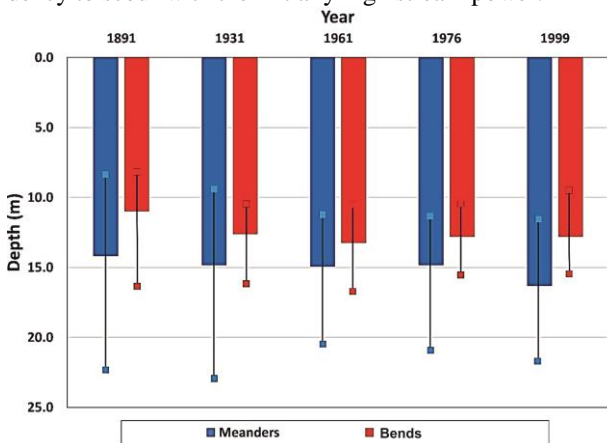


Fig. 13 Comparison of mean thalweg depths for cross-sections within meanders and bends, including the range (maximum-minimum) of thalweg depths

The mean thalweg depth within the reaches followed similar trends as of the entire section for both the non cut-off and cut-off segments (Fig. 14-15) although the magnitude in the depth changes was different. For the non cut-off segments, the upper reach had the least mean depths, and the lower reach had the highest magnitudes in mean thalweg depth. In case of artificial segments, decreasing temporal trends were found in the upper and middle reaches. However, in the lower reach, there was an increasing trend in mean thalweg depth values. Another important observation is the relatively larger ranges in the non cut-off segments compared with the artificial segments.

Effect of revetments and groynes

When evaluating the effects of revetments and groynes in the development of the thalweg depth, it should not be forgotten, that only the combined effect of revetments, groynes and cut-offs could be studied, as they are located very close to each other, and also temporally the responses of the river on these interventions overlap. The comparison of segments without any direct human impact to the artificially altered ones reflect very similar the trends, although the segments with human impacts tend to have smaller ranges (Fig. 16). This is understandable due to the fact that they were artificially created, therefore more evenly engineered than the natural development of the non-affected channel segments. This creates more uniformity within the artificial segments compared to the natural channel segments.

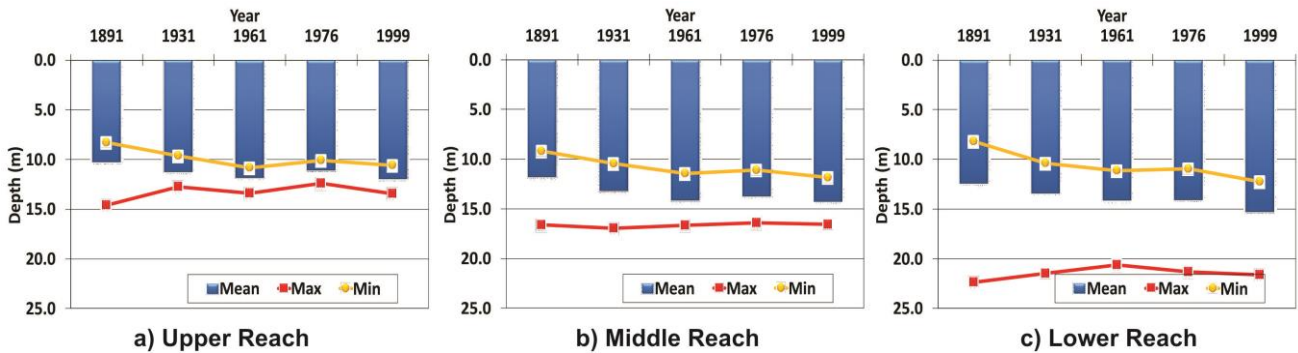


Fig. 14 Variations of the mean thalweg depth within non cut-off segments

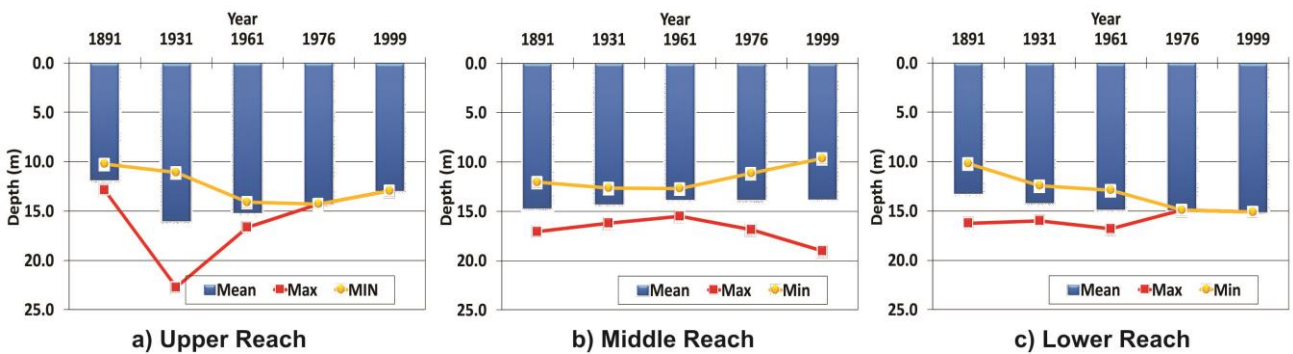


Fig. 15 Variations of the mean thalweg depth within artificial segments created by cut-offs

Focusing on the reaches, the three reaches do not exhibit similar patterns (Fig. 17-18). The absence of clear trends shows the deficiency of generalization to responses of human impacts by rivers in some cases.

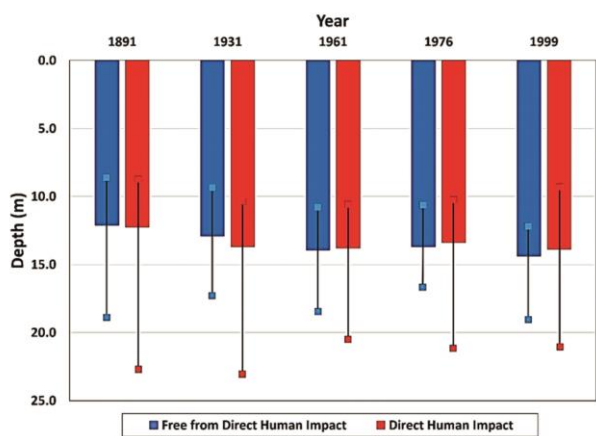


Fig. 16 Comparison of cross-sections with and without direct human impacts

The results indicate that between 1891 and 1999, the mean depth of the channel increased as a response to human interventions and this trend is similar to the response of rivers in Italy to various interventions with some incising by up to 10 m (Surian and Rinaldi, 2003). Using the periods in between the surveys as reference periods, the highest rate of incision occurred immediately after human interventions, similarly to European and North American rivers, which also showed considerable adjustments immediately after human interventions (Smith and Winkley, 1996; Surian and Rinaldi, 2003). As a fluvial response on mid- and late-19th century cut-offs the incision accelerated in the period of 1891-1931, whilst the revetment and groynes constructions of the 1930-1960s increased further the channel depth between 1976 and 1999.

The evolution of the thalweg depth shows that in the periods of 1891-1931, 1931-1961 and 1976-1999, the channel experienced incision while during 1961-1976 it was characterized by aggradation. It marks the attainment of equilibrium before the river readjusted to the construction of revetments. The mean thalweg depths in the upper reach were lower than the mean for the entire section with the highest values referring to the lower reach. The mean depth of the thalweg generally increased from upstream to downstream.

CONCLUSION

The study analyzed the changes in mean depth and thalweg depth of the Lower Tisza River from 1891 to 1999, focusing on the role of direct human impacts (mainly regulation works) in their evolution. Simon and Rinaldi (2006) indicated that degradation of channel beds represents a response to a disturbance in which an excess of flow energy, shear stress or stream power (sediment-transporting capacity) occurs relative to the amount of sediment supplied to the stream.

Acknowledgements

The research was supported by the Stipendium Hungaricum Programme and the Hungarian Research Foundation (OTKA 119193). Data were provided by the Water Directorate of the Lower Tisza District (ATIVIZIG).

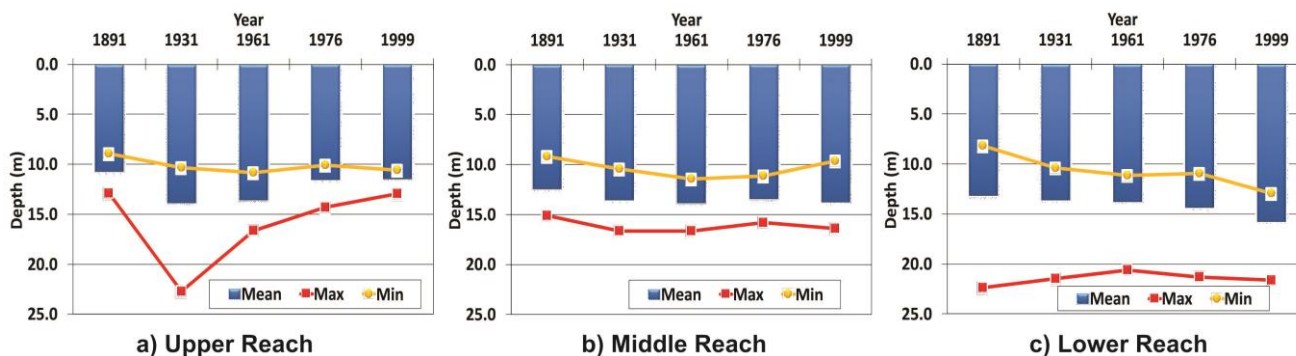


Fig. 17 Variation of the mean thalweg depth for the sections without direct human impact

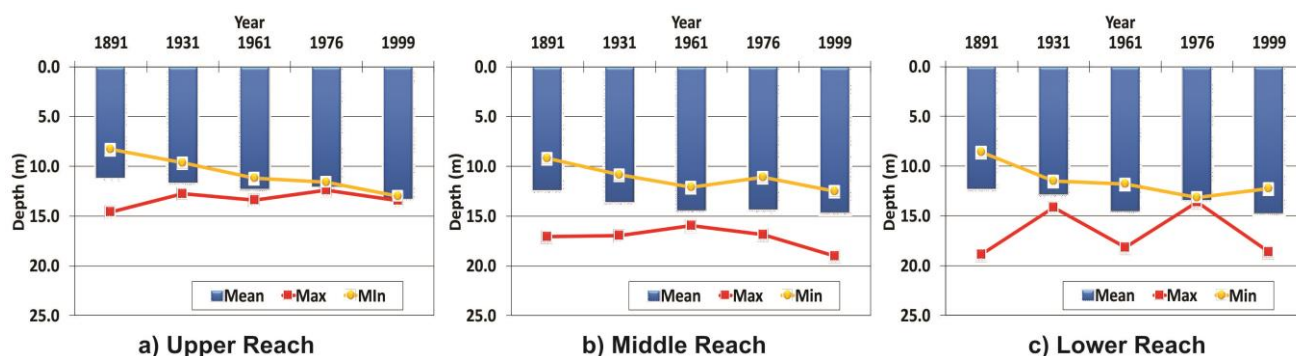


Fig. 18 Variation of the mean thalweg depth for the sections with direct human impact

References

- Anderson, R.S., Anderson, S.P. 2010. *Geomorphology: The Mechanics and Chemistry of Landscapes*. Cambridge University Press, UK, 340 p.
- Antonelli, C., Provansal, M., Vella, C. 2004. Recent morphological channel changes in a deltaic environment. The case of the Rhone River, France. *Geomorphology* 57, 385–402. DOI: 10.1016/s0169-555x(03)00167-3
- Bezdan, M. 2010. Characteristics of the flow regime of the regulated Tisza River reach downstream of Tiszafüred. *Journal of Env. Geogr.* 3 (1-4), 25–30.
- Bravard, J.P., Landon, N., Peiry, J.L., Piégay, H. 1999. Principles of engineering geomorphology for managing channel erosion and bedload transport, examples from French rivers. *Geomorphology* 31, 291–311. DOI: 10.1016/s0169-555x(99)00091-4
- Brierley, G.J., Fryirs, K.A. 2005. *Geomorphology and River Management: Applications of the river styles framework*. Blackwell Publishing, UK, 398 p.
- Chang, H.H. 2008. River Morphology and River Channel Changes. *Transactions of Tianjin Universities* 14 (4), 254–262. DOI: 10.1007/s12209-008-0045-3
- Church, M. 2006. Bed Material Transport and the Morphology of Alluvial River Channels. *Annual Review of Earth and Planetary Science* 34, 325–354. DOI: 10.1146/annurev.earth.33.092203.122721
- Dey, S. 2014: *Fluvial Hydrodynamics*. GeoPlanet Series, Springer-Verlag, Berlin, 670 p.
- Dunka, S., Fejér, L., Vágás, I. 1996. A veritékes honfoglalás: A Tisza szabályozás története. *Vízügyi Múzeum és Levéltár*, Budapest, 210 p. (in Hungarian)
- Ferguson, R. 2010. Time to abandon the Manning equation? *Earth Surf. Proc. Landf.* 38, 1873–1876. DOI: 10.1002/esp.2091
- Fryirs, K.A., Brierley, G.J. 2001. Variability in sediment delivery and storage along river courses in Bega catchment, NSW, Australia: implications for geomorphic recovery. *Geomorphology* 38, 237–265. DOI: 10.1016/s0169-555x(00)00093-3
- Fryirs, K.A., Brierley, G.J., Preston, N.J., Kasai, M. 2007. Buffers, barriers and blankets: The (dis)connectivity of catchment-scale sediment cascades. *Catena* 70, 49–67. DOI: 10.1016/j.catena.2006.07.007
- Fryirs, K.A., Brierley, G.J., Preston, N.J., Spencer, J. 2008. Catchment-scale (dis)connectivity in sediment flux in the upper Hunter catchment, New South Wales, Australia. *Geomorphology* 84 (3), 297–316. DOI: 10.1016/j.geomorph.2006.01.044
- Harmar, O.P., Clifford, N.J., Thorne, C. R., Biedenham, D. S. 2005. Morphological changes of the Lower Mississippi River: Geomorphological response to engineering intervention. *River Research Applications* 21 (10), 1107–1131. DOI: 10.1002/rra.887
- Hooke, J.M. 1995. River channel adjustment to meander cutoffs on River Bollin and River Dane, Northwest England. *Geomorphology* 14, 235–253. DOI: 10.1016/0169-555x(95)00110-q
- Huang, M.W., Liao, J.J., Pan, Y.W., Chen, M.H. 2014. Rapid channelization and incision into soft bedrock induced by human activity: Implication from the Bachang River in Taiwan. *Engineering Geology* 177, 10–24. DOI: 10.1016/j.enggeo.2014.05.002
- International Commission for Protection of the Danube River (ICPDR). 2008. *Analysis of the Tisza River Catchment 2007: Initial step towards the Tisza River Catchment Management Plan-2009*. Vienna, Austria.
- Kasse, C., Bohnake, S. J. P., Vandenberghe, J., Gabris, G. 2010. Fluvial style changes during the last glacial-interglacial transition in the middle Tisza Valley (Hungary). *Proceedings of the Geologists Association* 121, 180–194. DOI: 10.1016/j.pgeola.2010.02.005
- Kiss, T. 2014. Fluvialis Folyamatok antropogén hatásra megváltozó dinamikája: Egyensúly és érzékenység vizsgáta folyóvízi környezetben. *Akadémiai doktori értekezés*. Szeged, 165 p. (In Hungarian)
- Kiss, T., Balogh, M. 2015. Characteristics of point-bar development under the influence of a dam: Case study of the Dráva River at Sigelec, Croatia. *Journal of Env. Geogr.* 8 (1-2), 23–30. DOI: 10.1515/jengeo-2015-0003
- Kiss T., Fiala, K., Sipos, G. 2008. Alterations of channel parameters in response to river regulation works since 1840 on the Lower Tisza River (Hungary). *Geomorphology* 98, 96–110. DOI: 10.1016/j.geomorph.2007.02.027
- Kondolf, G.M., Piégay, H., Landon, N. 2002. Channel response to increased and decreased bedload supply from land use change: contrasts between two catchments. *Geomorphology* 45, 35–51. DOI: 10.1016/s0169-555x(01)00188-x
- Kroes, D.E., Kraemer, T.F. 2013. Human-induced stream channel abandonment/Capture and filling of floodplain channels within the Atchafalaya River Basin, Louisiana. *Geomorphology* 201, 148–156. DOI: 10.1016/j.geomorph.2013.06.016
- LacZay, I.A. 1982. A folyószabályozás tervezésének morfológiai alapjai. *Vízügyi Közlemények* 64 (2), 235–256. (in Hungarian)
- Landon, N., Piégay, H., Bravard, J.P. 1998. The Drôme River incision (France): from assessment to management. *Landscape and Urban Planning* 43 (1-3), 119–131. DOI: 10.1016/s0169-2046(98)00046-2
- Lászlóffy, W. 1982. *A Tisza*. Akadémiai Kiadó, Budapest. 610 p. (in Hungarian)
- Latapie, A., Camenen, B., Rodrigues, S., Paquier, A., Bouchard, J.P., Moatar, F. 2014. Assessing channel response of a long river influenced by human disturbance. *Catena* 121, 1–12. DOI: 10.1016/j.catena.2014.04.017
- Legleiter, C.J. 2014. A geostatistical framework for quantifying the reach-scale spatial structure of river morphology: 2. Application to restored and natural channels. *Geomorphology* 205, 85–101. DOI: 10.1016/j.geomorph.2012.01.017
- Liébault F., Piégay H. 2001. Assessment of channel changes due to long-term bedload supply decrease, Roubion River, France. *Geomorphology* 36, 167–186. DOI: 10.1016/s0169-555x(00)00044-1
- Liébault, F., Piégay, H. 2002. Causes of 20th century channel narrowing in Mountain and Piedmont Rivers of southeastern France. *Earth Surface Proc. and Landforms* 27, 425–444. DOI: 10.1002/esp.328
- Liébault, F., Gomez, B., Page, M., Marden, M., Peacock, D., Richard, D., Trotter, C.M. 2005. Land-use change, sediment production and channel response in upland regions. *River Research and Applications* 21, 739–756. DOI: 10.1002/rra.880
- Lóczy, D., Kis, É., Schweitzer, F. 2009. Local flood hazards assessed from channel morphology along the Tisza River in Hungary. *Geomorphology* 113, 200–209. DOI: 10.1016/j.geomorph.2009.03.013
- Mezősi, G. 2009. *The Physical Geography of Hungary*. Springer, Switzerland, 334 p.
- Morais, E.S., Rocha, P.C., Hooke, J. 2016. Spatiotemporal variations in channel changes caused by cumulative factors in a meandering river: The lower Peixe River, Brazil. *Geomorphology* 273, 348–360. DOI: 10.1016/j.geomorph.2016.07.026
- Nagy, J., Kiss, T. 2016. Hydrological and morphological changes of the Lower Danube near Mohács, Hungary. *Journal of Env. Geogr.* 9 (1-2), 1–6. DOI: 10.1515/jengeo-2016-0001
- Osei, N.A., Harvey, G.L., Gurnell, A.M. 2015. The early impact of large wood introduction on the morphology and sediment characteristics of a lowland river. *Limnologia* 54, 33–43. DOI: 10.1016/j.limno.2015.08.001
- Pinke, Z. 2014. Modernization and Decline: an eco-historical perspective on regulation of the Tisza Valley, Hungary. *Journal of Historical Geography* 45, 92–105. DOI: 10.1016/j.jhg.2014.02.001
- Pinter, A., Heine, R.A. 2005. Hydrodynamic and morphodynamic response to river engineering documented by fixed-discharge analysis, Lower Missouri River, USA. *Journal of Hydrology* 302, 70–91. DOI: 10.1016/j.jhydrol.2004.06.039
- Powell, D.M. 2014. Flow resistance in gravel-bed Rivers: Progress in research. *Earth Science Reviews* 136, 301–338. DOI: 10.1016/j.earscirev.2014.06.001
- Rinaldi, M. 2003. Recent channel adjustments in alluvial rivers of Tuscany, Central Italy. *Earth Surface Processes and Landforms* 28, 587–608. DOI: 10.1002/esp.464
- Rinaldi, M., Simon, A. 1998. Bed-level adjustments in the Arno River, Central Italy. *Geomorphology* 22, 57–71. DOI: 10.1016/s0169-555x(97)00054-8
- Rinaldi, M., Wyżga, B., Surian, N. 2005. Sediment mining in alluvial rivers: physical effects and management perspectives. *River Research and Application* 21, 805–828. DOI: 10.1002/rra.884
- Schweitzer, F. 2009. Strategy or disaster: flood prevention related issues and actions in the Tisza River Catchment. *Hung. Geogr. Bull.* 58, 3–17. DOI: 10.1007/978-94-011-4140-6_9

- Simon, A., Rinaldi, M. 2006. Disturbance, stream incision, and channel evolution. The roles of excess transport capacity and boundary materials in controlling channel response. *Geomorphology* 79 (3-4), 361–383. DOI: 10.1016/j.geomorph.2006.06.037
- Sipos, G., Kiss, T., Fiala, K. 2007. Morphological alterations due to channelization along the lower Tisza and Maros Rivers (Hungary). *Geografia Fisica E Dinamica Quaternaria* 30 (2), 239–247. DOI: 10.1016/j.geomorph.2007.02.027
- Smith, L.M., Winkley, B.R. 1996. The response of the Lower Mississippi River to river engineering. *Engineering Geology* 45, 433–455. DOI: 10.1016/s0013-7952(96)00025-7
- Surian, A. 1999. Channel changes due to river regulation: the case of the Piave River, Italy. *Earth Surface Processes Landforms* 24, 1135–1151. DOI: 10.1002/(sici)1096-9837(199911)24:12<1135::aid-esp40>3.3.co;2-6
- Surian, N., Rinaldi, M. 2003. Morphological response to river engineering and management in alluvial channels in Italy. *Geomorphology* 50, 307–326. DOI: 10.1016/s0169-555x(02)00219-2
- Szlávik, L. 2000. Az Alföld árvízi veszélyeztetettsége. In: Pálfai, J (Ed.): A víz szerepe és jelentősége. *Nagyalföld Alapítvány, Békéscsaba*, 64–84 (in Hungarian).
- Vágás, I. 1982. A Tisza árvizei. VÍZDOK, Budapest, 283 p. (in Hungarian)
- Van der Berg, J.H. 1995. Prediction of alluvial channel pattern of perennial rivers. *Geomorphology* 12, 259–279. DOI: 10.1016/0169-55x9(50)0014v-
- Wyżga, B. 2007. 20 A review on channel incision in Polish Carpathian Rivers during the 20th century. *Developments in Earth Surface Processes* 11, 525–553. DOI: 10.1016/s0928-2025(07)11142-1
- Xu, J. 2002. River sedimentation and channel adjustment of the lower Yellow River as influenced by low discharges and seasonal channel dry-ups. *Geomorphology* 43, 151–164. DOI: 10.1016/s0169-555x(01)00131-3
- Yang, S.L., Milliman, J.D., Xu, K.H., Deng, B., Zhang, X.Y., Luo, X.X. 2014. Downstream sedimentary and geomorphic impacts of the Three Gorges Dam on the Yangtze River. *Earth-Science Reviews* 138, 469–486. DOI: 10.1016/j.earscirev.2014.07.006
- Yates, R., Waldron, B., van Arsdale, R. 2003. Urban effects on flood plain natural hazards: Wolf River, Tennessee, USA. *Engineering Geology* 70, 1–15. DOI: 10.1016/s0013-7952(03)00088-7



DATING THE HOLOCENE INCISION OF THE DANUBE IN SOUTHERN HUNGARY

Orsolya Tóth¹, György Sipos^{1*}, Tímea Kiss¹, Tamás Bartyik¹

¹Department of Physical Geography and Geoinformatics, University of Szeged, Egyetem u. 2-6, H-6722 Szeged, Hungary

*Corresponding author, e-mail: gysipos@geo.u-szeged.hu

Research article, received 10 April 2017, accepted 20 June 2017

Abstract

The alluvial development of the Great Hungarian Plain has greatly been determined by the subsidence of different areas in the Pannonian Basin. The temporal variation of subsidence rates significantly contributed to the avulsion and shifting of main rivers. This was the case in terms of the Hungarian Lower Danube when occupying its present day N-S directional course. The considerable role of tectonic forcing is also supported by the presence of different floodplain levels. Although, several channel forms are identifiable on these the timing of floodplain development has been reconstructed up till now mostly by the means of geomorphological analysis, and hardly any numerical dates were available. The main aim of this study is to provide the first OSL dates for palaeo-channels located on the high floodplain surface of the Hungarian Lower Danube, and to determine the maximum age of low and high floodplain separation on the Kalocsa Plain. For the analysis two meanders were sampled close to the edge of the step slope between the two levels. According to the results, the development of the investigated palaeo-meanders could be rapid. The formation of the older meander was dated to the Late Atlantic, while the possible separation of the high and low floodplain surfaces could start in the beginning of the Subboreal Phase.

Keywords: Hungarian Lower Danube, floodplain development, Holocene, OSL dating

INTRODUCTION

The alluvial development of the Great Hungarian Plain (GHP) has greatly been determined by the selective subsidence of different areas in the Pannonian Basin. The significance of tectonic control on fluvial processes has been indicated by several earlier research (e.g. Somogyi, 1961; Borsy, 1992; Gábris and Nádor, 2007; Kiss et al., 2015). The temporal variation of subsidence rates at different areas lead to the time-to-time avulsion and shifting of the main rivers and related tributaries. Major shifts however were also influenced by geomorphological processes, namely alluvial fan building and subsequent sliding off the rivers from these elevated surfaces.

Concerning the Danube a significant, but presumably gradual diversion occurred during the Late Würm Period (Pécsi, 1959; Pécsi, 1991; Mezősi, 2011) on its GHP section, when the river had shifted from its earlier NW-SE course to a N-S direction by sliding off its alluvial fan, the Danube-Tisza Interfluve (Mezősi, 2011). The process can also be explained by the activation of the Kalocsa and Baja Depressions, located near the Hungarian-Serbian border. According to Jaskó and Krolopp (1991), this subsidence zone attracted the Danube to its present direction at around 30–40 ka, and fault lines related to the zone are still active, though only moderately (Mezősi, 2011).

Obviously, in case a river shifts to a depression, let it be of geomorphic or tectonic origin, incision is generated, which propagates upstream and leads to the devel-

opment of alluvial fan terraces indicating the major phases of changes (Bridge, 2003; Schumm, 1979). The age of fluvial forms on the abandoned floodplain (now terrace level) corresponds to the maximum, while that of active floodplain forms to the minimum age of incision. The numerical dating of fluvial forms therefore is crucial to reconstruct the timing of terrace formation and consequently the phases and sometimes even the rate of subsidence (Knighton, 1998).

The strath terraces of the Danube on its Hungarian upland section had been intensively studied with classical and more modern dating methods to assess the uplift rate of the adjacent members of the Transdanubian Mountains (Pécsi, 1991; Ruszkiczay-Rüdiger et al., 2005; Gábris, 2013).

Concerning the downstream GHP section of the river Pécsi (1959, 1967) investigated the geomorphological units, terrace materials and development of the floodplain and its levels. He concluded that the Northern part of the present GHP floodplain (Csepel-Solt Plain) is older than the Southern (Kalocsa Plain), and that the upper 10–20 m of sediments is almost completely reworked by the lateral movement of the Danube. Nevertheless, in both areas a low and a high floodplain surface (terrace) can be identified. The term high floodplain refers to the fact that although this surface lies 1–2 m higher it is still inundated by extreme floods. Consequently, Pécsi (1967) claims that fluvial deposits on the low and high floodplain cannot be separated in age, though the development of

the high floodplain can clearly be related to the Late Pleistocene activation of the Baja and Kalocsa Depressions.

So far the timing of floodplain development in the area has been reconstructed mostly by the means of geomorphological analysis, hardly any numerical dates are available concerning the sediments and forms of the high floodplain surface. Two radiocarbon dates from subfossil drift woods placed the age of the right bank side high floodplain surface of the Danube, just opposite to the Kalocsa Plain, to cca. 40 000 and 11 000 BP (Herzfeld et al., 1991). In terms of Late Pleistocene and Holocen terrace surfaces, where the fluvial forms are still identifiable a straightforward method of dating is using optically stimulated luminescence (OSL), which determines the last exposure of sediments to sunlight, i.e. the time of sediment deposition. The method has been extensively applied in studies related to the dating of

floodplain surfaces along several rivers (e.g. Kiss et al., 2013; Olszak et al., 2016; Ruszkiczay-Rüdiger et al., 2016; Meng et al., 2015).

By considering the above, the main aim of the present study is to provide the first OSL dates for palaeochannels located on the high floodplain surface of the Hungarian Lower Danube, and this way to provide a maximum age to the separation of the low and high floodplain levels on the Kalocsa Plain.

STUDY AREA AND SAMPLING

The study area is located on the Kalocsa Plain, which is situated at the middle section of the Hungarian Lower Danube (Fig. 1). The floodplain area is characterised by two floodplain levels: the elevation of the lower floodplain surface (A-level) is between 90 and 92 m asl, while that of the higher floodplain surface (B-level) is between

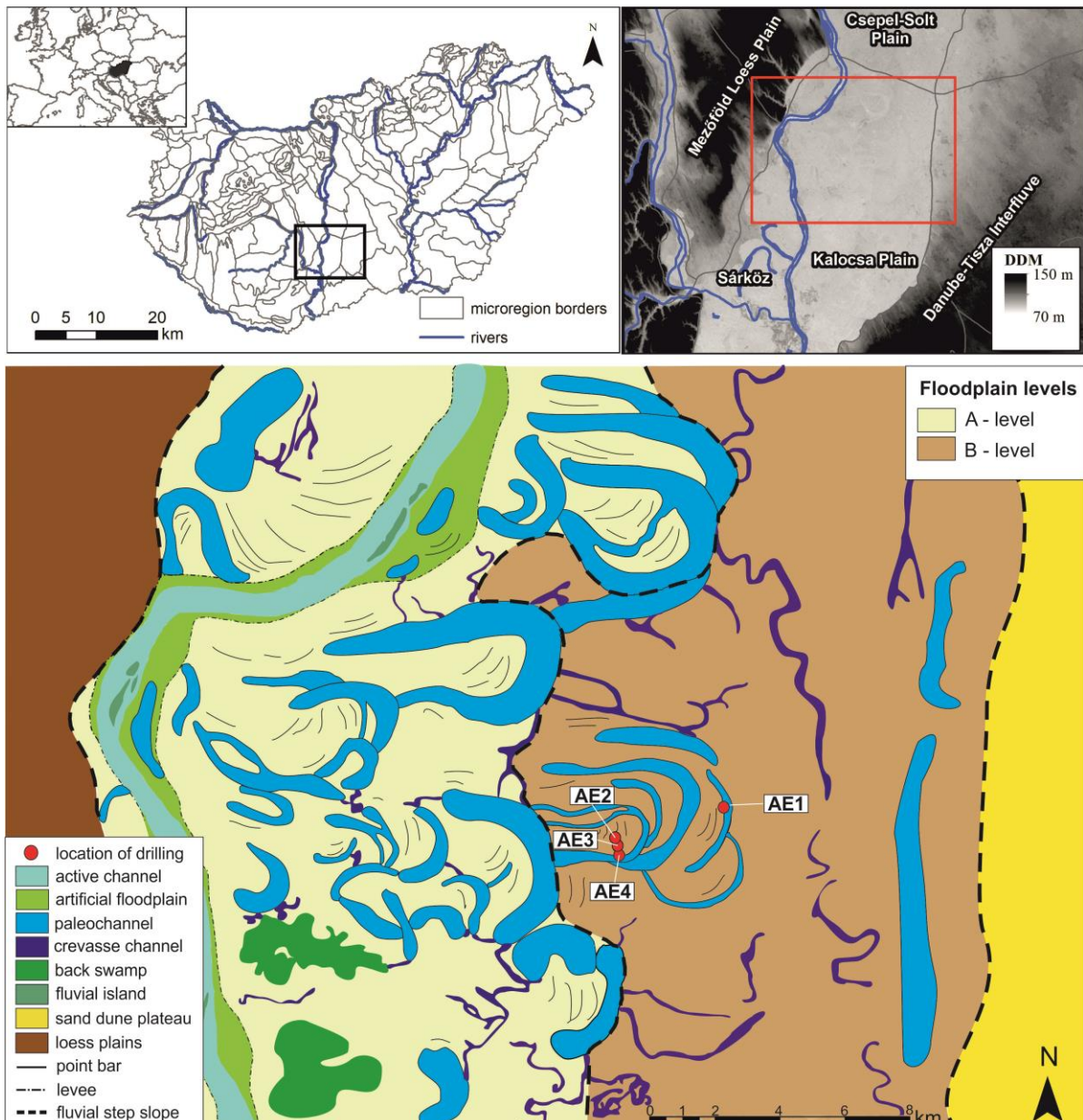


Fig. 1 Location of the study area, geomorphological setting, and sampling points

92 and 94 m asl. Eastwards the study area is adjacent to the Danube-Tisza Interfluvium covered by sand dunes and characterised by a relief between 96 and 105 m asl. Westwards loess plains border the Danube plains, with an elevation reaching even 150 m asl (Fig. 1).

Sediment samples were collected from two palaeo-meanders located on the B-level to determine the maximum age of floodplain surface differentiation, and the time of active B-level floodplain development. The two selected palaeo-channels belong to two separate meander systems. Based on the geomorphological map (Fig. 1), both systems developed through chute cut-offs and consequent meander growth, being characteristic in case of meanders on the lower floodplain as well.

In case of the eastern meander (width=170 m, R=1.7 km) one drilling was made (AE1) to sample channel sediments, as point bars were hardly recognisable on the field (Fig. 1). At the AE1 drilling point 3 OSL samples were collected from 60, 130 and 190 cm (AE1/1, AE1/2, AE1/3). In terms of the western meander (width: 370 m, R=720 m), right on the edge of the B-level, point bars were sampled at three locations (AE2, AE3, AE4), from depths 70, 70 and 110 cm, respectively.

OSL samples were mostly taken from layers of pure sand, however in terms of AE1 upper two samples were categorised on the field as sandy silt. Undisturbed sampling was made with steel cylinders applicable to an Eijkelkamp hand drill system. Samples weighed approximately 200 g. Background samples were also collected from above and from below each OSL sample.

METHODS

The geomorphological map of the study area was compiled on the basis of 1:10 000 scale topographical maps, with 1 m contour line interval, occasionally supplemented by 0.5 m contour lines,

The age of sediment samples was determined by optically stimulated luminescence. Samples were either composed of medium sand, or the mixture of fine sand and silt, though containing an adequate amount of medium sand in the latter case as well, thus the so called coarse grain quartz dating procedure was applied.

In terms of fluvial samples usually the sand sized quartz fraction is investigated anyway, assuming that it usually has more chance for complete bleaching during sediment transport. The preparation of the samples followed usual laboratory techniques (Aitken, 1998; Mauz et al., 2002). After removing the samples from the cylinders they were dried and the 90-150 μm fractions was separated by sieving. The carbonate and organic material content was removed by repeated treatment in 10% HCl and 10% H₂O₂. A Napolytungstanate (LST Fastfloat) heavy liquid flotation was applied for the separation of the quartz fraction. This step was followed by a 50 min etching in 40%

HF, aiming at removing any remaining feldspar contaminations and the outer layer of quartz. Purified quartz grains were adhered to stainless steel discs of 10 mm diameter by silicone spray. For OSL a $\varnothing 6$ mm mask for the final measurements $\varnothing 2$ mm mask was applied to control the number of grains on a disc. A number of aliquots were prepared for luminescence tests and for equivalent dose (D_e) determination. Measurements were made using a RISOE DA-15 TL/OSL luminescence reader by applying the single aliquot regeneration (SAR) protocol (Wintle and Murray 2006).

A preheat test was used for determining optimal heating parameters during the SAR measurements. Preheat temperatures were varied between 180 °C and 300 °C. During the tests 1) SAR recycling ratios (ratio of two sensitivity corrected luminescence signals generated by identical regeneration doses); 2) recuperation (thermal and photo transfer of electrons to OSL traps); and 3) dose recovery (ratios recycling ratio being within 1.00 ± 0.05 , D_e error being lower than 10%, recuperation being lower than 5%) were monitored to determine the best thermal treatment. A combined preheat and dose recovery test was performed. Preheat temperature was increased 200 °C SAR measurements were performed on 48–144 aliquots, depending on the proportion of acceptable measurements. Acceptability was assessed using the standard rejection criteria for each aliquot. Thresholds of rejection were the following: recycling ratio being within 1.00 ± 0.05 , D_e error being lower than 10%, recuperation being lower than 5%. Possible feldspar contamination was also monitored by measuring IRSL/OSL depletion ratio at the end of the SAR procedure. The first 0.5 s of OSL curves was taken as the signal, the last 10 s as the background of measurements. Sample D_e was calculated from aliquot D_e using either the minimum age model (MAM) (AE1/1, AE1/2), or the central age model (CAM) (AE1/3, AE2, AE3, AE4) depending on the dispersion D_e values (Galbraith et al. 1999). Environmental dose rate (D^*) was determined by using high-resolution, extended range gamma spectrometry (Canberra XtRa Coaxial Ge detector), using 500 cm³ Marinelli beakers. Dry dose rates were calculated using the conversion factors of Adamiec and Aitken (1998). Wet dose rates were assessed on the basis of in situ water contents. The rate of cosmic radiation was determined by considering burial depth following the method of Prescott and Hutton (1994).

RESULTS AND DISCUSSION

During the evaluation, a major problem was the low luminescence signal intensity and the low sensitivity of the samples (Fig. 2). Consequently, numerous aliquots did not pass the necessary criteria and were finally rejected from D_e calculation. Therefore, a high number of aliquots were measured finally to get an adequate amount of results for the statistical analysis

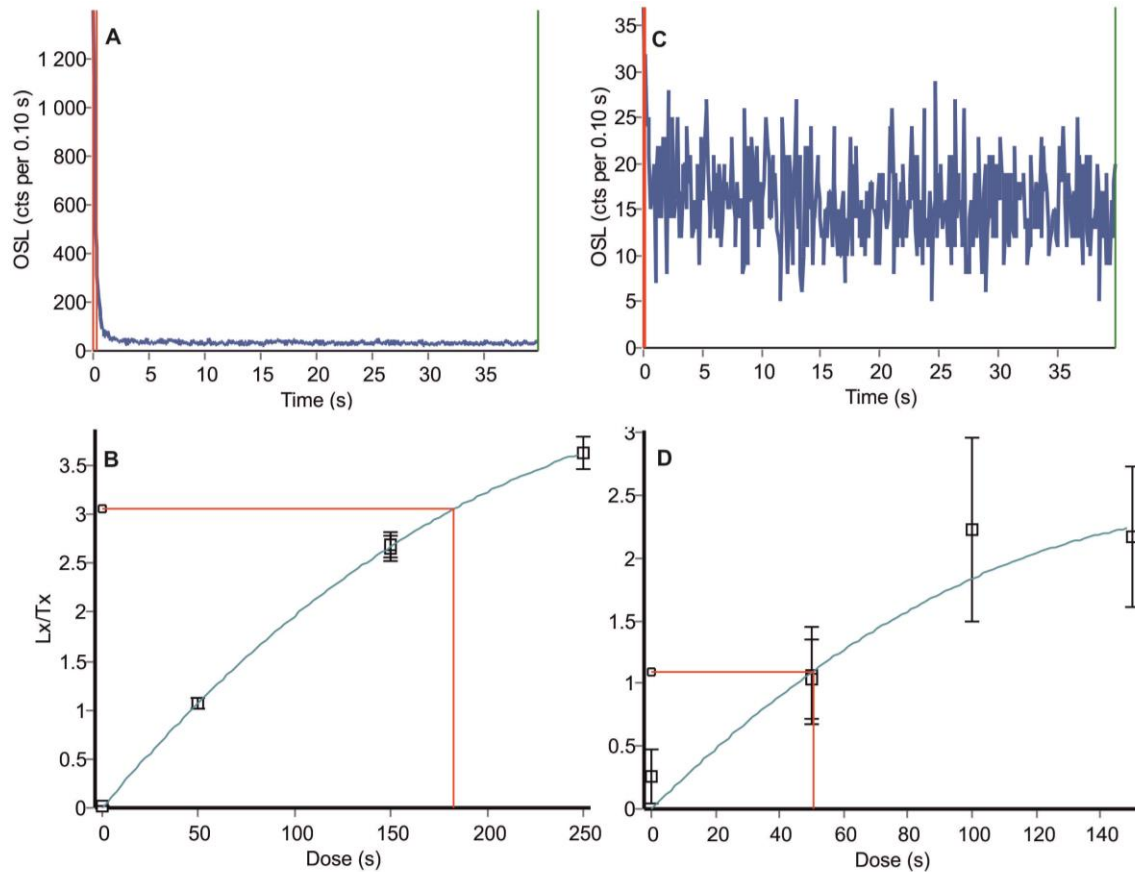


Fig. 2 Figures A and B show an appropriate shine-down curve (A) and dose response curve (B), meanwhile C and D figures represent the low intensity

of equivalent doses. In average 30-40% of the aliquots turned to be acceptable for sample D_e assessment (Table 1).

In case of preheat tests the problem of low sensitivity was a less significant issue, as due to the higher number of grains ($\varnothing 6$ mm mask) on the measurement discs luminescence response was considerably higher. The most appropriate preheat temperature for all samples was 200 °C for the SAR measurements (Fig. 3), since the dose recovery ratio at this temperature was well within the limits of acceptability. Nevertheless, the spread of the recycling ratios was wider in some cases and recuperation was over 5 % in case of samples AE1/2 and AE4. Consequently, the final SAR measurements were

carried out with using a hot bleach treatment, i.e. inserting a high temperature (280°C) optical bleaching at the end of each measurement cycle. By the application of the right temperature treatment the samples performed adequately to retrieve reliable results and ages.

Regarding drilling point AE1 the sampled sand layers at 70, 130 and 190 cm depth were dated to 6.7 ± 0.6 ka, 7.2 ± 0.4 ka and 6.1 ± 0.5 ka, respectively. The lowermost sand layer (AE1/3) was characterised almost exclusively by medium sand, and the distribution of individual D_e results showed a central tendency (Fig. 4), consequently, it is suggested that this sample had undergone the most complete resetting process during transportation and sedimentation. Therefore, both from a sedimentological, and

Table 1 Dose rate, equivalent dose and age data of the investigated samples

Sample	Aliquots (used/measured)	Depth (m)	Moisture content (%)	U (ppm)	Th (ppm)	K (%)	D^* (Gy/ka)	D_e (Gy)	Age (ka)
AE1/1	30/72	0.6	13±1.3	2.95±0.02	5.05±0.06	1.38±0.04	2.80±0.08	20.27±0.82	6.7±0.6
AE1/2	27/48	1.3	21±2.1	2.86±0.04	5.59±0.07	1.36±0.04	2.46±0.07	24.79±0.86	7.2±0.4
AE1/3	25/96	1.9	33±2	2.76±0.03	6.13±0.07	1.34±0.04	2.37±0.07	18.49±1.61	6.1±0.5
AE2	26/72	0.7	16±2	2.87±0.02	4.53±0.06	1.22±0.04	2.49±0.07	11.76±0.65	4.7±0.3
AE3	35/64	0.7	7±2	1.80±0.02	3.63±0.04	1.13±0.03	2.27±0.07	11.05±0.5	4.9±0.3
AE4	58/144	1.1	7±2	2.22±0.02	3.68±0.04	1.18±0.03	2.55±0.08	12.87±1.07	5.0±0.5

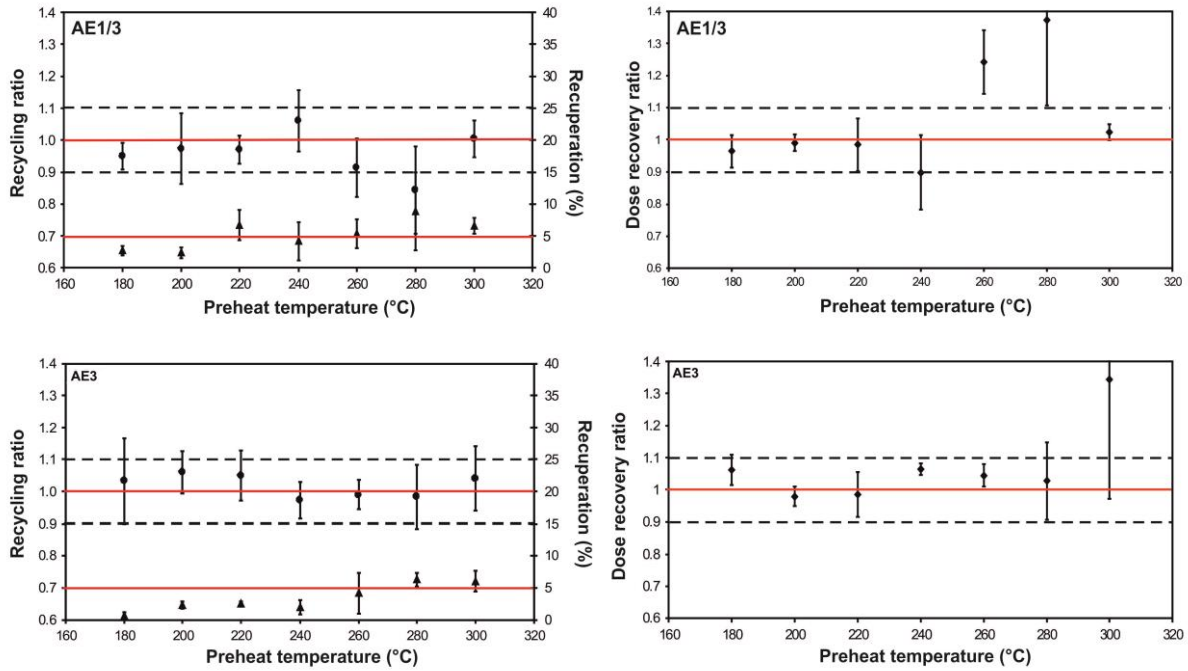


Fig. 3 Preheat and dose recovery tests of the samples. The red line and the dashed line mark the three criteria and the errors of the criteria

from an OSL point of view this sample can represent the time of major fluvial activity. This is in correspondence with the major findings of Tóth et al. (in press), who measured almost complete resetting in terms of modern coarse grain sediments along the present day Danube.

In the meantime the upper two samples yielded somewhat higher ages than AE1/3, which can be explained by their different sedimentology, i.e. the high proportion of fines, which refers to a post formational, lower energy deposition, being less favourable in terms of OSL signal resetting and leading to possible age overestimation. Based on the results, in case of sample AE1/2, characterised by the finest grain size, the age could be overestimated by more than 1 ka, while in case of the coarser AE1/1 by more than 0.6 ka (Fig. 5).

The ages of samples AE2, AE3 and AE4 were very similar and stayed within error, AE4: 4.7 ± 0.3 ka, AE6: 4.9 ± 0.3 ka, AE7: 5.0 ± 0.5 ka (Table 1). As the formation

age of point bars cannot be separated, results refer to a relatively fast meander development between 4.7 and 5.0 ka, reflecting the dynamic nature of Danube fluvial activity.

Based on the first age results from the area, the Danube was actively forming its present day high floodplain up till 5 ka. Consequently, the maximum age of incision and the development of the present day floodplain can be placed to the beginning of the Subboreal Phase. However, in order to question or reinforce the morphological interpretation of Pécsi (1967), i.e. the formation time of the higher and lower floodplain levels are hard to separate, needs further investigation in the area, especially focusing on lower floodplain palaeochannels. Nevertheless, the OSL dates presented here give a framework for further studies, and also imply that if there is a separation time between the two levels, it must be in the second half of the Holocene.

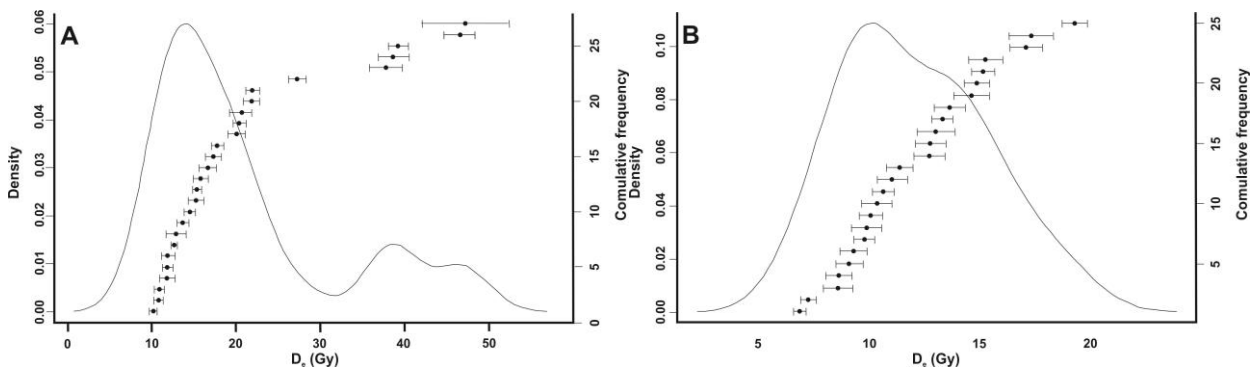


Fig. 4 Dose distribution of individual D_e of AE1/2 (A) and AE1/3 (B). In case of AE1/2 MAM, meanwhile in case of AE1/3 CAM was used for the calculations

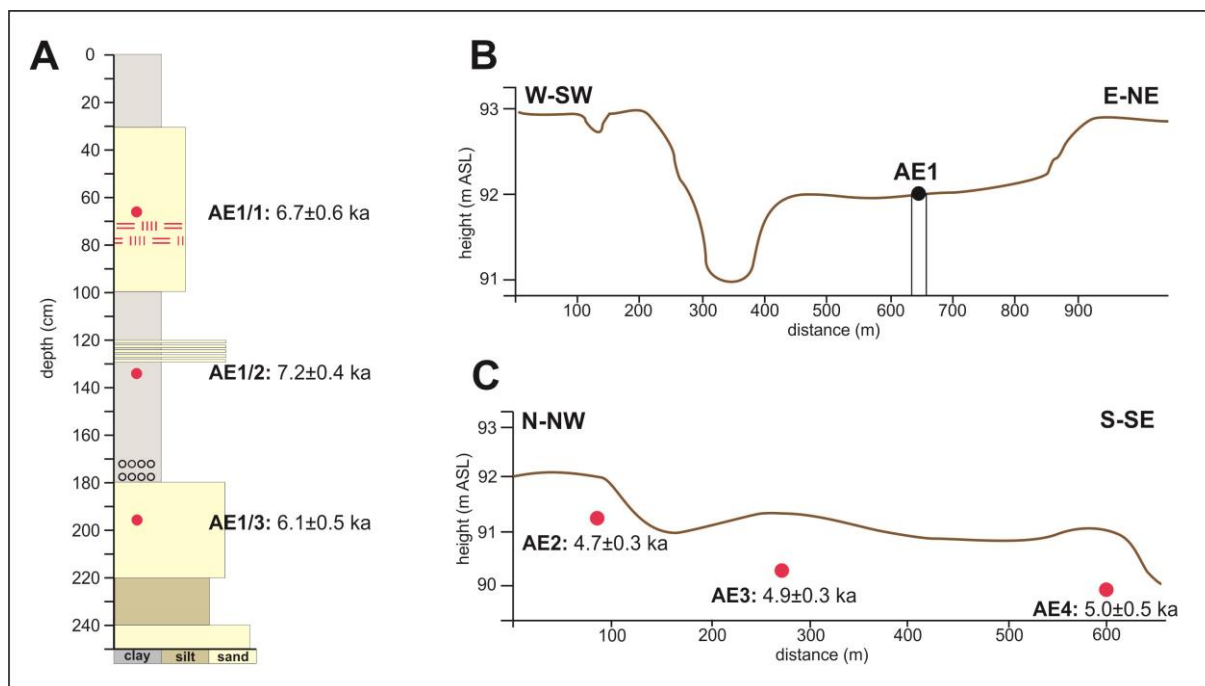


Fig. 5 The results of the two sample site. A: The AE1 drilling point, B: The ages of AE1 drilling point, C: The ages of the second site point bars

CONCLUSIONS

Floodplain development along the Hungarian Lower Danube has previously been reconstructed mainly on the basis of geomorphological evidence. The present study has provided the first OSL dates concerning the fluvial forms of the high floodplain surface on the Kalocsa Plain and therefore on the entire GHP section of the river.

The OSL sensitivity of the sampled sediments is low, therefore a high number of measurements is needed to get the necessary amount of results for the reliable statistical analysis of equivalent doses. However, by the application of the right temperature treatment the samples performed adequately to retrieve reliable results and ages.

The development of the investigated palaeo-meanders could be rapid. In case of the older meander the age of channel forming fluvial activity can be inferred from the lowermost sample, yielding a 6.1 ± 0.5 ka age placing the development of the meander to the Late Atlantic Phase. In terms of the younger meander, on the edge of the high floodplain the ages of consecutive pointbars were in the range of 4.7 ± 0.3 ka and 5.0 ± 0.5 ka, meaning, that the separation of the high and low surfaces could start in the beginning of the Subboreal Phase or later.

Acknowledgements

The research was funded by projects NKFI K 119309, NKFI K 119193 and HURO/1101/126 ENVIARCH

References

- Adamiec, G., Aitken, M. 1998. Dose-rate conversion factors: update. *Ancient TL* 16 (2), 37–50.
- Aitken, M. J. 1998. *An Introduction to Optical Dating*. Oxford University Press. London.

- Borsy, Z. 1992. *Általános természetföldrajz*. Nemzeti Tankönyvkiadó, Budapest. (In Hungarian)
- Bridge, J. S. 2003. *Rivers and Floodplains. Form, Processes and Sedimentary Record*. Blackwell Science Ltd.
- Galbraith, R. F., Roberts, R. G., Laslett, G. M., Yoshida, H., Olley, J. M. 1999. Optical dating of single and multiple grains of quartz from Jimmum rock shelter, northern Australia. Part I: Experimental design and statistical models. *Archaeometry* 41, 339–364. DOI: 10.1111/j.1475-4754.1999.tb00987.
- Gábris, Gy. 2013. A folyóvízi teraszok hazai kutatásának rövid áttekin-tése – A teraszok kialakulásának és korbeosztásának új magyarázata. *Földrajzi Közlemények* 137 (3), 240–247. (in Hungarian).
- Gábris, Gy., Nádor, A. 2007. Long-term fluvial archives in Hungary: response of the Danube and Tisza rivers to tectonic movements and climatic changes during the Quaternary: a review and new synthesis. *Quaternary Science Reviews* 26, 2758–2782. DOI: 10.1016/j.quascirev.2007.06.030
- Hertelendi, E., Petz, R., Scheuer, Gy., Schweitzer, F. 1991. Radiocarbon age of the formation in the Paks Szekszárd depression. – In: Pécsi, M., Schweitzer, F. (eds) *Quaternary environment in Hungary: contribution of the Hungarian National Committee to the XIIIth INQUA Congress Beijing, China*. *Akadémiai Kiadó*, Budapest, 85–89.
- Jaskó, S., Krolopp, E. 1991. Negyedidőszaki kéregmozgások és folyóvízi üledékfelhalmozódás a Duna-völgyében Paks és Mohács között. *A Földtani Intézet Évi Jelentése 1989-ről*, 65–84.
- Kiss, T., Hernesz, P., Sümeghy, B., Györgyövcis, K., Sipos, Gy. 2015. The evolution of the Great Hungarian Plain fluvial system – Fluvial processes in a subsiding area from the beginning of the Weichselian. *Quaternary International* 388 (3), 142–155. DOI: 10.1016/j.quaint.2014.05.050
- Kiss, T., Sümeghy, B., Hernesz, P., Sipos, Gy., Mezősi, G. 2013. Az Alsó-Tisza menti ártér és a Maros hordalékkúp késő-pleisztocén és holocén fejlődéstörténete. *Földrajzi Közlemények* 137: (3) 269–277. (In Hungarian)
- Knighton, D. 1998. *Fluvial forms and processes*. Hodder Arnold Publication, London.
- Mauz, B., Bode, T., Mainz, E., Blanchard, H., Hilger, W., Dikau, R., Zöller, L. 2002. The luminescence dating laboratory at the University of Bonn: Equipment and procedures. *Ancient TL* 20, 53–61.
- Meng, Y.M., Zhang, J.F., Qui, W.L., Fu, X., Guo, Y.J., Zhou, L.P. 2015. Optical dating of the Yellow River terraces in the Mengjin area (China). *Quaternary Geochronology*, 30, 219–225. DOI: 10.1016/j.quageo.2015.03.006

- Mezősi, G., 2011. Magyarország természetföldrajza. Akadémiai kiadó, Budapest (in Hungarian)
- Olszak, J., Kukulak, J., Alexandersonm H. 2016. Revision of river terrace geochronology in the Orawa-Nowy Targ Depression, south Poland: insights from OSL dating, *Proceedings of the Geologists' Association*, 127 (5), 595–605. DOI: 10.1016/j.pgeola.2016.09.004
- Pécsi, M. 1959: A magyarországi Duna-völgy kialakulása és felszínalaktana. Akadémiai kiadó, Budapest, 345. (in Hungarian)
- Pécsi, M. 1967. A dunai Alföld. Akadémiai kiadó, Budapest (in Hungarian)
- Pécsi, M. 1991. A magyarországi Duna-völgy teraszai és szintjei. In: Pécsi, M., Geomorfológia és domborzatminősítés. MTA FKI, Budapest, 36–47. (in Hungarian)
- Prescott, J. R., Hutton, J. T. 1994. Cosmic ray contributions to dose rates for luminescence and ESR dating: large depths and long-term time variations. *Radiation Measurements* 23, 497–500. DOI: 10.1016/1350-4487(94)90086-8
- Ruszkiczay-Rüdiger, Zs., Dunai, T. J., Bada, G., Fodor, L., Horváth, E. 2005: Middle to late Pleistocene uplift rate of the Hungarian Mountain Range at the Danube Bend, (Pannonian Basin) using in situ produced ^3He . *Tectonophysics*, Vol. 410, Iss. 1-4. 173-187. pp.
- Ruszkiczay-Rüdiger, Zs., Braucher, R., Novothny, Á., Csillag, G., Fodor, L., Molnár, G., Madarász, B., ASTER Team. 2016. Tectonic and climatic control on terrace formation: Coupling in situ produced ^{10}Be depth profiles and luminescence approach, Danube River, Hungary, Central Europe. *Quaternary Science Reviews* 131, 127-147. DOI: 10.1016/j.quascirev.2015.10.041
- Somogyi, S. 1961: Hazánk folyóhálózatának fejlődéstörténeti vázlat. *Földrajzi Közlemények* 9 (85), 25–50. (In Hungarian)
- Schumm, S. A. 1979: Geomorphic thresholds: The concept and its applications. *Transactions of the Institute of British Geographers* 4, 485–515. DOI: 10.2307/622211
- Tóth, O., Sipos, Gy., Kiss, T., Bartyik, T.: Variation of OSL residual doses in terms of coarse and fine grain modern sediments along the Hungarian section of the Danube. *Geochronometria* (in press)
- Wintle, A. G., Murray, A. S. 2006. A review of quartz optically stimulated luminescence characteristic and their relevance in single-aliquot regeneration dating protocols. *Radiation Measurement* 41, 369–391. DOI: 10.1016/j.radmeas.2005.11.001